

Final Report for Project
“EVALUATION OF REFLECTIVE CRACKING MITIGATION TREATMENTS USING THE
COMPOSITE SPECIMEN INTERFACE CRACKING (CSIC) TEST”

| |
|--|
| UF Project No.: 120852 Contract No.: BDV31 977-39 |
|--|

Submitted to:

Florida Department of Transportation
605 Suwannee Street MS-30
Tallahassee, FL, 32399



Dr. Reynaldo Roque, P.E.
Cristian Cocconcelli
Dr. Jian Zou
Bongsuk Park
George Lopp

Department of Civil and Coastal Engineering
College of Engineering
365 Weil Hall, P.O. Box 116580
Gainesville, FL, 32611-6580
Tel: (352) 392-9537 extension 1458
Fax: (352) 392-3394

June 2018

DISCLAIMER

The opinions, findings, and conclusions expressed in this publication are those of the authors and not necessarily those of the State of Florida Department of Transportation.

Prepared in cooperation with the State of Florida Department of Transportation.

SI* (MODERN METRIC) CONVERSION FACTORS

APPROXIMATE CONVERSIONS TO SI UNITS

| SYMBOL | WHEN YOU KNOW | MULTIPLY BY | TO FIND | SYMBOL |
|--|-----------------------------|-----------------------------|-----------------------------|---------------------|
| LENGTH | | | | |
| in | inches | 25.4 | millimeters | mm |
| ft | feet | 0.305 | meters | m |
| yd | yards | 0.914 | meters | m |
| mi | miles | 1.61 | kilometers | km |
| AREA | | | | |
| in ² | square inches | 645.2 | square millimeters | mm ² |
| ft ² | square feet | 0.093 | square meters | m ² |
| yd ² | square yard | 0.836 | square meters | m ² |
| ac | acres | 0.405 | hectares | ha |
| mi ² | square miles | 2.59 | square kilometers | km ² |
| VOLUME | | | | |
| fl oz | fluid ounces | 29.57 | milliliters | mL |
| gal | gallons | 3.785 | liters | L |
| ft ³ | cubic feet | 0.028 | cubic meters | m ³ |
| yd ³ | cubic yards | 0.765 | cubic meters | m ³ |
| NOTE: volumes greater than 1000 L shall be shown in m ³ | | | | |
| MASS | | | | |
| oz | ounces | 28.35 | grams | g |
| lb | pounds | 0.454 | kilograms | kg |
| T | short tons (2000 lb) | 0.907 | megagrams (or "metric ton") | Mg (or "t") |
| TEMPERATURE (exact degrees) | | | | |
| °F | Fahrenheit | 5 (F-32)/9 or (F-32)/1.8 | Celsius | °C |
| ILLUMINATION | | | | |
| fc | foot-candles | 10.76 | lux | lx |
| fl | foot-Lamberts | 3.426 | candela/m ² | cd/m ² |
| FORCE and PRESSURE or STRESS | | | | |
| lbf | poundforce | 4.45 | newtons | N |
| lbf/in ² | poundforce per square inch | 6.89 | kilopascals | kPa |
| APPROXIMATE CONVERSIONS FROM SI UNITS | | | | |
| SYMBOL | WHEN YOU KNOW | MULTIPLY BY | TO FIND | SYMBOL |
| LENGTH | | | | |
| mm | millimeters | 0.039 | inches | in |
| m | meters | 3.28 | feet | ft |
| m | meters | 1.09 | yards | yd |
| km | kilometers | 0.621 | miles | mi |
| AREA | | | | |
| mm ² | square millimeters | 0.0016 | square inches | in ² |
| m ² | square meters | 10.764 | square feet | ft ² |
| m ² | square meters | 1.195 | square yards | yd ² |
| ha | hectares | 2.47 | acres | ac |
| km ² | square kilometers | 0.386 | square miles | mi ² |
| VOLUME | | | | |
| mL | milliliters | 0.034 | fluid ounces | fl oz |
| L | liters | 0.264 | gallons | gal |
| m ³ | cubic meters | 35.314 | cubic feet | ft ³ |
| m ³ | cubic meters | 1.307 | cubic yards | yd ³ |
| MASS | | | | |
| g | grams | 0.035 | ounces | oz |
| kg | kilograms | 2.202 | pounds | lb |
| Mg (or "t") | megagrams (or "metric ton") | 1.103 | short tons (2000 lb) | T |
| TEMPERATURE (exact degrees) | | | | |
| °C | Celsius | 1.8C+32 | Fahrenheit | °F |
| ILLUMINATION | | | | |
| lx | lux | 0.0929 | foot-candles | fc |
| cd/m ² | candela/m ² | 0.2919 | foot-Lamberts | fl |
| FORCE and PRESSURE or STRESS | | | | |
| N | newtons | 0.225 | poundforce | lbf |
| kPa | kilopascals | 0.145 | poundforce per square inch | lbf/in ² |

*SI is the symbol for the International System of Units. Appropriate rounding should be made to comply with Section 4 of ASTM E380.

(REVISED MARCH 2003)

| | | | |
|--|--|---|-----------|
| 1. Report No. | 2. Government Accession No. | 3. Recipient's Catalog No. | |
| 4. Title and Subtitle Evaluation of Reflective Cracking Mitigation Treatments Using the Composite Specimen Interface Crack (CSIC) Test | | 5. Report Date June 2018 | |
| | | 6. Performing Organization Code | |
| 7. Author(s) Reynaldo Roque, Cristian Cocconcelli, Jian Zou, Bongsuk Park, and George Lopp | | 8. Performing Organization Report No. 120852 | |
| 9. Performing Organization Name and Address University of Florida Department of Civil and Coastal Engineering 365 Weil Hall, PO Box 116580 Gainesville, FL 32611-6580 | | 10. Work Unit No. (TRAIS) | |
| | | 11. Contract or Grant No. BDV31-977-39 | |
| 12. Sponsoring Agency Name and Address Florida Department of Transportation Research Center, MS 30 605 Suwannee Street Tallahassee, FL, 32399-0450 | | 13. Type of Report and Period Covered Final 03/11/15-06/30/18 | |
| | | 14. Sponsoring Agency Code | |
| 15. Supplementary Notes | | | |
| 16. Abstract: Reflective cracking is frequently reported as the most common distress affecting resurfaced pavements. The Florida Department of Transportation (FDOT) has traditionally used an asphalt rubber membrane interlayer (ARMI) approach to mitigate reflective cracking. However, recent field evidence has raised doubts about the effectiveness of the ARMI when placed near the surface, indicating questionable benefits to reflective cracking and increased instability rutting potential. The main purpose of this research was to develop guidelines for an effective alternative to the ARMI that is less expensive than a geotextile system for mitigation of near-surface reflective cracking in overlays on asphalt pavement. Fourteen interlayer mixtures, covering a broad range of gradation, were designed based on the dominant aggregate size range – interstitial component (DASR-IC) model, which provides a framework for the design and modification of gradation to ensure sufficient aggregate interlock to resist permanent deformation as well as adequate cracking resistance. A composite specimen interface cracking (CSIC) test developed in an earlier FDOT research project was enhanced with a new loading device, specimen preparation procedure, and loading procedure to more consistently evaluate reflective cracking performance of interlayer systems. In addition, asphalt pavement analyzer (APA) tests were performed to determine whether the interlayer mixtures had sufficient rutting resistance. The results demonstrated that interlayer mixtures designed with lower compaction effort, reduced design air voids, and coarser gradation led to more cost-effective fracture-tolerant and shear resistant (FTSR) interlayers. Therefore, preliminary design guidelines including minimum effective film thickness (EFT) requirements (20 µm for 4.75-mm NMAS and 35 µm for 9.5-mm NMAS FTSR mixtures) were proposed to mitigate near-surface reflective cracking. | | | |
| 17. Key Words: Fracture-tolerance, shear-resistance, interlayer mixture, reflective cracking, instability rutting | | 18. Distribution Statement No restrictions | |
| 19. Security Classif. (of this report) Unclassified | 20. Security Classif. (of this page) Unclassified | 21. No of Pages 95 | 22. Price |

Form DOT F 1700.7 (8-72)

ACKNOWLEDGEMENT

The authors would like to acknowledge and thank the Florida Department of Transportation (FDOT) for providing technical and financial support and materials for this project. Special thanks go to project manager Wayne Rilko and engineers and technicians of the Bituminous Section of the State Materials Office for their contributions throughout the various phases of this project.

EXECUTIVE SUMMARY

Reflective cracking is a discontinuity in the rehabilitated surface with a pattern similar to the existing cracking in the old pavement surface. It is frequently reported as the most common distress affecting resurfaced pavements. The Florida Department of Transportation (FDOT) has traditionally used an asphalt rubber membrane interlayer (ARMI) approach to mitigate reflective cracking in overlays on asphalt pavement. The intent of this treatment is to absorb the stresses induced by horizontal movements of cracks in the existing pavement before they reach the overlay. However, recent field evidence has raised doubts about the effectiveness of the ARMI when placed near the surface, indicating questionable benefits to reflective cracking and increased instability rutting potential.

Two existing systems were identified in the literature as potentially more effective alternatives to the ARMI: fracture-tolerant interlayer and stone matrix asphalt (SMA) interlayer. The fracture-tolerant interlayer system involves 9.5-mm nominal maximum aggregate size (NMAS) crack attenuating mixture (CAM) and 4.75-mm NMAS binder rich intermediate course (BRIC) mixture, which are dense-graded mixtures specially designed to allow for higher asphalt content for higher fracture tolerance. Lower compaction effort, reduced design air void content, and even finer gradation relative to the Superpave gradation band were used in the system to achieve higher asphalt content. However, increasing asphalt content does not necessarily enhance fracture tolerance and may reduce shear resistance. SMA mixture belongs to the family of gap-graded mixtures, which are designed to achieve stone-on-stone contact for enhanced shear resistance. Also, SMA is known to provide improved cracking resistance. However, characteristic stone-on-stone design requires strong aggregate. Furthermore, gap-grading requires both additional asphalt binder and the introduction of fibers, which may result in higher cost and potential construction issues. Therefore, it was determined that a more suitable interlayer system was needed to mitigate near-surface reflective cracking in overlays on asphalt pavement.

The main purpose of this study was to develop guidelines for fracture-tolerant and shear-resistance (FTSR) interlayer mixtures to mitigate near-surface reflective cracking. Fourteen interlayer mixtures, covering a broad range of gradation, were designed based on the dominant

aggregate size range – interstitial component (DASR-IC) model, which provided a framework for the design and modification of gradation to ensure sufficient aggregate interlock to resist permanent deformation as well as adequate cracking resistance. Two key mixture parameters from the DASR-IC model, DASR porosity and effective film thickness (EFT), were used to ensure the twelve designed dense-graded interlayer mixtures covered a broad range of gradation, including the finest and coarsest within the gradation bands used to define CAM and BRIC mixtures. In addition, two gap-graded mixtures were designed to achieve the highest coarseness with available stockpiles in Florida. According to the DASR-IC model, coarser gradation results in lower DASR porosity and higher EFT which enhance shear resistance and fracture tolerance.

Both granite and limestone aggregate types widely used in the state of Florida were employed to produce interlayer mixtures for laboratory testing, including Georgia granite, Nova Scotia granite, and Florida limestone. Two polymer-modified asphalt (PMA) binders that have been shown to improve mixture cracking and rutting performance were used: a performance-grade (PG) 76-22 PMA, and a PG 76-22 high polymer (HP) asphalt binder. Based on discussion with the FDOT research panel, three interlayer thicknesses in combination with two nominal maximum aggregate sizes were selected for interlayer system evaluation, i.e., 0.5-in and 0.75-in for 4.75-mm mixtures, and 0.75-in and 1.0-in for 9.5-mm mixtures.

A composite specimen interface cracking (CSIC) test developed in an earlier FDOT research project was enhanced with a new loading device, specimen preparation procedure, and loading procedure to more consistently evaluate reflective cracking performance of interlayer systems. In addition, asphalt pavement analyzer (APA) tests were performed to determine whether the interlayer mixtures had sufficient rutting resistance. Results showed that 9.5-mm dense-graded mixtures, with a minimum EFT of 35 μm , are suitable as FTSR mixtures for good reflective cracking and rutting performance. Both granite and limestone worked well. However, the Florida limestone used required greater interlayer thickness (1.0-in, as opposed to 0.75-in for granite) and more asphalt binder. As compared to CAM, 9.5-mm dense-graded FTSR mixtures exhibited equivalent performance with less asphalt binder when granite aggregate was used, or better performance and less sensitivity to interlayer thickness with less asphalt binder when limestone was used. Furthermore, the 4.75-mm dense-graded limestone mixture with a minimum EFT of

20 μm exhibited good reflective cracking performance at 0.75-in thickness and good rutting performance. However, due to higher asphalt content required, it is costlier than the 9.5-mm mixtures with the same thickness. The 4.75-mm dense-graded granite mixture with a minimum EFT of 20 μm also exhibited good reflective cracking performance at 0.75-in thickness, but were not suitable as an FTSR mixture due to high APA rut depth. Therefore, rutting resistance of 4.75-mm mixtures must be checked to ensure adequate shear resistance. As compared to BRIC mixture, 4.75-mm dense-graded FTSR mixtures exhibited better performance and less sensitivity to interlayer thickness. In addition, the 9.5-mm gap-graded granite mixture provided superior performance at 1.0-in thickness. However, it is a costlier option relative to dense-graded mixtures due to greater thickness and more asphalt binder required. Florida limestone was not suitable for gap-graded design due to breakage of aggregates.

Results of CSIC and APA tests demonstrated that interlayer mixtures designed with lower compaction effort, reduced design air voids, and coarser gradation led to more cost-effective FTSR interlayers than existing CAM and BRIC systems. Therefore, preliminary design guidelines, including minimum EFT requirements (20 μm for 4.75-mm and 35 μm for 9.5-mm FTSR mixtures), were proposed to mitigate near-surface reflective cracking in overlays on asphalt pavement. A broader range of aggregate types, gradations, and interlayer thickness should be tested to refine the design guidelines. Development of a simpler test system (i.e. Superpave IDT along with HMA fracture mechanics) is recommended to complete the work needed for refinement of design guidelines. Furthermore, an HVS test or an experimental road test should be performed to verify further the design guidelines that were identified based on laboratory tests.

TABLE OF CONTENTS

| | |
|--|------|
| DISCLAIMER | ii |
| SI* (MODERN METRIC) CONVERSION FACTORS | iii |
| TECHNICAL REPORT DOCUMENTATION PAGE | iii |
| ACKNOWLEDGEMENT | v |
| EXECUTIVE SUMMARY | vi |
| LIST OF TABLES | xii |
| LIST OF FIGURES | xiii |
| CHAPTER 1 INTRODUCTION | 1 |
| 1.1 Background..... | 1 |
| 1.2 Objectives | 3 |
| 1.3 Scope..... | 3 |
| 1.4 Research Approach..... | 4 |
| CHAPTER 2 MECHANISMS AND MITIGATION TREATMENTS..... | 6 |
| 2.1 Reflective Cracking Mechanisms | 6 |
| 2.2 Mitigation Treatments | 9 |
| 2.2.1 Existing Asphalt Surface Modification | 10 |
| 2.2.2 Overlay Layer/Mixture Modification | 10 |
| 2.2.3 Overlay Reinforcement..... | 10 |
| 2.2.4 Stress or Strain Relieving Interlayers | 11 |
| 2.3 Concluding Remarks | 13 |
| CHAPTER 3 DEVELOPMENT OF FRACTURE-TOLERANT SHEAR-RESISTANT INTERLAYER MIXTURES..... | 14 |
| 3.1 Mix Design Methods | 14 |
| 3.1.1 DASR-IC Model..... | 14 |

| | |
|--|----|
| 3.1.2 Promising Treatments and Key Mixture Characteristics | 17 |
| 3.1.3 Preliminary Mix Design Criteria for FTSR Interlayer Mixtures | 18 |
| 3.2 Materials | 19 |
| 3.3 Mix Design Results..... | 20 |
| 3.3.1 Mixture Gradations..... | 20 |
| 3.3.2 Volumetric Property and DASR-IC Parameters..... | 25 |
| CHAPTER 4 MIXTURE TESTS AND EXPERIMENTAL PLAN..... | 26 |
| 4.1 Composite Specimen Interface Cracking Test | 26 |
| 4.1.1 Specimen Preparation | 26 |
| 4.1.2 CSIC Test Procedure | 29 |
| 4.1.3 Data Collection and Interpretation..... | 31 |
| 4.2 Asphalt Pavement Analyzer Test..... | 32 |
| 4.2.1 Sample Preparation..... | 32 |
| 4.2.2 APA Test Procedure | 33 |
| 4.2.3 Data Collection and Interpretation..... | 34 |
| 4.3 Experimental Plan..... | 34 |
| CHAPTER 5 TEST RESULTS AND ANALYSIS | 36 |
| 5.1 Introduction..... | 36 |
| 5.2 Test Results..... | 36 |
| 5.2.1 9.5-mm NMAS Granite Interlayer Mixtures | 37 |
| 5.2.2 4.75-mm NMAS Granite Interlayer Mixtures | 39 |
| 5.2.3 9.5-mm NMAS Limestone Interlayer Mixtures | 41 |
| 5.2.4 4.75-mm NMAS Limestone Interlayer Mixtures | 43 |
| 5.3 Identification of Preliminary Design Guidelines | 45 |
| 5.3.1 Minimum EFT for 9.5-mm NMAS Interlayer Mixtures | 45 |
| 5.3.2 Minimum EFT for 4.75-mm NMAS Interlayer Mixtures | 48 |
| 5.3.3 Preliminary Design Guidelines..... | 50 |
| CHAPTER 6 CLOSURE | 52 |
| 6.1 Summary of Findings | 52 |

| | |
|--|-----------|
| 6.2 Conclusions..... | 54 |
| 6.3 Recommendations and Future Work | 54 |
| APPENDIX A REVIEW OF REFLECTIVE CRACKING MITIGATION TREATMENT | 55 |
| A.1 Existing Asphalt Surface Modification..... | 55 |
| A.1.1 Milling and Replacing | 55 |
| A.1.2 Hot-in-Place Recycling (HIPR)..... | 55 |
| A.1.3 Full-Depth-Reclamation (FDR)..... | 56 |
| A.2 Overlay Layer/Mixture Modification | 57 |
| A.2.1 Thick asphalt Overlays | 57 |
| A.2.2 Modified Asphalt and Specialty Mixtures..... | 57 |
| A.3 Overlay Reinforcement..... | 58 |
| A.3.1 Geosynthetics..... | 58 |
| A.3.2 Steel Mesh..... | 60 |
| A.4 Stress or Strain Relieving Layers..... | 61 |
| A.4.1 Crack Relief Layer (CRL) | 61 |
| A.4.2 Stress Absorbing Membrane Interlayers (SAMI)..... | 62 |
| APPENDIX B AGGREGATE STOCKPILE INFORMATION | 66 |
| APPENDIX C GRADATIONS DESIGNED FOR INTERLAYER MIXTURES..... | 67 |
| APPENDIX D ENHANCEMENT OF THE CSIC TEST | 68 |
| D.1 New Loading Device | 68 |
| D.2 New Specimen Configuration..... | 70 |
| D.3 New Loading Procedure | 73 |
| APPENDIX E MIXTURE TEST RESULTS | 74 |
| LIST OF REFERENCES | 77 |

LIST OF TABLES

| | |
|---|----|
| Table 2-1. Possible reflective cracking treatments (adapted from Von Quintus et al., 2009). | 9 |
| Table 3-1. Key mixture characteristics. | 17 |
| Table 3-2. Mix design requirements for dense-graded and gap-graded FTSR interlayer mixtures..... | 19 |
| Table 3-3. DASR porosity and EFT estimated for granite mixtures. | 21 |
| Table 3-4. DASR porosity and EFT estimated for limestone mixtures..... | 24 |
| Table 3-5. Volumetric properties and final DASR porosity and EFT values..... | 25 |
| Table 5-1. Mix design requirements for FTSR interlayer mixtures..... | 50 |
| Table B-1. Aggregate stockpiles used for granite mixtures..... | 66 |
| Table B-2. Aggregate stockpiles used for limestone mixtures. | 66 |
| Table C-1. Granite interlayer mixture gradations..... | 67 |
| Table C-2. Limestone interlayer mixture gradations | 67 |
| Table E-1. CSIC test results for 9.5-mm mixtures and the control at 1.0-in thickness. | 74 |
| Table E-2. CSIC test results for 9.5-mm mixtures and the control at 0.75-in thickness. | 74 |
| Table E-3. CSIC test results for 4.75-mm mixtures and the control at 0.75-in thickness. | 75 |
| Table E-4. CSIC test results for 4.75-mm mixtures and the control at 0.50-in thickness. | 75 |
| Table E-5. APA test results for interlayer mixtures..... | 76 |

LIST OF FIGURES

| | |
|--|----|
| Figure 2-1. Reflective cracking in asphalt overlays..... | 6 |
| Figure 2-2. Typical failure modes associated with reflective cracking. | 7 |
| Figure 2-3. Typical failure modes associated with reflective cracking. | 8 |
| Figure 3-1. DASR-IC model: (a) Schematic representation; (b) Mixture components by volume..... | 15 |
| Figure 3-2. 9.5-mm NMAS granite mixture gradations. | 21 |
| Figure 3-3. 4.75-mm NMAS granite mixture gradations. | 22 |
| Figure 3-4. 9.5-mm NMAS limestone mixture gradations. | 23 |
| Figure 3-5. 4.75-mm NMAS limestone mixture gradations. | 24 |
| Figure 4-1. Preparation of composite layers: (a) Overlay compaction, (b) Tack coat application, and (c) Interlayer compaction on top of the thin tack coat. | 27 |
| Figure 4-2. Assembly of CSIC composite specimen: (a) Cutting to obtain two symmetrical parts (plan view), (b) Two symmetrical parts aligned and glued to the central metal spacer, and (c) Complete CSIC specimen installed with gauge points..... | 28 |
| Figure 4-3. CSIC test setup: (a) Loading device, (b) Placement of CSIC specimen into the loading device, and (c) Connection of loading device to the MTS loading frame. | 29 |
| Figure 4-4. Repeated loading and response for two consecutive cycles: (a) Loading applied through two yolks, (b) Resilient deformation obtained at the extensometers..... | 30 |
| Figure 4-5. Typical load and response for reflective cracking performance evaluation: (a) Amplitude sweep loading, (b) Evolution of resilient deformation in the CSIC specimen. | 31 |
| Figure 4-6. Determination of specimen failure: (a) Slope of resilient deformation calculated for the last load level when the specimen failed, (b) A cracked composite specimen. | 32 |
| Figure 4-7. APA test procedure: (a) Two APA sets placed in the molds, (b) Steel wheel and pressurized hose to load each APA set, and (c) A deformed sample after APA test..... | 33 |

| | |
|--|----|
| Figure 4-8. Overall experimental plan. | 35 |
| Figure 5-1. APA test result for 9.5-mm NMAS granite mixtures. | 37 |
| Figure 5-2. CSIC test results for 9.5-mm NMAS granite interlayers. | 38 |
| Figure 5-3. APA test result for 4.75-mm NMAS granite mixtures. | 39 |
| Figure 5-4. CSIC test results for 4.75-mm NMAS granite interlayers. | 40 |
| Figure 5-5. Evaluation of 4.75-mm DC granite mixture with HP binder: (a) APA test results; (b) CSIC test results. | 41 |
| Figure 5-6. Crack jumping phenomenon (Bennert et al., 2011) | 41 |
| Figure 5-7. APA test result for 9.5-mm NMAS limestone mixtures. | 42 |
| Figure 5-8. CSIC test results for 9.5-mm NMAS limestone interlayers. | 43 |
| Figure 5-9. Comparison of failure surfaces between limestone and granite mixtures. | 43 |
| Figure 5-10. APA test result for 4.75-mm NMAS limestone mixtures. | 44 |
| Figure 5-11. CSIC test results for 4.75-mm NMAS limestone interlayers. | 44 |
| Figure 5-12. Effect of EFT on performance of 9.5-mm dense-graded granite mixtures. | 45 |
| Figure 5-13. Effect of EFT on asphalt content of 9.5-mm dense-graded granite mixtures. | 46 |
| Figure 5-14. Effect of EFT on performance of 9.5-mm dense-graded limestone mixtures. | 46 |
| Figure 5-15. Effect of EFT on asphalt content of 9.5-mm dense-graded limestone mixtures and minimum EFT requirement. | 47 |
| Figure 5-16. Effect of EFT on reflective cracking performance and asphalt content of 4.75- mm dense-graded limestone mixtures. | 48 |
| Figure 5-17. Effect of EFT on rutting performance of 4.75-mm dense-graded limestone mixtures and minimum EFT requirement. | 49 |
| Figure 5-18. Comparison of gradation bands for 9.5-mm DG FTSR mixture and CAM. | 51 |
| Figure 5-19. Comparison of gradation bands for 4.75-mm DG FTSR mixture and BRIC. | 51 |
| Figure A-1. Existing asphalt surface modification. | 56 |

| | |
|---|----|
| Figure A-2. Overlay layer/mixture modification. | 58 |
| Figure A-3. Reinforcement of asphalt overlays. | 60 |
| Figure A-4. Cushion or crack relief layer. | 61 |
| Figure A-5. Stress and strain relief interlayer. | 65 |
| Figure D-1. Original loading device. | 69 |
| Figure D-2. New loading assembly. | 69 |
| Figure D-3. Test setup with new loading device. | 70 |
| Figure D-4. Original specimen configuration. | 71 |
| Figure D-5. New specimen assembly. | 72 |
| Figure D-6. New loading procedure. | 73 |

CHAPTER 1
INTRODUCTION
1.1 Background

Hot mix asphalt (HMA) overlay is one of the most common techniques used to restore initial pavement condition of a cracked surface. However, after the overlay is placed, cracking may develop in the new surface in a pattern similar to the existing cracks in the old pavement. This phenomenon was named reflective cracking, and is recognized as a major distress mode for asphalt overlays (Sherman, 1974).

An asphalt rubber membrane interlayer (ARMI) system has been traditionally used by the Florida Department of Transportation (FDOT) to mitigate reflective cracking. This system is placed between the existing cracked pavement and the new overlay. The ARMI consists of coarse aggregates seated in a thick layer of asphalt rubber binder. The intent of the treatment is to absorb the stresses induced by horizontal movements of cracks in the existing pavement before they reach the overlay. However, recent field evidence has raised doubts about the effectiveness of the ARMI when placed near the surface, indicating questionable benefits to reflective cracking and increased instability rutting potential.

The FDOT conducted studies to evaluate further performance of ARMI. Greene et al. (2012) focused on evaluating whether ARMI contributes to instability rutting and on its effectiveness in mitigating reflective cracking. Results showed that rut depth of sections containing an ARMI was at least twice that of control sections (without an ARMI). Reflective cracking was observed on all Portland cement concrete (PCC) joints on sections with and without ARMI. Chen et al. (2013) conducted a study using the composite specimen interface cracking (CSIC) test which showed that control specimens exhibited better reflective cracking resistance than specimens with an ARMI.

Based on the findings of these two research projects, the FDOT decided to search for an alternative reflective cracking mitigation strategy. A theoretical analysis was conducted by Nam et al. (2014), which included a conventional numerical analysis to better understand the

mechanism of reflective cracking in HMA overlays on flexible pavement and a general multi-criteria decision making (MCDM) study to select the best mitigation techniques. Two treatments were recommended: i) fabric, and ii) 4-in milling and replacement. The first approach was very promising according to their theoretical analysis. However, other studies have indicated that difficulties encountered during installation and high cost make the fabrics impractical and non-cost-effective (Barazone, 1990, 2000; Buttlar et al., 2000). The second treatment has been found to be questionable in arresting the development of reflective cracking (Housel, 1962; Van Breeman, 1963). This conventional approach was not meant to prevent reflective cracking from occurring, but rather to delay the appearance of cracks in the surface with a thicker overlay. In addition, Nam et al. (2014) mentioned that the MCDM analysis requires important details for accurate evaluation, which are often not available. Thus, moving forward with these recommendations without further investigation and proven performance appeared to be risky at this point in time.

Based on an extensive literature review, two treatments that are less expensive than a geotextile system were identified as alternatives to the ARMI interlayer. The first one uses a fracture-tolerant interlayer, which is a thin HMA interlayer of fairly small aggregate particles mixed with a high percentage of polymer-modified asphalt (PMA) binder. The design of these interlayer mixtures is based on the idea that higher asphalt content results in mixtures with higher fracture resistance. Lower compaction effort and reduced design air void content were used to achieve higher asphalt content. Compared to specialty systems such as geosynthetics, this treatment involves fairly conventional construction techniques, making it easier to install and more economical. The second treatment involves SMA mixtures, which belong to the category of gap-graded mixtures. Gap-grading is used to achieve stone-on-stone contact to maximize resistance to permanent deformation, which has been shown to be a problem associated with the ARMI. SMA is also known to provide enhanced cracking resistance.

However, both treatments have posed challenges. In the case of fracture-tolerant interlayer mixtures, higher asphalt content does not necessarily enhance fracture tolerance and may reduce shear resistance. Finer gradation results in higher asphalt content, but also makes the mixture stiffer and more brittle, which may actually result in less fracture-tolerant mixtures. In addition,

finer gradation may result in poor shear resistance. The characteristic stone-on-stone design of gap-graded mixtures requires strong aggregate, so a weak aggregate such as Florida limestone may not be suitable. Furthermore, gap-grading requires both additional asphalt binder and fibers, which results in higher cost and potential construction issues. Therefore, there is a need to design a more suitable interlayer system to mitigate near-surface reflective cracking in overlays on flexible pavements.

1.2 Objectives

The primary objective of this research was to develop guidelines for an effective alternative to ARMI for mitigation of near-surface reflective cracking in overlays on asphalt pavement that is less expensive than a geotextile system. Detailed objectives are as follows:

- Identify key mixture characteristics that provide high fracture tolerance and shear resistance;
- Refine a test device and loading procedure to more consistently evaluate reflective cracking performance of interlayer mixtures; and
- Develop preliminary design guidelines for fracture-tolerant and shear-resistant interlayer (FTSR) systems for mitigation of near-surface reflective cracking in overlays on asphalt pavement.

1.3 Scope

In order to meet the objectives of this research, it was necessary to evaluate a range of mixtures designed according to the key characteristics identified to provide high fracture tolerance and shear resistance for mitigation of near-surface reflective cracking. Two laboratory tests were selected for purposes of this study: the composite specimen interface cracking (CSIC) test for evaluation of reflective cracking performance of interlayer systems, and the asphalt pavement analyzer (APA) test for evaluation of rutting performance of interlayer mixtures.

Three aggregate types widely used in the state of Florida were employed to produce interlayer mixtures for laboratory testing: Georgia granite, Nova Scotia granite, and Florida limestone. Two polymer-modified asphalt (PMA) binders that have been shown to improve mixture cracking and rutting performance were used: a performance-grade (PG) 76-22 PMA, and a PG 76-22 high polymer (HP) asphalt binder. Based on discussion with the FDOT research panel, two nominal maximum aggregate sizes, 9.5-mm and 4.75-mm, in combination with three interlayer thicknesses were selected for interlayer system evaluation as described below:

- 0.5-in and 0.75-in for 4.75-mm mixtures
- 0.75-in and 1.0-in for 9.5-mm mixtures

A 12.5-mm dense-graded granite asphalt mixture commonly employed by the FDOT as a structural layer was used to produce a 1.5-in overlay for the composite specimens to be evaluated using the CSIC test. The asphalt binder used for the overlay mixture was PG 67-22 at an asphalt content of 4.8%.

1.4 Research Approach

This study primarily focused on developing preliminary design guidelines for FTSR interlayer mixtures to mitigate near-surface reflective cracking. The overall approach used to meet the objectives of this project involved the following steps:

- Review available literature to achieve better understanding of reflective cracking mechanisms in overlays on asphalt pavement, to identify promising treatments to mitigate reflective cracking, and to define key mixture characteristics that provide high fracture tolerance and shear resistance.
- Design a range of interlayer mixtures according to the key characteristics identified for mitigation of near-surface reflective cracking, including higher asphalt content obtained through lower compaction effort and reduced design air voids, and sufficient gradation coarseness achieved following the dominant aggregate size range-interstitial component (DASR-IC) model for design and modification of mixture gradation.

- Enhance the composite specimen interface cracking (CSIC) test for more consistent and more efficient evaluation of reflective cracking performance of interlayer mixtures, including a more efficient specimen preparation procedure, a more repeatable loading device, and a loading and data interpretation procedure to achieve more relevant results in less time.
- Perform CSIC tests to evaluate reflective cracking performance of interlayer systems and conduct APA tests to determine whether the interlayer mixtures have sufficient rutting resistance.
- Develop preliminary design guidelines for FTSR interlayer mixtures based on thorough evaluation and analysis of the test results.

CHAPTER 2
MECHANISMS AND MITIGATION TREATMENTS

Reflective cracking has been reported to occur in overlays on both Portland cement concrete (PCC) and asphalt pavements. Generally, overlays on rigid pavements show more severe reflective cracking compared to those on flexible pavements due to larger differential movements underneath the overlay (Mukhtar & Dempsey, 1996). This chapter provides a description of reflective cracking mechanisms and an introduction of reflective cracking treatments available in the literature. More detailed information on findings obtained from the literature review is presented in Appendix A.

2.1 Reflective Cracking Mechanisms

When hot mix asphalt (HMA) overlay is placed on distressed flexible or rigid pavement, it is only a matter of time before cracks in existing pavement reflect to the new overlay surface (Chen et al., 2013). The development of reflective cracking may take several years or few months after rehabilitation. Once reflective cracking reaches the surface (Figure 2-1), it creates a path through the pavement structure allowing water to enter. If action is not taken rapidly, pavement conditions may deteriorate, resulting in even more severe damage (Ghauch & Abou-Jaoude, 2013).

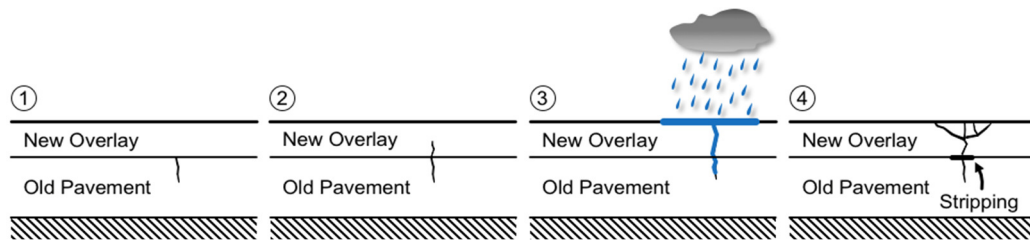


Figure 2-1. Reflective cracking in asphalt overlays.

Reflective cracking is caused by stresses concentrated by localized discontinuities or cracks remaining underneath the overlay. This type of distress is typically considered a fatigue phenomenon under repeated load (Lea and Harvey, 2004, Wu, 2005). The stresses induced by repeated wheel load and/or temperature variation have magnitudes below the ultimate tensile

strength. The application of repeated loading triggers a progressive and localized weakening process that leads to material failure (Luther et al., 1976). There are generally two major mechanisms: horizontal differential movements due to temperature changes and/or bending due to moving wheel loading, and vertical differential movements across cracks due to moving wheel loading. Because of the bond between the existing pavement and the overlay, horizontal movements induce tensile stresses in the overlay, which lead to cracks that initiate at the bottom of the overlay and propagate upward. The shear stresses from vertical movements also lead to crack initiation and propagation in the overlay.

Typically, two failure modes are associated with the aforementioned mechanisms: Mode I (or opening mode) due to horizontal tensile stresses induced by bending or horizontal-differential movements (Figure 2-2(a)), and Mode II (or in-plane shear mode) controlled by shear stresses caused by differential vertical movements (Figure 2-2(b)). Wu et al. (2005) showed that failure mode, development rate, and severity of reflective cracking depend on the magnitude of these stresses, which are mainly affected by pavement stiffness, load transfer (primarily controlled by spacing and length of the crack), and base conditions.

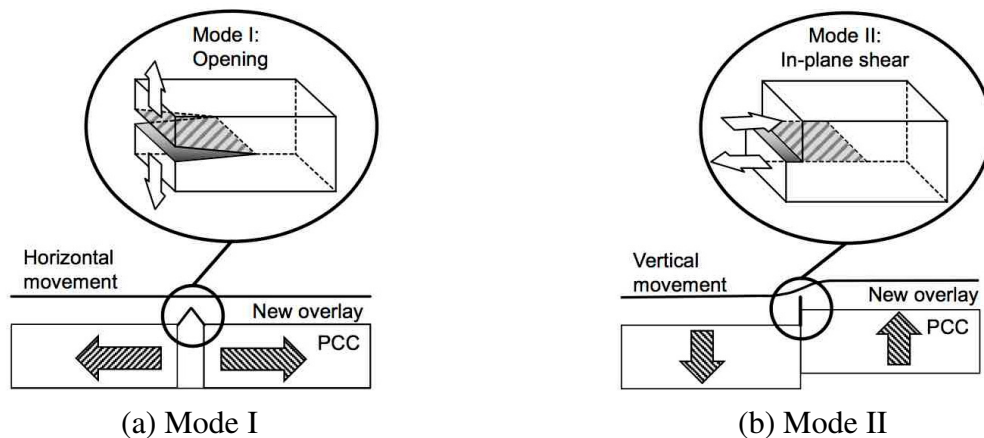


Figure 2-2. Typical failure modes associated with reflective cracking.

In Florida, top-down cracking is the most common distress in asphalt pavements due for rehabilitation (Roque et al., 2011). Top-down cracks typically have a wider opening near the surface and get narrower with depth. Although in a few cases top-down cracks have been

observed to propagate through the entire asphalt layer, most cracks generally stop at around mid-depth of the asphalt layer. Therefore, milling is commonly used to remove deteriorated asphalt pavements before placement of overlay. However, standard milling may not remove the existing cracks completely (Nam et al., 2014). As compared to a full-depth crack, a localized crack remaining in the milled asphalt pavement does not completely eliminate the integrity of the pavement structure (Figure 2-3(a)). The partial structural continuity allows load transfer near the localized crack and reduces shear stresses in the overlay right above the crack, indicating low potential for mode II failure. However, this partial structural continuity in conjunction with the relatively low stiffness of the underlying asphalt layer renders mode I failure to be the primary mechanism for reflective cracking.

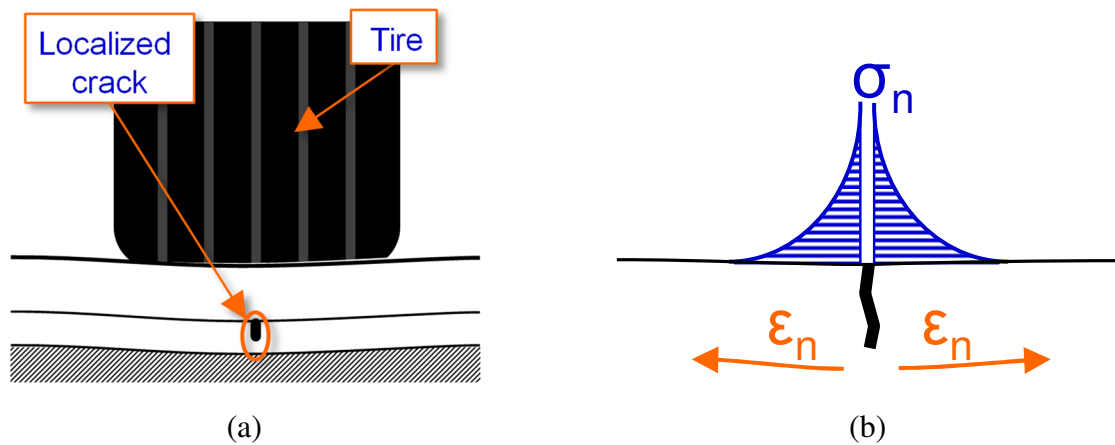


Figure 2-3. Typical failure modes associated with reflective cracking.

As shown in Figure 2-3(b), bending occurs when the wheel load moves over the pavement section, which tends to open the partial crack. Since existing pavement and overlay are bonded, this movement induces intensified tensile stresses in the overlay immediately above the crack normal to the plane of the discontinuity. Under repeated loading condition, cracks in the existing pavement may propagate and reflect in the surface of the overlay. In other words, partial cracks in combination with moving wheel load is the primary source of reflective cracking in overlay on milled asphalt pavement in Florida. It should be noted that longitudinal top-down cracks in asphalt pavement are typically located in the wheel path and relatively close to each other. So, the amount of relative thermal movement that may occur between the asphalt overlay and the

milled flexible pavement is very limited, especially in a warm climate. Consequently, the thermal stresses induced in the overlay right above the crack are negligible.

2.2 Mitigation Treatments

Starting from the early 1950s, numerous materials and methods have been used to mitigate reflective cracking with varying degrees of success. Generally, mitigation treatments for reflective cracking can be classified into four categories shown in Table 2-1, including existing asphalt surface modification, overlay layer/mixture modification, overlay reinforcement, and stress or strain relieving interlayers.

Table 2-1. Possible reflective cracking treatments (adapted from Von Quintus et al., 2009).

| |
|--|
| 1. EXISTING ASPHALT SURFACE MODIFICATION |
| <ul style="list-style-type: none"> - <i>Milling and replacing asphalt surface</i> - <i>Hot-in-place recycling (HIPR)</i> - <i>Full-depth reclamation (FDR)</i> |
| 2. OVERLAY LAYER/MIXTURE MODIFICATION |
| <ul style="list-style-type: none"> - <i>Thick asphalt overlays</i> - <i>Modified asphalt and specialty mixtures</i> |
| 3. OVERLAY REINFORCEMENT |
| <ul style="list-style-type: none"> - <i>Geosynthetics (reinforced geotextiles, geogrids, or geocomposites)</i> - <i>Steel mesh</i> |
| 4. STRESS OR STRAIN RELIEVING INTERLAYERS |
| <ul style="list-style-type: none"> - <i>Crack relief layer (CRL)</i> - <i>Stress absorbing membrane interlayer (SAMI)</i> <ul style="list-style-type: none"> ○ <i>Non-woven geotextile</i> ○ <i>Interlayer stress absorbing composite (ISAC)</i> ○ <i>Asphalt rubber membrane interlayer (ARMI)</i> ○ <i>Fracture-tolerant interlayer</i> |

2.2.1 Existing Asphalt Surface Modification

Modification of the existing asphalt surface is aimed at removing cracks in the existing pavement prior to placement of a new asphalt overlay. This category mainly includes three methods: milling and replacing, hot-in-place recycling (HIPR), and full-depth reclamation (FDR). As mentioned earlier, milling and replacing is the most suitable method for Florida pavement conditions, where cracks are confined to the surface or upper asphalt layers. However, this method may not completely remove the discontinuities. Therefore, it needs to be used in combination with other mitigation techniques (Von Quintus et al., 2009).

2.2.2 Overlay Layer/Mixture Modification

This category includes two main methods: thick asphalt overlay and modified asphalt and specialty mixtures. Increasing overlay thickness has been found to be the least cost-effective technique to delay reflective cracking (Von Quintus et al., 2009). The general "rule of thumb" states that reflective cracking propagates at a rate of one inch per year (Penman and Hook, 2008). Mixture modification such as gap-grading can improve reflective cracking performance by enhancing the fracture resistance of the overlay (Chen et al., 2005; Lu & Harvey, 2012). This method does help reduce the severity of reflective cracks, however, it does not prevent reflective cracking from occurring (Von Quintus et al., 2009).

2.2.3 Overlay Reinforcement

Reinforcement of asphalt overlays are generally composed of geosynthetics (e.g., reinforced geotextiles and geogrids) and steel, which are used to increase the tensile resistance of the overlay. Methods in this category do not prevent reflective cracking from occurring when large differential vertical movement exists, but help hold the cracks tightly together. It is important to note that a minimum overlay thickness is typically recommended for these treatments to ensure reinforcement works in tension. For instance, the Federal Aviation Administration (2006) recommends not using reinforcement if the overlay thickness is less than three inches. Therefore,

in addition to the higher cost of the reinforcing materials relative to materials used in the other categories, the minimum thickness requirement itself appeared to have a negative impact on the cost-effectiveness of these treatments (Buttlar et al., 2000, Maurer & Malasheskie, 1989).

2.2.4 Stress or Strain Relieving Interlayers

Stress or strain relieving interlayers are relatively low-stiffness systems that dissipate energy by deforming horizontally and/or vertically. Two subcategories are included: crack relief layer (CRL) and stress absorbing membrane interlayer (SAMI).

2.2.4.1 Crack Relief Layer

A crack relief layer (CRL) can be defined as an interlayer that is greater than three inches in thickness, which can consist of open-graded asphalt mixture with large aggregate or an unbound base material. This layer absorbs or dissipates horizontal movements and differential vertical deflections developed at discontinuities in the existing pavement. However, due to the large air voids and the relatively high layer thickness, the crack relief layer has a potential of acting as a water conduit or reservoir between the overlay and the underlying pavement (Von Quintus et al., 2009).

2.2.4.2 Stress Absorbing Membrane Interlayer

A stress absorbing membrane interlayer (SAMI) consists of a layer of material with relatively low-stiffness installed between the existing pavement and the new overlay. SAMI is thinner than the CRL and able to deform horizontally without breakage, allowing the stress induced by horizontal movement at the discontinuity to dissipate before reaching the overlay. This subcategory includes the following systems:

- Non-woven geotextile. This system has high elongation and low stiffness, which provide high strain tolerance. However, in addition to high cost, special care needs to be taken during installation to avoid the formation of wrinkles and overlaps in the fabric

(additional source of reflective cracking). Tack coat application is another issue. Insufficient tack coat may induce debonding, whereas excessive tack coat may cause slippage (Barazone, 1990, 2000).

- Interlayer stress-absorbing composite (ISAC). The ISAC was designed to relieve stress intensity at the crack-tip and simultaneously provide reinforcement to the overlay. It consists of a low stiffness geotextile as the bottom layer, a viscoelastic membrane layer as the core, and a very high stiffness geotextile as the surface layer. In essence, it is a composite that combines the benefits of geotextile and stress-absorbing interlayer. High cost and potential installation difficulties are the main issues associated with this system (Von Quintus et al., 2009).
- Asphalt rubber membrane interlayer (ARMI). The ARMI is constructed of a single application of a No.6 stone seated into a layer of asphalt rubber binder (ARB). A minimum initial overlay thickness of 1.5-in is required to provide sufficient heat to properly bond the ARMI with the overlay (Greene et al., 2012). The ARMI has been the primary reflective cracking mitigation technique used by the FDOT since the early 1990s. However, recent studies showed the system did not effectively mitigate reflective cracking when placed near the surface and it increased instability rutting potential (Chen et al., 2013, Greene et al., 2012).
- Fracture-tolerant interlayer. This system involves a thin layer of asphalt mixture composed of fairly small aggregates and rich polymer-modified asphalt (PMA) binder. This composition results in higher fracture tolerance than that of conventional mixtures. Strata reflective cracking relief interlayer, a proprietary product designed to dissipate tensile stress and strain under horizontal movements, is one example of the system (Blankenship et al., 2004). Recently, 9.5-mm NMA crack attenuating mixture (CAM) and 4.75-mm NMA binder-rich intermediate course (BRIC) mixture were added to this category (Scullion, 2010, Bennert et al., 2011). Generally, the fracture-tolerant interlayer system has shown promise in terms of its effectiveness to control reflective cracking, but

shear resistance of the system remains the concern (Baek & Al-Qadi, 2011; Elseifi & Dhaka, 2015).

2.3 Concluding Remarks

Reflective cracking in Florida generally occurs in overlay on relatively sound asphalt pavement with remaining partial top-down cracks. This distress is mainly induced by traffic load and is limited to mode I failure. Therefore, systems that are aimed at mitigating large shear and horizontal movements associated with more aggressive reflective cracking, such as reinforced overlays on PCC, are not required. The fracture-tolerant interlayer and stone matrix asphalt (SMA) mixtures appear to be potential candidates to mitigate reflective cracking in Florida. Promising results have been reported in terms of their effectiveness to control reflective cracking (Baek & Al-Qadi, 2011, Smit et al., 2011, Lu & Harvey, 2012).

- As compared to specialty systems such as geotextiles that are known to have installation difficulties, the fracture-tolerant interlayer system involves fairly conventional construction techniques that make them easy to install and more economical.
- SMA is known to provide improved cracking resistance. Furthermore, it is designed to achieve stone-on-stone contact to resist instability rutting, which is a problem associated with ARMI.

However, both treatments have posed challenges. In the case of fracture-tolerant interlayer mixtures, higher asphalt content does not necessarily enhance fracture-tolerance and may reduce shear resistance. Finer gradation results in higher asphalt content, but also makes the mixture stiffer and more brittle, which may actually result in less fracture-tolerant mixtures. In addition, finer gradation may result in poor shear resistance. The characteristic stone-on-stone design of gap-graded mixtures requires strong aggregate, so a relatively weak aggregate such as Florida limestone may not be suitable. Furthermore, gap-grading requires both additional asphalt binder and fibers, which results in higher cost and potential construction issues. Therefore, both treatments need to undergo a mix design optimization process to more effectively mitigate near-surface reflective cracking in overlays on asphalt pavement.

CHAPTER 3

DEVELOPMENT OF FRACTURE-TOLERANT SHEAR-RESISTANT INTERLAYER MIXTURES

The main purpose of this study was to develop guidelines for fracture-tolerant and shear-resistance (FTSR) interlayer mixtures to mitigate near-surface reflective cracking in overlays on asphalt pavement. Fourteen interlayer mixtures, covering a broad range of gradation, were designed based on the dominant aggregate size range – interstitial component (DASR-IC) model, which provides a framework for the design and modification of gradation to ensure sufficient aggregate interlock to resist permanent deformation as well as adequate cracking resistance. Two key mixture parameters from the DASR-IC model, DASR porosity and effective film thickness (EFT), were used to ensure the twelve designed dense-graded interlayer mixtures covered a broad range of gradation, including the finest and coarsest within the gradation bands used to define CAM and BRIC mixtures. In addition, two gap-graded mixtures were designed to achieve the highest coarseness with available stockpiles in Florida. According to the DASR-IC model, coarser gradation results in lower DASR porosity and higher EFT which enhance shear resistance and fracture tolerance.

3.1 Mix Design Methods

3.1.1 DASR-IC Model

As mentioned earlier, the DASR-IC model provides a framework for the design and modification of gradation to ensure sufficient aggregate interlock to resist permanent deformation as well as adequate durability and fracture resistance (Roque et al., 2011). According to this model, mixture behavior is dominated by two primary components:

- DASR, which is composed of the coarse aggregates that form the structural interactive network of aggregate to resist shear;

- IC, which is the combination of fine aggregates, binder, and air voids. This component fills the interstitial volume (IV) within the DASR and resists primarily tension and, to a lesser extent, shear.

DASR can be composed of one size or multiple contiguous sizes of coarse particles. The composition of DASR can be determined by conducting particle interaction analysis based on packing theory. Particles larger than DASR will simply float in the DASR matrix and will not play a major role in the aggregate structure. Particles finer than DASR fill the IV and do not interact with the coarser portion in properly designed mixtures (Kim et al., 2006). Figure 3-1 schematically illustrates these concepts.

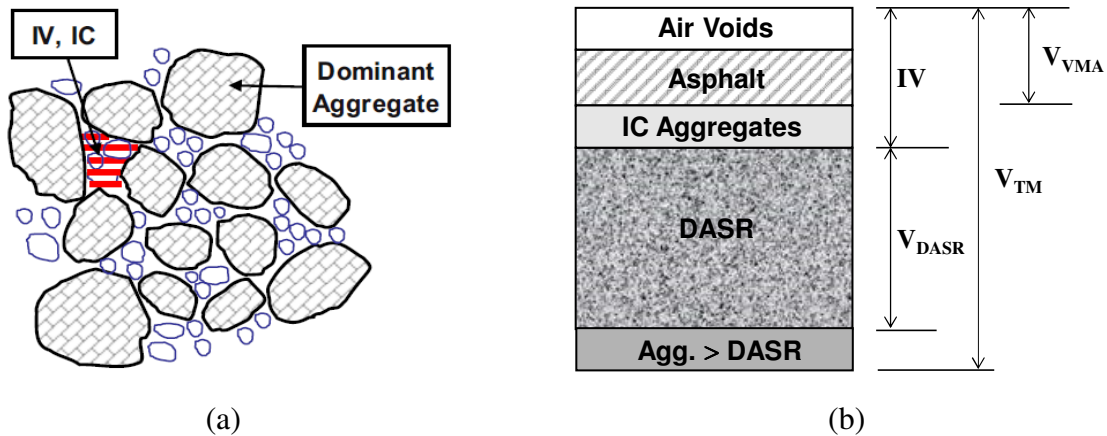


Figure 3-1. DASR-IC model: (a) Schematic representation; (b) Mixture components by volume.

Based on results of laboratory studies and long-term field evaluation of 9.5 to 12.5-mm structural course mixtures, three key parameters and associated criteria for potentially good mixture performance have been developed: DASR porosity (η_{DASR} : 38-48 percent), disruption factor (DF: 0.50-0.95), and effective film thickness (EFT: 12.5-25.0 μm). The DASR porosity criterion was used to ensure adequate interlocking to provide resistance to deformation and fracture.

DASR porosity can be calculated using the following equation:

$$\eta_{DASR} = \frac{V_{V(DASR)}}{V_{T(DASR)}} = \frac{V_{ICAGG} + V_{VMA}}{V_{TM} - V_{AGG(>DASR)}}$$

where, $V_{V(DASR)}$ is the volume of voids within DASR (i.e., IV), $V_{T(DASR)}$ is the total volume available for DASR particles, V_{ICAGG} is the volume of IC aggregates, V_{TM} is the total volume of mixture, and $V_{AGG(>DASR)}$ denotes volume of particles greater than DASR (Figure 3-1(b)).

The DF criterion was developed to ensure that IC aggregates form a secondary structure in the IV to help resist deformation and fracture without disrupting the DASR structure (Guarin, et al., 2013). DF can be calculated using the equation below.

$$DF = \frac{\text{Volume of IC Particles in the potentially disruptive range (PDR)}}{\text{Volume of DASR packing voids}}$$

The volume of DASR packing voids is a function of void size and number of voids determined based on DASR void structure through three-dimensional packing analyses. Assuming a single-sized DASR, the void size is 0.732D for cubical packing and 0.414D for close hexagonal packing, where D denotes DASR particle size. IC particles that are greater than the DASR void size have the potential of disrupting the DASR structure. The size range of these IC particles was defined as the potentially disruptive range (PDR), which typically includes one single size below the DASR.

The EFT criterion was established to ensure adequate durability and fracture resistance of the mixture (Isola et al., 2014). EFT (μm) can be calculated using the following equation:

$$EFT = \frac{V_{be}}{SA_F \cdot M_{TM} \cdot \frac{P_{SF}}{100}} \times 10^3 = \frac{P_{be}}{SA_F \cdot G_b \cdot P_{SF}} \times 10^3$$

where, V_{be} is the volume of effective asphalt binder (cm^3), SA_F is the surface area per unit mass (m^2/kg) of fine particles passing 2.36-mm sieve size, M_{TM} is the total mass of mixture (g), P_{SF} is fine aggregate content, P_{be} is effective asphalt content, and G_b denotes specific gravity of asphalt binder.

3.1.2 Promising Treatments and Key Mixture Characteristics

Two existing systems were identified in the literature as potentially more effective alternatives to the ARMI: fracture-tolerant interlayer and stone matrix asphalt (SMA) interlayer. The fracture-tolerant interlayer system involves 9.5-mm nominal maximum aggregate size (NMAS) crack attenuating mixture (CAM) and 4.75-mm NMAS binder rich intermediate course (BRIC) mixture, which are dense-graded mixtures specially designed to allow for higher asphalt content for higher fracture tolerance. Lower compaction effort, reduced design air void content, and even finer gradation relative to the Superpave gradation band were used in these mixtures to achieve higher asphalt content. However, increasing asphalt content does not necessarily enhance fracture tolerance and may reduce shear resistance. Based on the experience of the UF research team, the distribution of asphalt in the mixture is as important as or even more important than the amount of asphalt (Roque et al., 2011). Table 3-1 presents key characteristics for CAM and BRIC mixtures (Scullion, 2010, Bennert et al., 2011).

Table 3-1. Key mixture characteristics.

| Parameter | CAM | BRIC | SMA |
|-------------------|------------|-----------|-----------|
| V_a (%) | 2 | 2 | 4 |
| N_d (gyration) | 50 | 50 | 75 or 100 |
| AC_{min} (%) | 7 | 7 | 6 |
| VMA_{min} (%) | 17 | 18 | 17 |
| Dust proportion | ≤ 1.4 | 0.6 – 1.2 | - |
| Draindown (% max) | - | 0.1 | 0.3 |

The optimum asphalt content of CAM or BRIC mixture is determined at 2.0 percent air voids (V_a) at a design number of gyrations (N_d) of 50 using the Superpave gyratory compactor (SGC). The minimum asphalt content (AC_{min}) is 7.0 percent for CAM designed with PG 76-22 binders. The minimum asphalt content of 7.0 percent is also required for BRIC mixture, for which the grade of asphalt binder is required to be at least a PG 70-28. Additional volumetric requirements in terms of minimum voids in mineral aggregate (VMA_{min}), dust proportion, and maximum draindown are also included in Table 3-1. More detailed information regarding CAM and BRIC interlayer mixtures are described elsewhere (Scullion, 2010, Bennert et al., 2011).

SMA mixture with a NMAS ranging from 4.75 to 25 mm belongs to the family of gap-graded mixtures, which are designed to achieve stone-on-stone contact for enhanced shear resistance (Cooley and Brown, 2003). Also, SMA is known to provide improved cracking resistance. However, characteristic stone-on-stone design requires strong aggregate. Furthermore, gap-grading requires both additional asphalt binder and the introduction of fibers, which may result in higher cost and potential construction issues. As shown in Table 3-1, the optimum asphalt content of SMA is chosen to produce 4.0 percent air voids at an N_d of 75 or 100 using the SGC. The minimum asphalt content is based on the combined bulk specific gravity of the aggregate used in the mix (NCHRP Report 673, 2011). A minimum asphalt content of 6.0 percent was selected for the materials used in this study to meet the minimum VMA of 17 percent at 4.0 percent air voids. Additional volumetric requirements in terms of dust proportion, and maximum draindown are also included in Table 3-1. More detailed information regarding SMA mixtures can be found elsewhere (Cooley & Brown, 2003, NCHRP Report 673, 2011).

3.1.3 Preliminary Mix Design Criteria for FTSR Interlayer Mixtures

FTSR interlayer mixtures were designed primarily based on the DASR-IC system. Specifically, it was hypothesized that better reflective cracking performance and shear resistance will be achieved for mixtures with lower DASR porosity and higher EFT. In addition, key mixture characteristics identified from two fracture-tolerant mixtures (i.e., CAM and BRIC mixture) and from SMA (Scullion, 2010, Bennert et al., 2011, Cooley & Brown, 2003, NCHRP Report 673) were considered in the course of developing preliminary mix design criteria for FTSR interlayer mixtures. Table 3-2 summarizes preliminary design requirements for FTSR interlayer mixtures.

As shown in Table 3-2, a maximum DASR porosity (η_{DASR}) of 50 percent was selected to ensure interlocking for adequate shear resistance, and a minimum EFT of 25 μm was selected for enhanced fracture tolerance for 9.5-mm dense-graded FTSR mixture. Also, this mixture type was required to have characteristics similar to the CAM (see Table 3-1). As for 4.75-mm dense-graded FTSR mixture, η_{DASR} was selected to be no greater than 60 percent for minimum shear resistance. EFT was selected to be no less than 20 μm for minimum fracture tolerance. In

addition, this mixture type was required to have characteristics similar to the BRIC mixture as listed in Table 3-1.

Table 3-2. Mix design requirements for dense-graded and gap-graded FTSR interlayer mixtures.

| Parameter | Dense-Graded FTSR | | Gap-Graded FTSR |
|--|-------------------|-----------|-----------------|
| | 9.5mm | 4.75 mm | 9.5 mm |
| $\eta_{DASRmax}$ (%) | 50 | 60 | 50 |
| EFT _{min} , (μm) | 25 | 20 | 25 |
| V _a (%) | 2 | 2 | 4 |
| N _d (gyration) | 50 | 50 | 50 |
| AC _{min} (%) | 7 | 7 | 6 |
| VMA _{min} , (%) | 17 | 18 | 17 |
| Dust proportion | ≤ 1.4 | 0.6 – 1.2 | – |
| Draindown (% max) | – | 0.1 | 0.3 |

As shown in Table 3-2, 9.5-mm gap-graded FTSR mixture was required to have a maximum η_{DASR} of 50 percent and a minimum EFT of 25 μm . Also, this mixture type was required to have characteristics similar to the SMA mixture as listed in the Table 3-1. The gap-graded mixtures were designed to achieve coarsely distributed asphalt and stone-on-stone contact (Cooley and Brown, 2003). Consequently, they should automatically satisfy the η_{DASR} and EFT criteria. It is important to note that an N_d of 50 (as opposed to 75 or 100) was selected for gap-graded interlayer mixtures based on a similar value used by others for interlayer mixtures (e.g., CAM and BRIC mixtures). These are not structural mixtures, but more intended for stress relief. Furthermore, gap-graded mixtures cannot be developed with the 4.75-mm stockpiles typically available in Florida.

3.2 Materials

Both granite and limestone aggregate types widely used in the state of Florida were employed to produce interlayer mixtures for laboratory testing, including Georgia granite, Nova Scotia granite, and Florida limestone. Two polymer-modified asphalt (PMA) binders that have been shown to improve mixture cracking and rutting performance were used: a performance-grade (PG) 76-22 PMA, and a PG 76-22 high polymer (HP) asphalt binder. Based on discussion with the FDOT research panel, three interlayer thicknesses in combination with two nominal maximum aggregate sizes were selected for interlayer system evaluation, i.e., 0.5-in and 0.75-in

for 4.75-mm mixtures, and 0.75-in and 1.0-in for 9.5-mm mixtures. Detailed information on aggregate stockpiles used for design of interlayer mixtures is included in Appendix B.

3.3 Mix Design Results

Mix design for interlayer mixtures was conducted in two phases. In Phase I, fourteen mixture gradations were developed for both dense-graded and gap-graded gradation types with stockpiles typically available in Florida and by referring to gradation bands found in the literature (Cooley & Brown, 2003, Scullion, 2010, Bennert et al., 2011). DASR-IC parameters were estimated based on VMA values assumed according to minimum VMA requirements. In Phase II, Rice tests were conducted to determine theoretical maximum specific gravity for each gradation and optimum asphalt content was obtained for the desired air void content at N_d . The final values for DASR-IC parameters were calculated based on measured volumetric properties. Results of mix design are summarized below.

3.3.1 Mixture Gradations

Gradations for three 9.5-mm dense-graded granite interlayer mixtures (9.5DC GGr, 9.5DI GGr, and 9.5DF GGr) and one 9.5-mm gap-graded granite mixture (9.5GG GGr) are shown in Figure 3-2, where D denotes dense-graded, GG denotes gap-graded, GGr denotes Georgia granite, and C, I, and F denote coarse, intermediate, and fine, respectively. Superpave 9.5-mm gradation band (SP 9.5), CAM gradation band and SMA gradation band (SMA 9.5) were also included for comparison. DASR porosity and EFT estimated based on assumed VMA values are presented in Table 3-3. A brief description of 9.5-mm interlayer mixtures is provided below:

- The 9.5DC GGr mixture with a η_{DASR} of 40.1 percent and an EFT of 38.1 μm satisfies the DASR-IC criteria. It was designed by minimizing η_{DASR} and maximizing EFT using stockpiles typically employed in Florida. The gradation of the mixture is within the Superpave gradation band, and it is slightly below the lower-bound of CAM gradation band (i.e., it is similar to coarse CAM mixtures).
- The 9.5 DF GGr mixture with a η_{DASR} of 50.5 percent and an EFT of 20.0 μm does not satisfy the DASR-IC criteria. It was designed by approaching as close as possible the

upper bound of CAM gradation band using available Florida stockpiles. The gradation of the mixture is within both Superpave and CAM gradation bands.

- The 9.5 DI GGr mixture with a η_{DASR} of 44.9 percent and an EFT of 27.4 μm satisfies the DASR-IC criteria. It was designed to introduce an intermediate gradation between the coarse and fine gradations to help identify the boundary of proper coarseness for use as a 9.5-mm FTSR interlayer mixture.
- The 9.5 GG GGr mixture has a gradation within the SMA gradation band, which is coarser than all three dense-graded mixtures. This mixture has the lowest η_{DASR} (36.6 percent) and the highest EFT (42.4 μm).

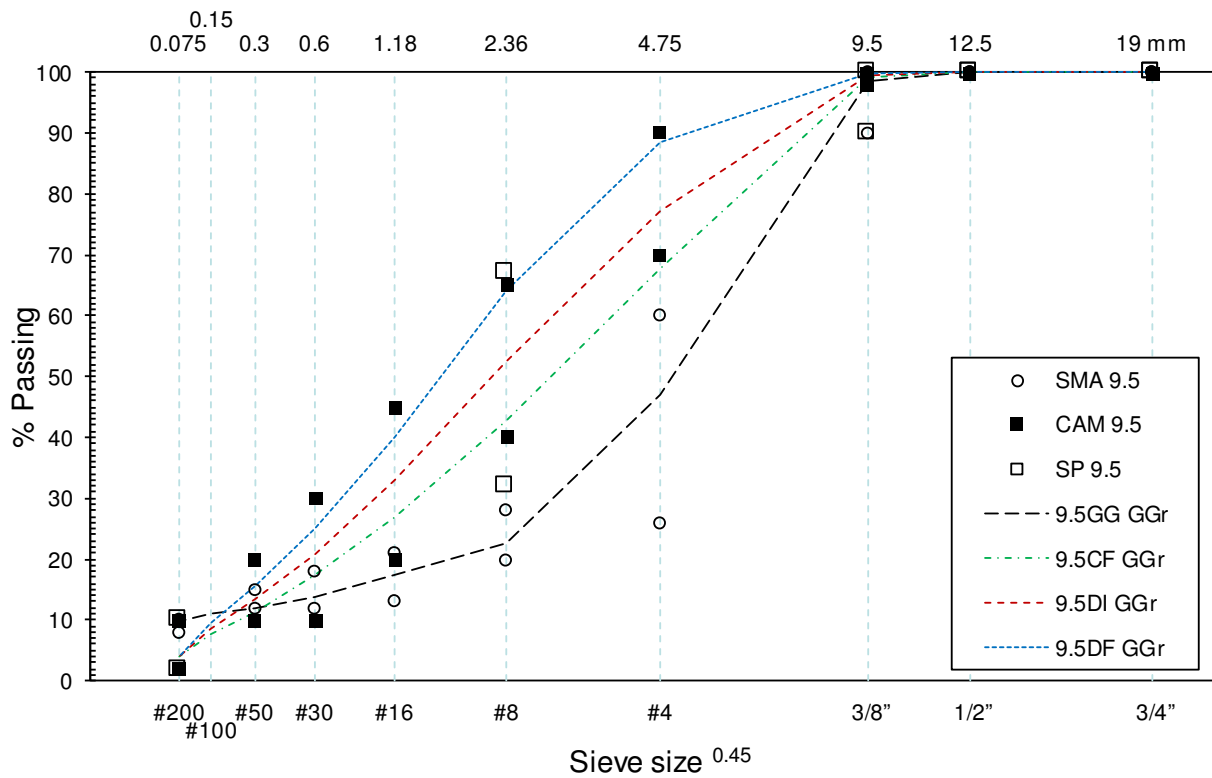


Figure 3-2. 9.5-mm NMAS granite mixture gradations.

Table 3-3. DASR porosity and EFT estimated for granite mixtures.

| Parameters | 9.5-mm NMAS | | | | 4.75-mm NMAS | | |
|-----------------------|-------------|------|------|------|--------------|------|------|
| | DF | DI | DC | GG | DF | DI | DC |
| η_{DASR} (%) | 50.5 | 44.9 | 40.1 | 36.6 | 74.4 | 62.1 | 56.0 |
| EFT (μm) | 20.0 | 27.4 | 38.1 | 42.4 | 8.2 | 13.1 | 22.9 |

Figure 3-3 presents gradations for three 4.75-mm dense-graded granite interlayer mixtures (4.75DC NGr, 4.75DI GGr, and 4.75DF GGr), where NGr denotes Nova Scotia granite. The Superpave 4.75-mm gradation band (SP 4.75) and the BRIC gradation band were also included for comparison. The estimated values for DASR porosity and EFT are shown in Table 3-3.

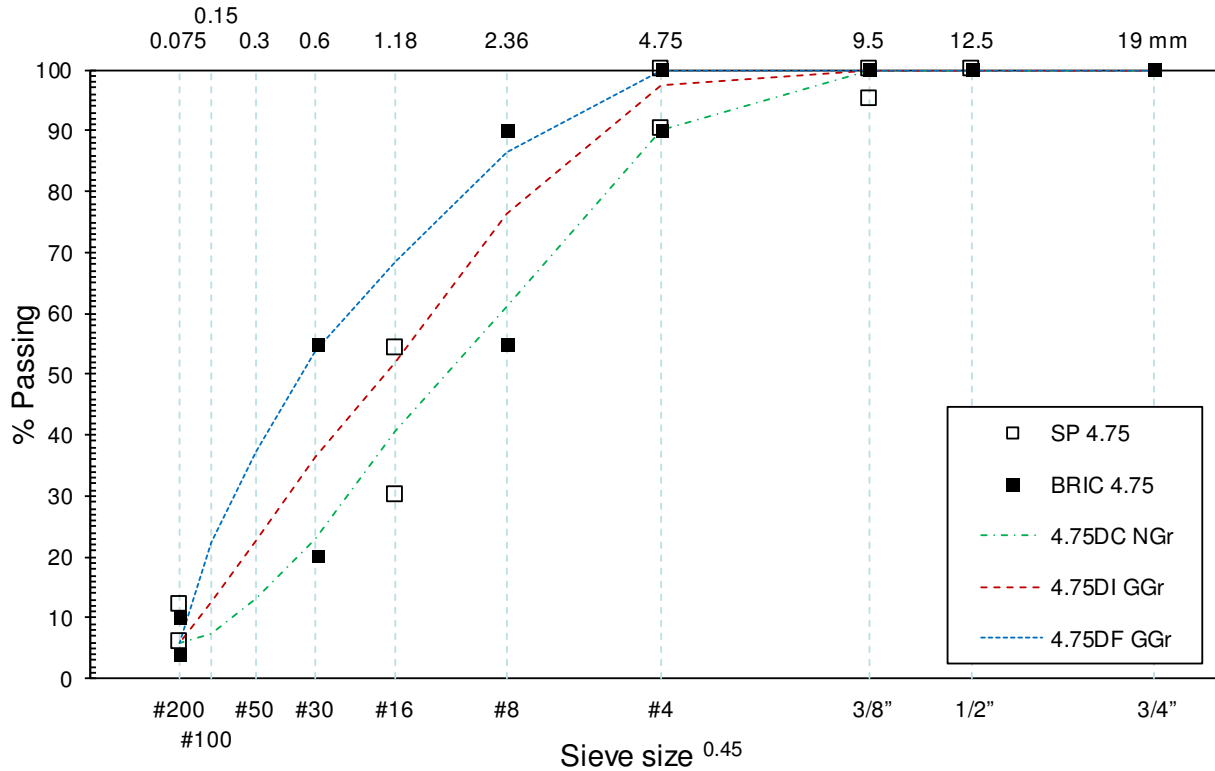


Figure 3-3. 4.75-mm NMAS granite mixture gradations.

A brief description of the 4.75-mm interlayer mixtures is provided below:

- The 4.75DC NGr mixture with a η_{DASR} of 56.0 percent and an EFT of 22.9 μm was designed by minimizing η_{DASR} and maximizing EFT using available stockpiles in Florida. It satisfies the DASR-IC criteria proposed for 4.75-mm FTSR interlayer mixtures (Table 3-2). The gradation of the mixture is within both Superpave and BRIC gradation bands.
- The 4.75DF GGr mixture with a η_{DASR} of 74.4 percent and an EFT of 8.2 μm was designed by approaching as close as possible the upper bound of BRIC gradation band. It does not satisfy the DASR-IC criteria. The gradation of the mixture is within BRIC gradation band, and it is above the upper bound of Superpave gradation band (i.e., it is finer than Superpave mixtures).

- The 4.75DI GGr mixture with a η_{DASR} of 62.1 percent and an EFT of 13.1 μm does not satisfy the DASR-IC criteria. It was designed to introduce an intermediate gradation to help identify the boundary of proper coarseness for use as a 4.75-mm FTSR interlayer mixture.

The limestone mixture gradations were designed following the same procedure adopted for developing granite mixture gradations using typical stockpiles available in Florida. For each NMAS, one dense-graded coarse (DC) mixture was designed by minimizing η_{DASR} porosity and maximizing EFT, one dense-graded fine (DF) mixture was designed by approaching as close as possible the upper bound of gradation band for existing fracture tolerant interlayer mixtures (i.e., CAM or BRIC), and one dense-graded intermediate (DI) mixture was introduced between the coarse and fine gradations. One gap-graded (GG) mixture was developed for 9.5-mm NMAS based on available Florida stockpiles. The 9.5-mm and 4.75-mm limestone mixture gradations are shown in Figure 3-4 and Figure 3-5, respectively. DASR porosity and EFT values estimated based on assumed VMA values for these mixtures are presented in Table 3-4.

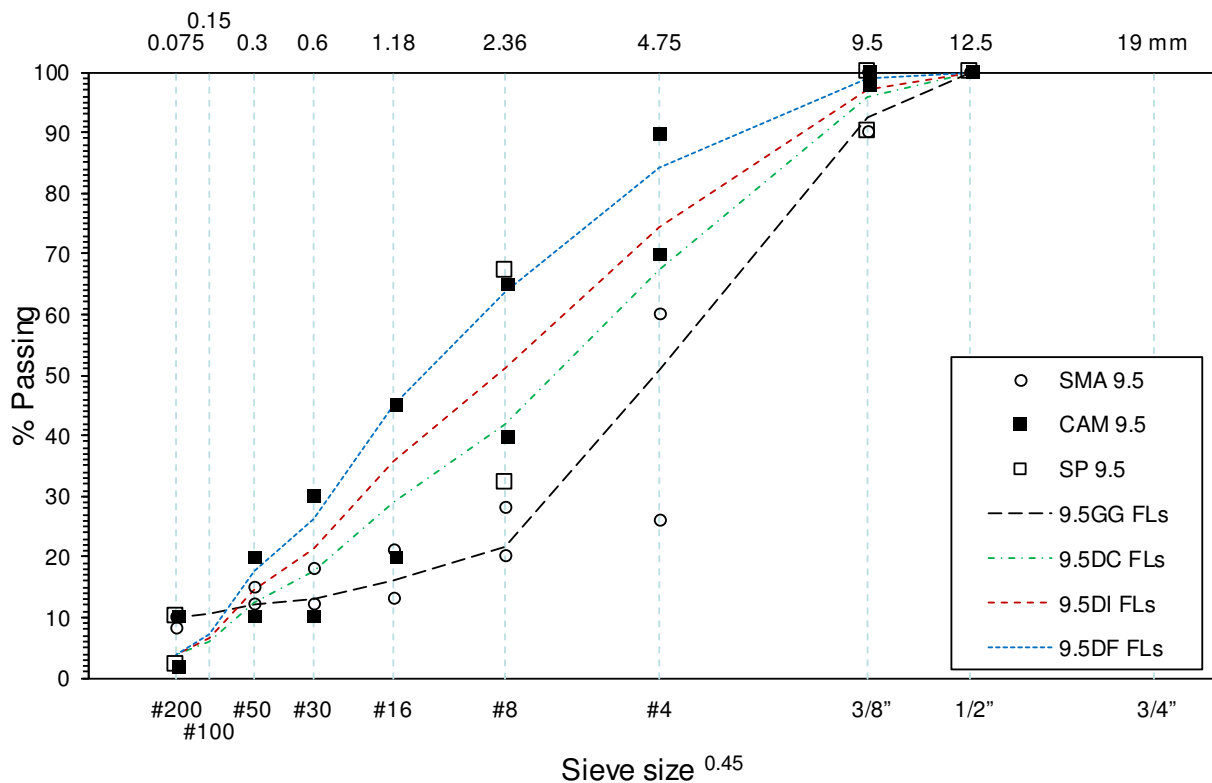


Figure 3-4. 9.5-mm NMAS limestone mixture gradations.

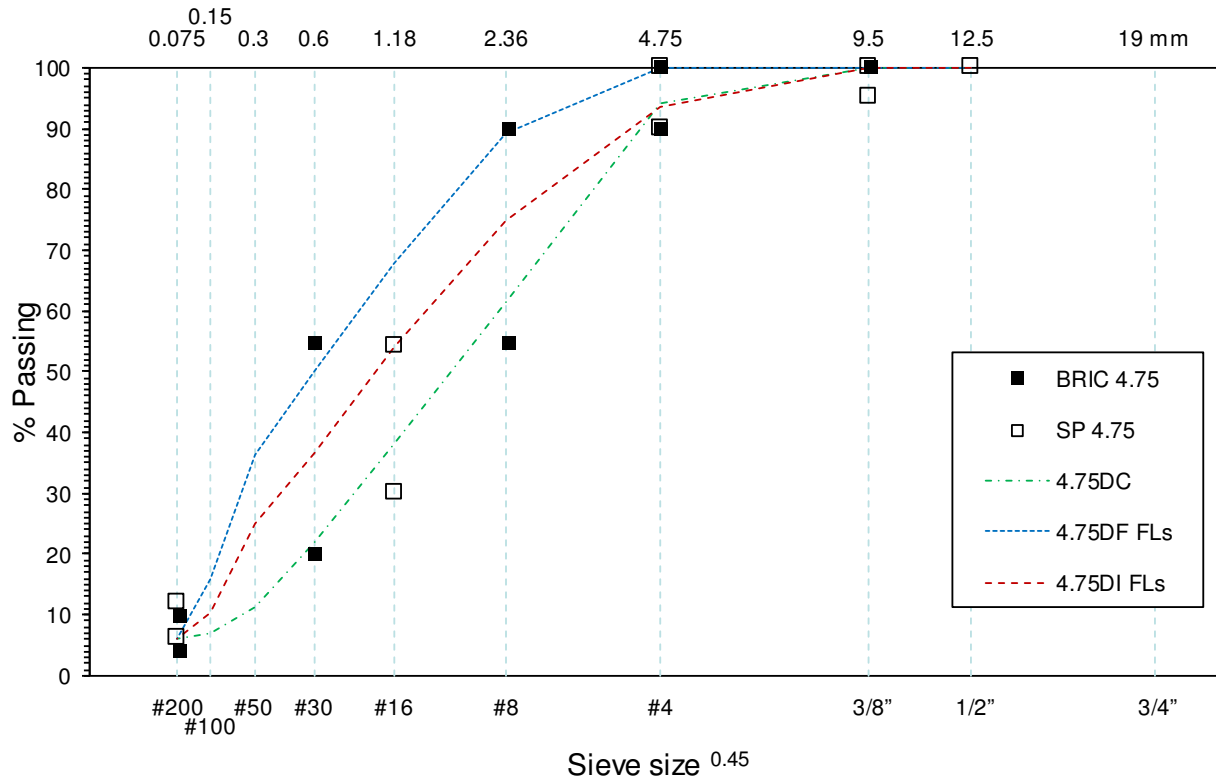


Figure 3-5. 4.75-mm NMAS limestone mixture gradations.

Table 3-4. DASR porosity and EFT estimated for limestone mixtures.

| Parameters | 9.5-mm NMAS | | | | 4.75-mm NMAS | | |
|-----------------------|-------------|------|------|------|--------------|------|------|
| | DF | DI | DC | GG | DF | DI | DC |
| η_{DASR} (%) | 54.2 | 47.1 | 41.8 | 36.5 | 73.3 | 65.3 | 51.3 |
| EFT (μm) | 20.0 | 28.9 | 39.7 | 45.2 | 8.6 | 13.2 | 24.0 |

For both granite and limestone mixtures, it appeared that the minimum DASR porosity and maximum EFT approach resulted in dense-graded gradations on the coarser side of the gradation bands for CAM and BRIC mixtures. In other words, not all CAM and BRIC mixtures may function properly as FTSR interlayer mixtures unless they satisfy the DASR-IC criteria. Complete gradations for all designed interlayer mixtures are included in Appendix C.

3.3.2 Volumetric Property and DASR-IC Parameters

Theoretical maximum specific gravity was determined for each interlayer mixture by conducting Rice tests on loose samples following the standard method (FM1-T209). Optimum asphalt content was obtained based on desired air void content (V_a) at the design number of gyrations (N_d) presented in Table 3-2. As shown in Table 3-5, the asphalt content (AC) and voids in mineral aggregate (VMA) were generally significantly higher than the minimum requirements specified for each mixture. As a result, the final EFT values calculated based on measured volumetric properties were generally greater than the estimates obtained based on assumed VMA values. The final η_{DASR} values were only slightly higher than the estimated values since the gradations remained the same for all interlayer mixtures.

Table 3-5. Volumetric properties and final DASR porosity and EFT values.

| Aggregate | Parameter | 9.5-mm NMAS | | | | 4.75-mm NMAS | | |
|-----------|-----------------------|-------------|-------|-------|-------|--------------|-------|-------|
| | | DF | DI | DC | GG | DF | DI | DC |
| Granite | AC (%) | 8.9 | 8.3 | 7.9 | 9.0 | 12.2 | 8.4 | 9.7 |
| | G_{mm} | 2.429 | 2.456 | 2.465 | 2.442 | 2.264 | 2.434 | 2.320 |
| | VMA | 20.7 | 19.4 | 18.9 | 22.5 | 28.7 | 19.6 | 21.4 |
| | η_{DASR} (%) | 52.5 | 46.3 | 41.1 | 40.5 | 77.6 | 62.6 | 57.7 |
| | EFT (μm) | 25.0 | 31.6 | 42.4 | 62.0 | 15.3 | 14.2 | 28.0 |
| Limestone | AC (%) | 9.8 | 9.1 | 8.9 | 9.7 | 11.5 | 9.6 | 12.0 |
| | G_{mm} | 2.242 | 2.251 | 2.244 | 2.193 | 2.225 | 2.265 | 2.185 |
| | VMA | 19.6 | 17.6 | 17.0 | 20.0 | 22.1 | 19.3 | 18.4 |
| | η_{DASR} (%) | 56.2 | 48.2 | 42.6 | 39.7 | 74.9 | 66.3 | 52.1 |
| | EFT (μm) | 26.3 | 33.0 | 43.1 | 63.4 | 12.3 | 15.6 | 26.7 |

CHAPTER 4

MIXTURE TESTS AND EXPERIMENTAL PLAN

A composite specimen interface cracking (CSIC) test developed in an earlier FDOT research project was enhanced with a new specimen preparation procedure, loading device, and loading procedure to more consistently evaluate reflective cracking performance of interlayer systems. In addition, asphalt pavement analyzer (APA) test was selected to determine whether the interlayer mixtures had sufficient rutting resistance. This chapter describes the enhanced CSIC test, the APA test, and the overall experimental plan for evaluation of interlayer mixture performance.

4.1 Composite Specimen Interface Cracking Test

The composite specimen interface cracking (CSIC) test was developed in an earlier FDOT research project (Roque et al., 2009) and successfully employed to evaluate the effects of interface condition characteristics as well as the effects of ARMI on pavement reflective cracking performance (Chen et al., 2013a, 2013b). This test simulates the propagation of existing cracks through the interlayer and into the HMA overlay under repeated load, so that reflective cracking performance of various interlayers can be properly evaluated. Detailed information regarding enhancement of the CSIC test is included in Appendix D. Specimen preparation, test, and data interpretation procedures used in this study are summarized below.

4.1.1 Specimen Preparation

A composite layer was prepared by compacting loose mixture to desired thickness on top of a layer of pre-compacted dense-graded mixture (representing the overlay) using the Superpave gyratory compactor (SGC). Two identical parts obtained from the composite layer were aligned and glued to a central metal spacer to form a symmetrical specimen for CSIC testing. Detailed steps used to prepare the CSIC specimen are described below.

4.1.1.1 Preparation of Composite Layers

Loose dense-graded overlay mixture was compacted to the desired thickness of 1.5 in at 7.0 percent air voids content (Figure 4-1(a)). For batching purposes, the weight of the overlay mixture ($W_{Overlay}$) was calculated using the following equation.

$$W_{Overlay} = \pi \cdot \frac{D^2}{4} \cdot h_{Overlay} \cdot G_{mm,Overlay} \cdot (1 - V_a/100)$$

where, D represents the diameter of the Superpave gyratory pill, $h_{Overlay}$ is the height of the overlay, $G_{mm,Overlay}$ is the theoretical maximum specific gravity of the overlay mixture, and V_a is the air void content.

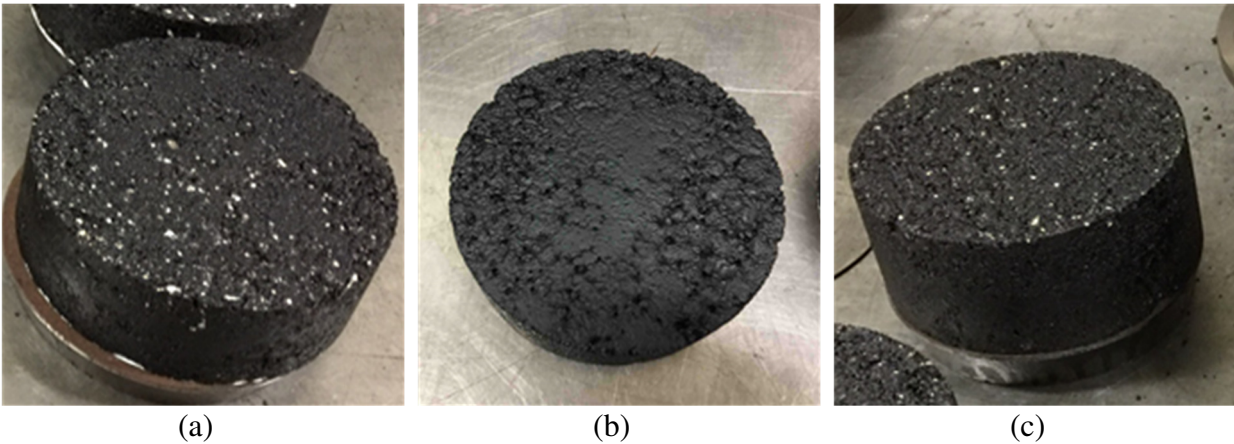


Figure 4-1. Preparation of composite layers: (a) Overlay compaction, (b) Tack coat application, and (c) Interlayer compaction on top of the thin tack coat.

Figure 4-1(b) shows a thin layer of trackless tack emulsion applied to the surface of the overlay at room temperature at a rate of 0.06 gallon/yd². The amount of trackless tack emulsion (W_{TE}) was calculated using the following equation.

$$W_{TE} = \pi \cdot \frac{D^2}{4} \cdot Application\ rate \cdot G_{TE} \cdot \frac{100}{Percent\ residual}$$

where, D denotes the diameter of Superpave gyratory pills, G_{TE} is the specific gravity of tack emulsion (1.0 according to specification), and percent residual is the remaining amount of tack emulsion after water evaporation (50 percent according to FDOT specification). In this study, the rate was determined to be 9.6 ml per 6-in diameter specimen. Once the tack emulsion was set, loose interlayer mixture was compacted on top of the tack coat to the desired thickness (i.e., 0.5-in and 0.75-in for 4.75-mm NMAS mixture, and 0.75-in and 1.0-in for 9.5-mm NMAS mixture) at the desired air void content (4 percent for dense-graded and 7 percent for gap-graded mixture). Figure 4-1(c) shows a completed composite layer.

4.1.1.2 Assembly of CSIC Composite Specimen

As shown in Figure 4-2(a), two central parts were obtained by cutting off the edges of the composite layer. The two parts were aligned and glued to a central metal spacer along the surface of the interlayer to produce a symmetrical CSIC specimen. Gauge points were installed 0.375 in above and below the interlayers with the aid of a positioning metal panel (Figure 4-2(b)), which led to the completed composite specimen for CSIC testing (Figure 4-2(c)).

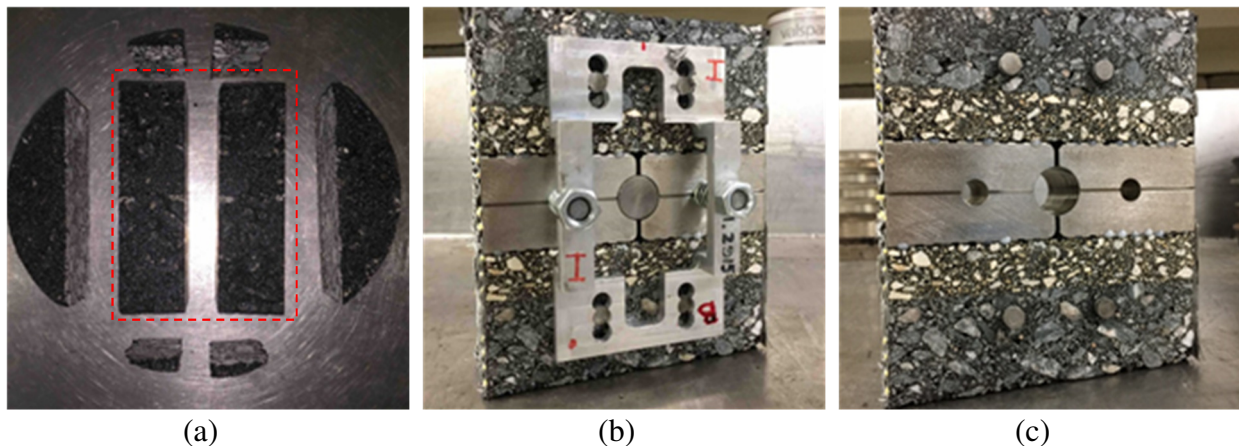


Figure 4-2. Assembly of CSIC composite specimen: (a) Cutting to obtain two symmetrical parts (plan view), (b) Two symmetrical parts aligned and glued to the central metal spacer, and (c) Complete CSIC specimen installed with gauge points.

4.1.2 CSIC Test Procedure

The CSIC test was conducted in an environmental chamber at 10°C using the MTS loading system. A composite specimen was placed into a loading device with specially designed loading yokes (Figure 4-3(a)-(b)). The loading device was connected to the MTS loading frame in the environmental chamber. Two extensometers were mounted at 1.5-in gauge-length on each face of the specimen (Figure 4-3(c)). The specimen was cooled to the test temperature of 10°C for at least three hours before testing. A seating load of 10 to 30 lb was applied to ensure proper contact between the specimen and the loading yokes.

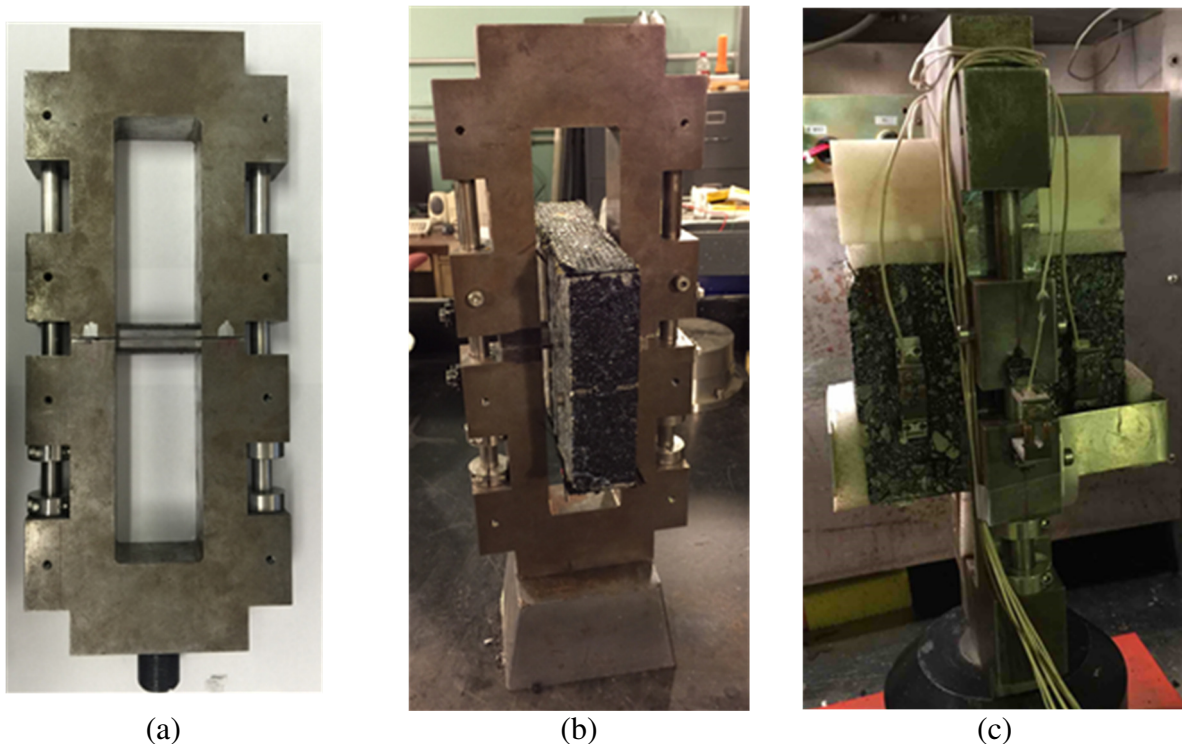


Figure 4-3. CSIC test setup: (a) Loading device, (b) Placement of CSIC specimen into the loading device, and (c) Connection of loading device to the MTS loading frame.

The specimen was loaded by applying a repeated haversine tensile load by way of two yokes placed inside the central hole of the specimen (Figure 4-4(a)). A repeated load consisting of 0.1 s loading and 0.9 s rest period was used. Figure 4-4(b) shows typical vertical deformation measured for two consecutive cycles by extensometers installed 0.375 in away from the

interlayer. Resilient deformation (δ_R) was determined as the difference between the total and permanent deformation for each cycle as shown in Figure 4-4(b).

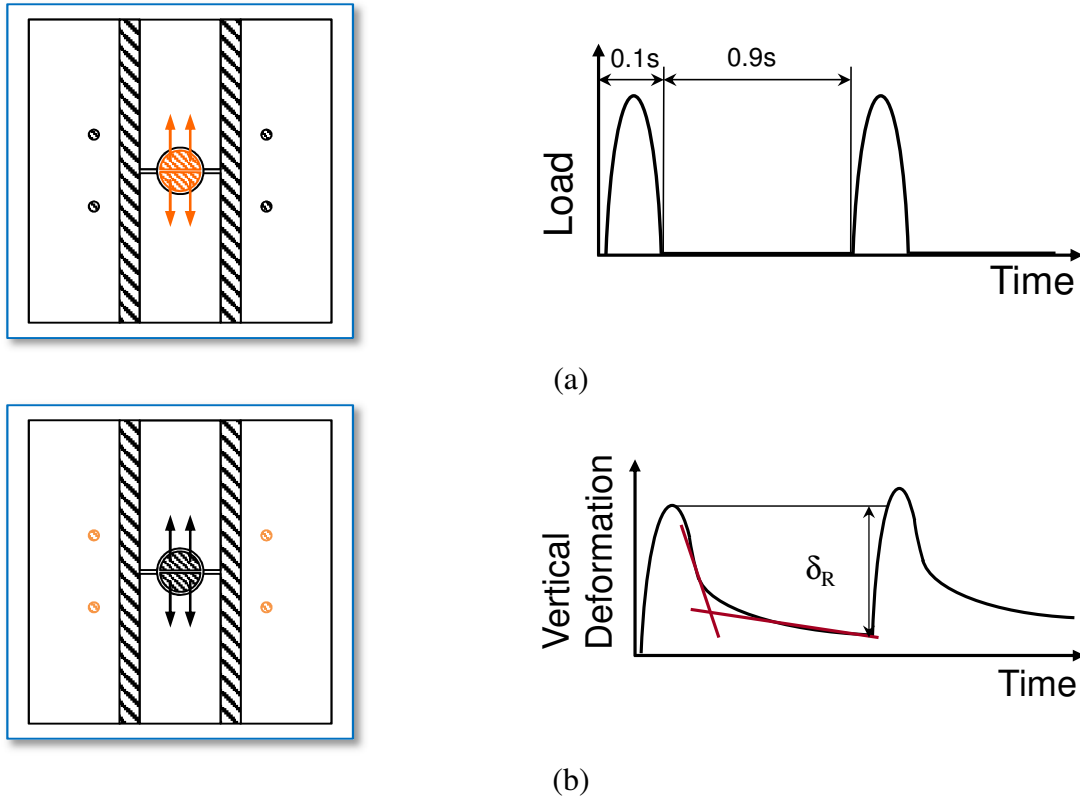


Figure 4-4. Repeated loading and response for two consecutive cycles: (a) Loading applied through two yolks, (b) Resilient deformation obtained at the extensometers.

Based on trial tests conducted on composite specimens with a range of interlayer mixtures, an amplitude sweep loading procedure was established with an initial load of 700 lb and a constant increment of 150 lb for every one hour of loading until specimen failure (Figure 4-5(a)). It was observed that almost no damage was induced to the specimen below the 700-lb load level. The constant load increment of 150 lb resulted in gradual accumulation of damage over a series of load levels. All specimens evaluated failed before reaching 1600 lb and the test duration was typically no greater than 6 hours (i.e., within one working day).

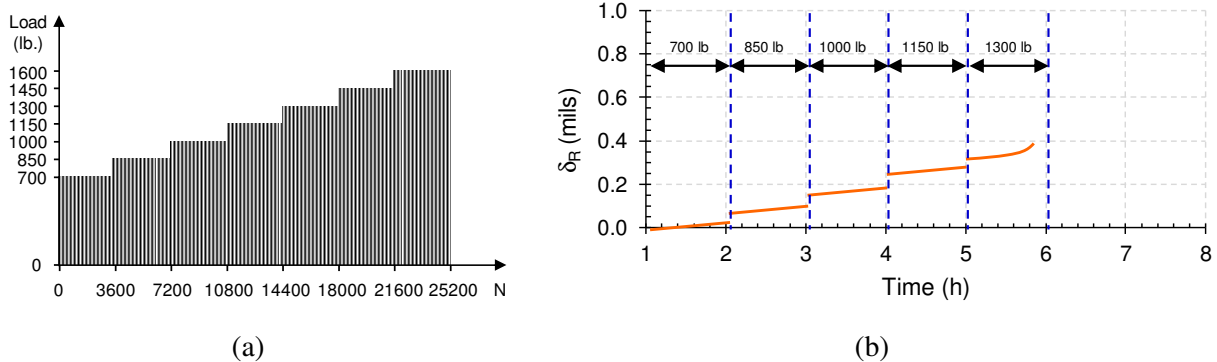


Figure 4-5. Typical load and response for reflective cracking performance evaluation: (a) Amplitude sweep loading, (b) Evolution of resilient deformation in the CSIC specimen.

4.1.3 Data Collection and Interpretation

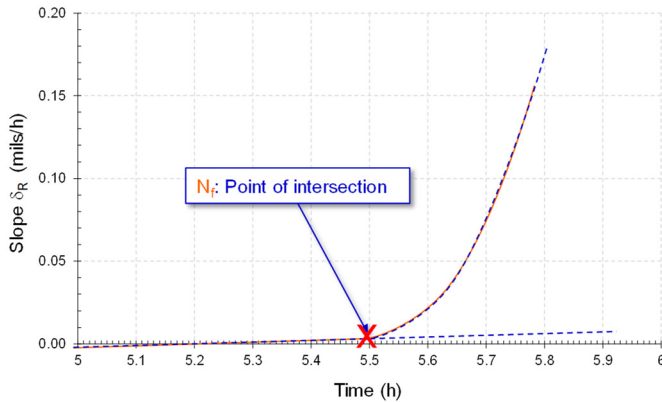
As mentioned earlier, the composite specimen was instrumented with four extensometers (two on each face) to obtain local deformation in the overlay 0.375 in away from the interlayer. In addition, the MTS measurement system was used to obtain global deformation and external load as a function of time. Test data were acquired every 200 seconds for four seconds at a rate of 512 data points per second, so a minimum of three complete loading cycles were recorded every 200 seconds.

Figure 4-5(b) shows evolution of averaged resilient deformation (average of the four gauges) in a composite specimen subjected to amplitude sweep loading until specimen failure. The number of cycles to failure (N_f) was obtained based on slope of resilient deformation calculated using the equation below for the last load level, during which the specimen failed.

$$\dot{\delta}_{R,i} = \frac{\delta_{R,i} - \delta_{R,i-1}}{t_i - t_{i-1}}$$

where, $\delta_{R,i}$, and $\delta_{R,i-1}$ are resilient deformation values at time t_i and t_{i-1} , respectively. The slope of resilient deformation generally remains unchanged for load levels before failure, then starts to increase rapidly under the load level when failure occurs. Figure 4-6(a) presents the approach taken to determine the number of cycles to failure (i.e., instant of specimen failure). The linear portion of the last load level data for slope of resilient deformation versus time was fitted using a

straight line, while the non-linear portion was fitted using a second-order polynomial. N_f was determined as the point of intersection for the two fitted curves. Figure 4-6(b) presents a cracked composite specimen after completion of the CSIC test.



(a)

(b)

Figure 4-6. Determination of specimen failure: (a) Slope of resilient deformation calculated for the last load level when the specimen failed, (b) A cracked composite specimen.

4.2 Asphalt Pavement Analyzer Test

4.2.1 Sample Preparation

Batched aggregate and asphalt binder were heated in the oven to mixing temperature (325°F for polymer modified asphalt binder) for approximately three hours. The materials were mixed until aggregate particles were completely coated with asphalt binder. The resulting loose mixture was kept in the oven for two hours and then compacted using the Superpave gyratory compactor (SGC) to the target air void content (i.e., 4 percent for dense-graded and 7 percent for gap-graded mixture). The compacted specimen was allowed to cool down for approximately five minutes before being extracted from the mold. The bulk specific gravity of each sample was measured in accordance with the AASHTO T 166 procedure to verify air void content.

4.2.2 APA Test Procedure

The APA test was conducted in the APA environmental control chamber at 64°C (AASHTO T 340). As shown in Figure 4-7(a), four specimens (replicates) were produced for each interlayer mixture and placed in two molds for testing. Every two specimens held in one mold was called one APA set, so two APA sets were tested simultaneously to evaluate rutting resistance of interlayer mixtures developed in this study. A load of 100 lb was applied through a concave steel wheel moving back and forth across a pressurized hose placed on top of each APA set (Figure 4-7(b)). The hose pressure was 100 psi. Each APA test was conducted for 8,000 cycles or until a rut depth of 14 mm (the machine limit value) was reached. Figure 4-7(c) shows a deformed sample after the APA test. A summary of the test procedure is provided below.

- Place APA specimens into the molds and preheat the APA sets in the oven at 64°C for at least 6 hours;
- Set the hose pressure to 100 psi and set the load cylinder pressure for each wheel to reach a load of 100 lb;
- Stabilize the APA environmental chamber at 64°C;
- Secure the preheated APA sets in the APA;
- Initialize the APA computer software and start the test;
- Save the rut-depth data file upon completion of the test.

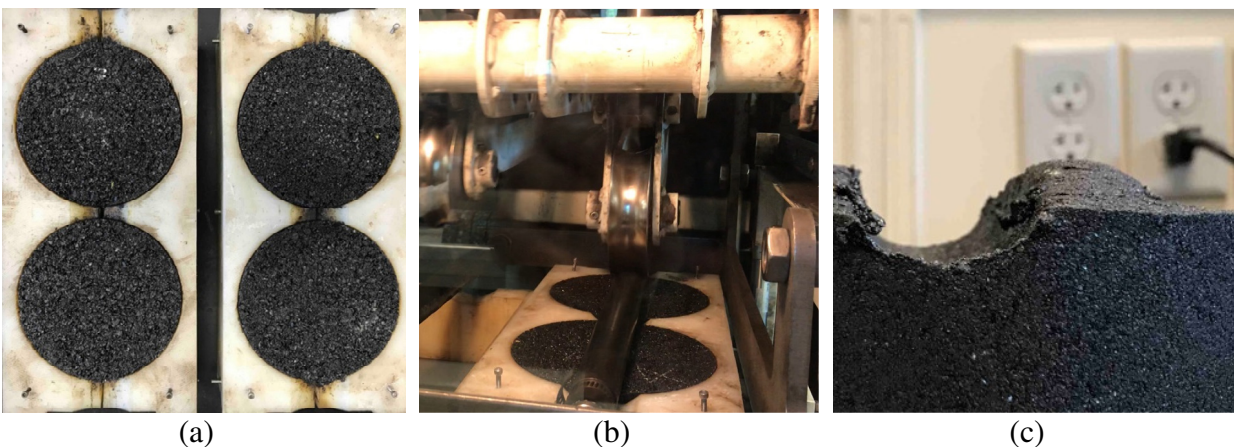


Figure 4-7. APA test procedure: (a) Two APA sets placed in the molds, (b) Steel wheel and pressurized hose to load each APA set, and (c) A deformed sample after APA test.

4.2.3 Data Collection and Interpretation

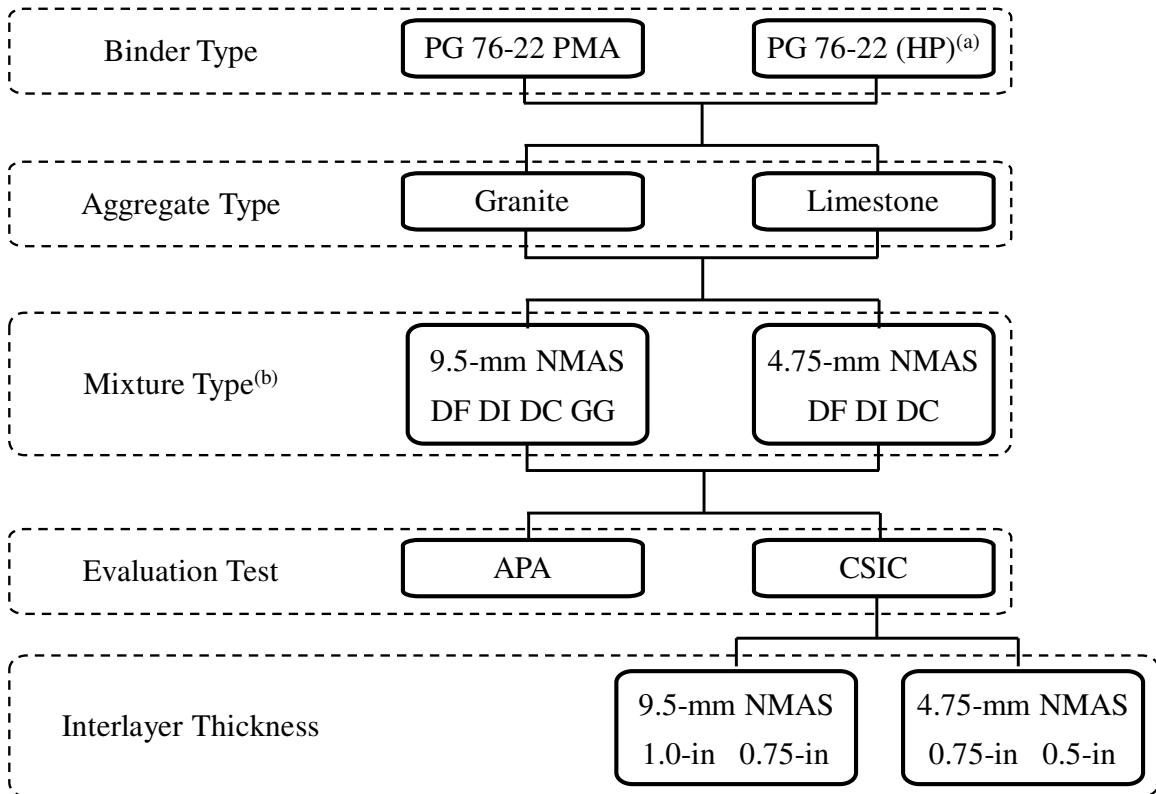
The rut depth of each APA set was recorded by the APA system as the average of permanent deformations measured at four locations along the wheel track. If permanent deformation at any location of one APA set reached 14 mm before the end of 8,000 cycles, the test was stopped and 14 mm was reported as the rut depth of the APA set. The average of rut depths from two APA sets was used as an indicator of interlayer mixture's resistance to rutting.

4.3 Experimental Plan

The experimental plan was developed with the main purpose of evaluating variables that could potentially influence reflective cracking performance of interlayer systems. As shown in Figure 4-8, both granite and limestone aggregates widely used in the state of Florida were employed to study the effect of aggregate on interlayer performance. According to the key mixture characteristics identified during the course of mix design, seven gradation types were selected to evaluate the impact of gradation on performance, including four (DF, DI, DC, and GG) associated with 9.5-mm nominal maximum aggregate size (NMAS) and three (DF, DI, DC) for 4.75-mm NMAS. DF, DI, DC, and GG denote dense-fine, dense-intermediate, dense-coarse, and gap-graded, respectively. The 4.75-mm GG mixture was not included in the experimental plan because it could not be developed with stockpiles typically used in Florida (Chapter 3). Two polymer-modified asphalt (PMA) binders, which have been shown to improve cracking and rutting performance of dense-graded structural mixtures were selected: a performance grade (PG) 76-22 PMA, and a PG 76-22 high polymer (HP) asphalt binder. It should be noted that the PG 76-22 HP binder was only used for mixtures that exhibited improved reflective cracking performance but did not meet the APA requirement.

Performance evaluation involved two types of mixture tests: CSIC test and APA test. The CSIC test was selected to evaluate the reflective cracking performance of the 14 interlayer mixtures designed. Based on discussion with the FDOT research panel, three interlayer thicknesses in

combination with two nominal aggregate sizes were selected for interlayer system evaluation, i.e., 0.5-in and 0.75-in for 4.75-mm mixtures, and 0.75-in and 1.0-in for 9.5-mm mixtures. APA test was employed to determine whether the interlayer mixtures had sufficient rutting resistance.



Note: ^(a) indicates that this binder type will only be used for mixtures that exhibited improved reflective cracking performance but did not meet the APA requirement. ^(b) DF, DI, DC, and GG denote dense-graded fine, dense-graded intermediate, dense-graded coarse, and gap-graded, respectively.

Figure 4-8. Overall experimental plan.

CHAPTER 5

TEST RESULTS AND ANALYSIS

5.1 Introduction

According to the experimental plan presented in Chapter 4, a total of fourteen interlayer mixtures were evaluated using the composite specimen interface cracking (CSIC) and the asphalt pavement analyzer (APA) tests. Thirty-three sets of CSIC tests were conducted at 10°C for evaluation of reflective cracking resistance, including: i) twenty-eight sets for interlayer mixtures (two aggregate types, seven gradations, and two interlayer thickness levels) with PG 76-22 asphalt binder; ii) three sets for control dense-graded mixtures (three interlayer thickness levels) with PG 67-22 binder; and iii) two additional sets for the 4.75-mm dense-coarse granite mixture (two interlayer thickness levels) with PG 76-22 high polymer (HP) binder. Since each set included three replicates, a total of ninety-nine specimens were prepared and tested using the CSIC test.

Fifteen sets of APA tests were performed at 64 °C for evaluation of rutting resistance, including: i) fourteen sets for interlayer mixtures (two aggregate types and seven gradations) with PG 76-22 asphalt binder, and ii) one additional set for the 4.75-mm dense-coarse granite interlayer mixture with PG 76-22 HP binder. Since each set included four replicates, a total of sixty specimens were prepared using a Superpave gyratory compactor and tested using the APA test.

This chapter documents test results obtained for these interlayer mixtures and preliminary design guidelines identified for fracture tolerant and shear resistant (FTSR) interlayer mixtures.

5.2 Test Results

This section reports the APA rut depth and the number of cycles to failure (N_f) for CSIC test for the interlayer mixtures tested. The mixtures were grouped according to nominal maximum aggregate size (NMAS) and aggregate type as described below:

- 9.5-mm NMAS granite interlayer mixtures;

- 4.75-mm NMAS granite interlayer mixtures;
- 9.5-mm NMAS limestone interlayer mixtures;
- 4.75-mm NMAS limestone interlayer mixtures.

For each mixture, the N_f results for two interlayer thicknesses were included, i.e., 1.0-in. and 0.75-in. for 9.5-mm NMAS mixtures, and 0.75-in. and 0.5-in. for 4.75-mm NMAS mixtures. More detailed information on CSIC and APA test results for both granite and limestone interlayer mixtures is included in Appendix E.

5.2.1 9.5-mm NMAS Granite Interlayer Mixtures

Figure 5-1 presents the APA rut depth for four 9.5-mm Georgia granite mixtures: three dense-graded mixtures (i.e. dense-fine (DF), dense-intermediate (DI), and dense-coarse (DC)) and one gap-graded mixture (GG). The DASR porosity (η_{DASR}) calculated for each mixture is included in the figure. As described in Chapter 3, the preliminary maximum requirement for DASR porosity was 50% for 9.5-mm mixtures to ensure interlocking for adequate shear resistance.

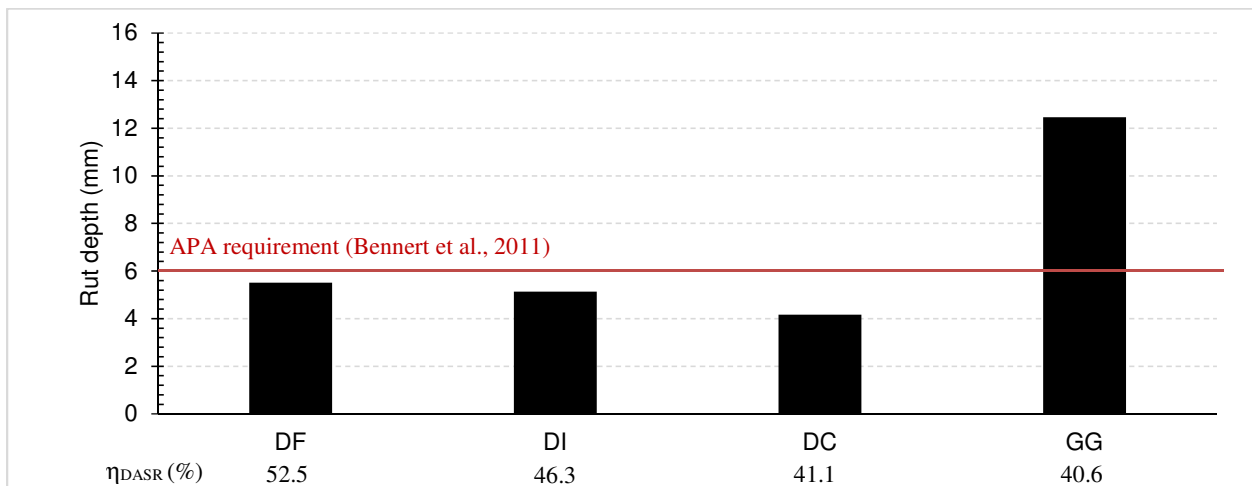


Figure 5-1. APA test result for 9.5-mm NMAS granite mixtures.

Figure 5-1 shows that all dense-graded mixtures (i.e. DF, DI, and DC) met the APA requirement used by Bennert et al. (2011) for design of binder rich intermediate course (BRIC) mixtures. APA test results also revealed that the rutting performance of the dense-graded mixtures improved as DASR porosity decreased. The gap-graded (GG) mixture did not meet the APA

requirement. This apparently inconsistent result may have been caused by the characteristics of the APA loading mechanism, which involves the application of the load through a pressurized hose. The resulting loading strip of about 1/8-in width does not provide confinement in a manner similar to a real tire (Drakos et al. 2005). Gap-graded mixture requires confinement to perform well, especially when aggregate surface roughness and angularity are insufficient to provide shear resistance independently.

Figure 5-2 presents the CSIC results in terms of N_f for four 9.5-mm granite mixtures: three dense-graded mixtures (i.e., DF, DI, and DC defined earlier) and one gap-graded mixture (GG) compared to the control (i.e., the specimen with no interlayer). For each mixture, results were presented for two interlayer thicknesses (i.e., 1.0-in and 0.75-in). The effective film thickness (EFT) for each mixture is included in the figure. As described in Chapter 3, the preliminary minimum requirement for EFT was 25 μm for 9.5-mm mixtures for enhanced fracture tolerance.

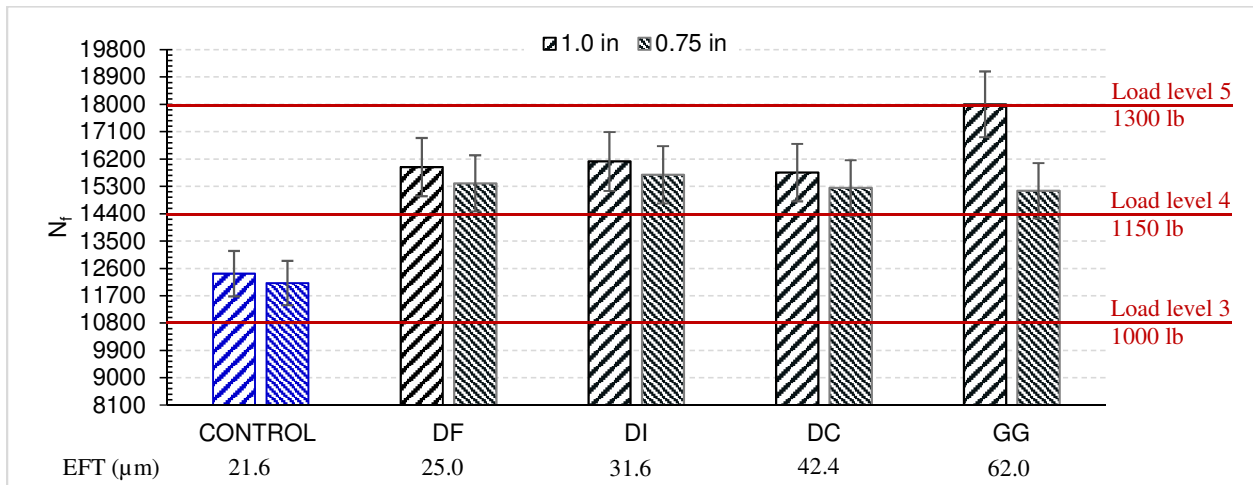


Figure 5-2. CSIC test results for 9.5-mm NMAS granite interlayers.

Figure 5-2 shows that the gap-graded (GG) and all dense-graded (DF, DI, and DC) mixtures had better performance than the control for both interlayer thicknesses. The 1.0-in gap-graded interlayer, which lasted throughout Load Level 4 outperformed the other interlayers. This superior performance is likely associated with both good interlocking between the large aggregate particles and coarser binder distribution as reflected by the higher EFT. CSIC results also revealed that, unlike the dense-graded mixtures, the gap-graded mixture was sensitive to

interlayer thickness. It appeared that a minimum interlayer thickness of 1.0 in was necessary for the gap-graded mixture to achieve proper interlocking between large particles. For all dense-graded (DF, DI, and DC) interlayer mixtures, 0.75-in thickness appeared to be sufficient to provide adequate reflective cracking performance.

5.2.2 4.75-mm NMAAS Granite Interlayer Mixtures

Design of 4.75-mm granite mixtures required the use of a second granite (Nova Scotia granite) since the dense-graded coarse (DC) gradation could not be achieved with the Georgia granite. For dense-graded fine (DF) and intermediate (DI) mixtures, which were produced with Georgia granite, permanent deformation reduced as DASR porosity decreased (Figure 5-3). The dense-graded coarse mixture, which was produced with Nova Scotia granite, showed higher rut depth than the intermediate mixture even though its DASR porosity was lower (Figure 5-3). It is well known that aggregate characteristics including texture, angularity, and toughness may affect rutting performance of a mixture. The change in rock may have led to a weaker system that was not able to perform as expected. Overall, no 4.75-mm granite mixture met the APA requirement.

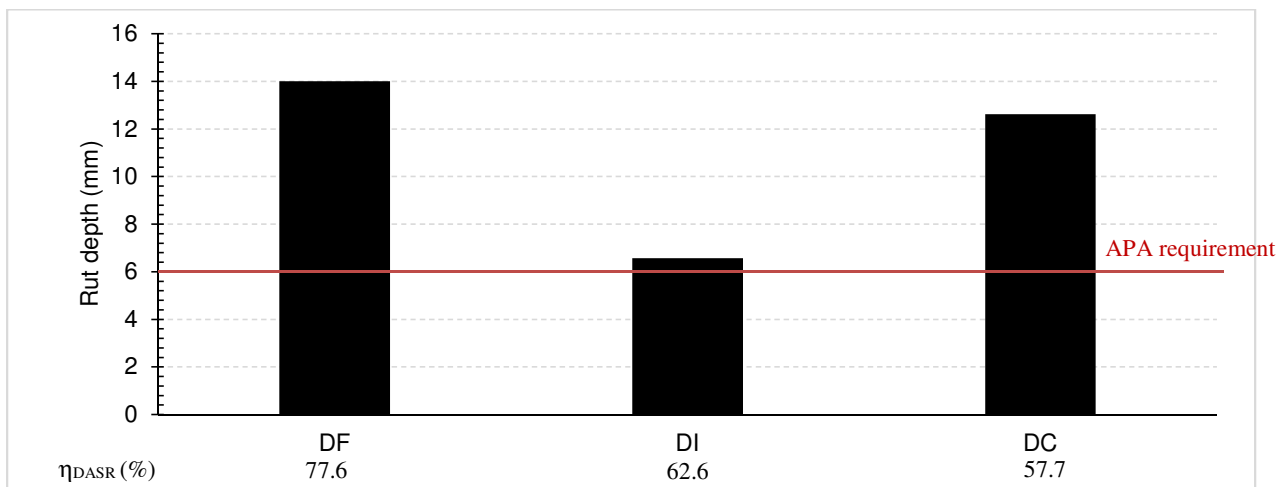


Figure 5-3. APA test result for 4.75-mm NMAAS granite mixtures.

As shown in Figure 5-4, the dense-graded coarse (DC) mixture exhibited better reflective cracking performance than both dense-graded intermediate (DI) and fine (DF) mixtures, as well as the control. Sensitivity to interlayer thickness was observed for both dense-graded

intermediate and fine mixtures. It is important to note that these two mixtures did not meet the preliminary EFT requirement (i.e. $\geq 20 \mu\text{m}$) established in Chapter 3 for the 4.75-mm FTSR interlayer mixtures. Overall, the 0.50-in interlayer with the dense-graded coarse mixture appeared to be most promising for this group of interlayers. However, since the dense-graded coarse mixture exhibited poor rutting performance, further APA and CSIC tests were conducted with a premium high-polymer (HP) asphalt binder.

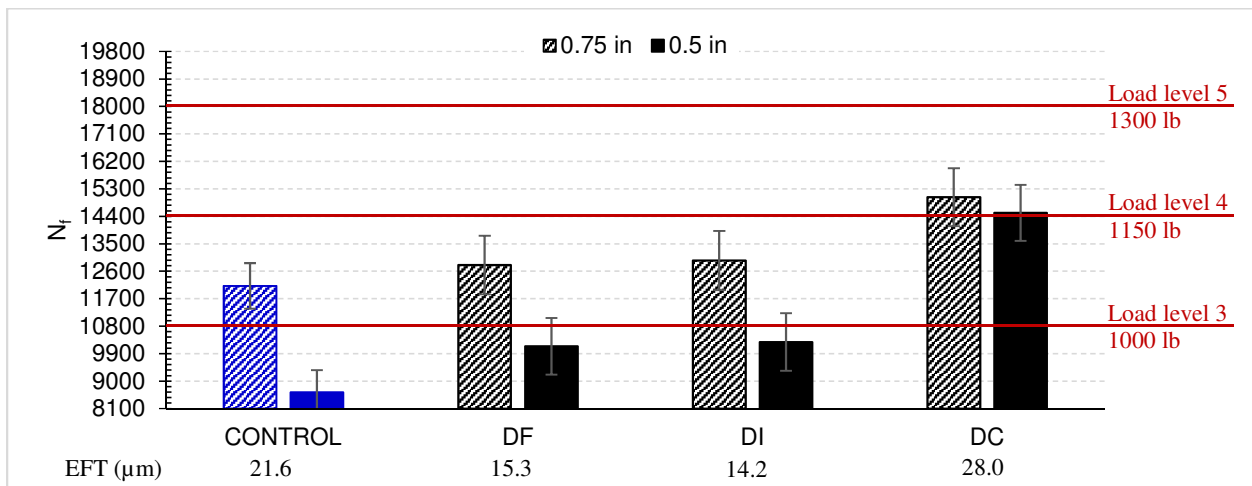


Figure 5-4. CSIC test results for 4.75-mm NMAS granite interlayers.

As expected, the rutting performance of the 4.75-mm dense-graded coarse (DC) interlayer mixture with the HP binder improved significantly relative to the mixture with PG 76-22 binder (Figure 5-5a). However, the HP binder had a negative effect on reflective cracking performance (Figure 5-5b). It is important to note that because of the small level of deformation experienced during the CSIC test, the stresses in the interlayer were dominated by the softer base binder used to produce the HP asphalt binder. Consequently, the lower stiffness interlayer resulted in the load being transferred directly to the overlay, so the crack advanced into the overlay without failing the interlayer. This phenomenon has been called “crack jumping” by Bennert et al. (2011) based on a similar observation (Figure 5-6). They reported that when a ductile layer was placed underneath a brittle overlay, the crack in the existing pavement can propagate into the overlay, bypassing the interlayer. Therefore, none of the 4.75-mm dense-graded granite interlayers were suitable as a fracture-tolerant shear-resistant (FTSR) interlayer.

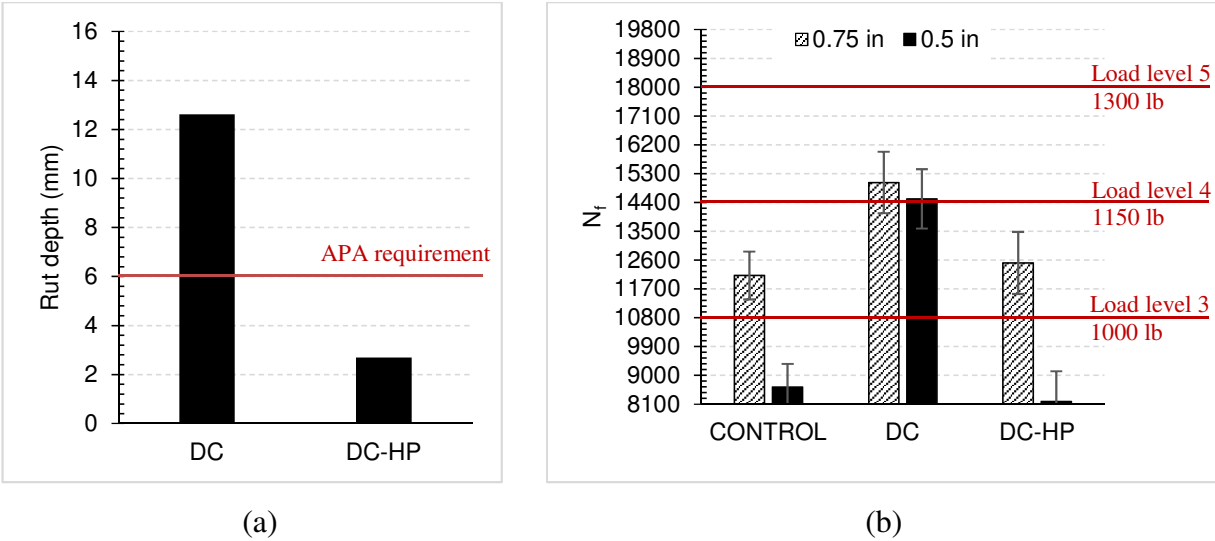


Figure 5-5. Evaluation of 4.75-mm DC granite mixture with HP binder: (a) APA test results; (b) CSIC test results.



Figure 5-6. Crack jumping phenomenon (Bennert et al., 2011)

5.2.3 9.5-mm NMAS Limestone Interlayer Mixtures

Figure 5-7 shows that all 9.5-mm dense-graded limestone interlayer mixtures met the APA requirement and that rutting performance improved as DASR porosity decreased. Although the 9.5-mm gap-graded limestone interlayer mixture met the APA requirement, it did not perform as well as dense-graded mixtures. This observation demonstrates once again the issue with the APA loading mechanism that does not provide confinement in a manner similar to a real tire (Drakos et al. 2005). However, the rough surface and high angularity in combination with the high binder absorption of the Florida limestone created a strong bond between aggregates and asphalt binder

that may have partially compensated for the need of confinement for the gap-graded mixture to perform.

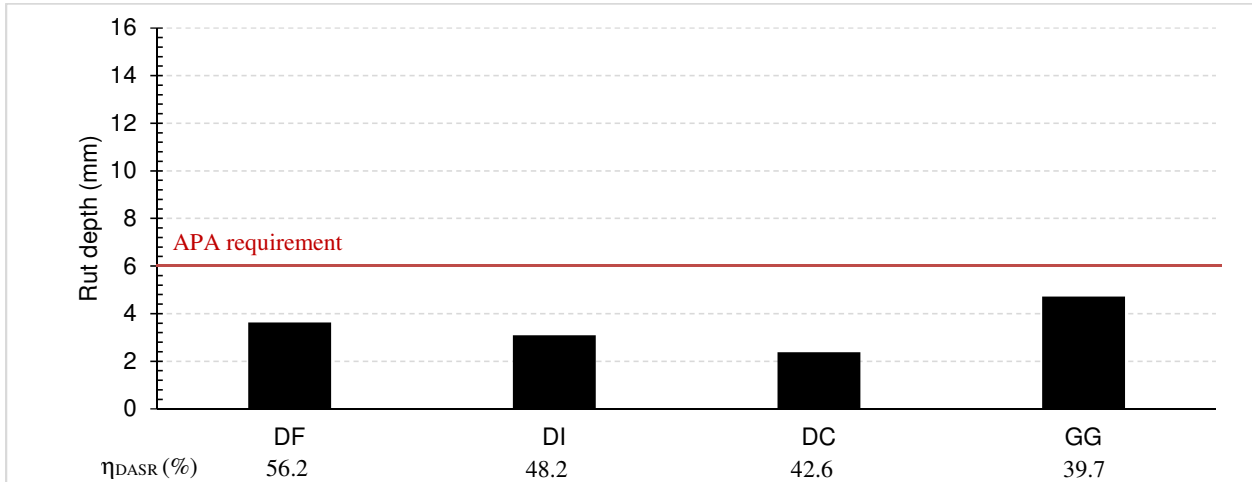


Figure 5-7. APA test result for 9.5-mm NMAS limestone mixtures.

Figure 5-8 shows that all 1.0-in dense-graded limestone interlayers improved the reflective cracking performance relative to the control. The results also revealed that performance of dense-graded mixtures was sensitive to interlayer thickness and that sensitivity reduced as EFT increased. The 1.0-in gap-graded limestone interlayer showed marginal improvement relative to the control. The 0.75-in gap-graded interlayer exhibited worse performance than the control. It appeared that the characteristic stone-on-stone gap-graded design resulted in breakage of the weaker Florida limestone aggregates which led to poorer reflective cracking performance (Figure 5-9).

For all 9.5-mm dense-graded limestone interlayer mixtures, 1.0-in thickness appeared to be necessary to provide adequate reflective cracking performance. The 9.5-mm gap-graded limestone mixture appeared to be unsuitable due to its lower performance relative to dense-graded mixtures.

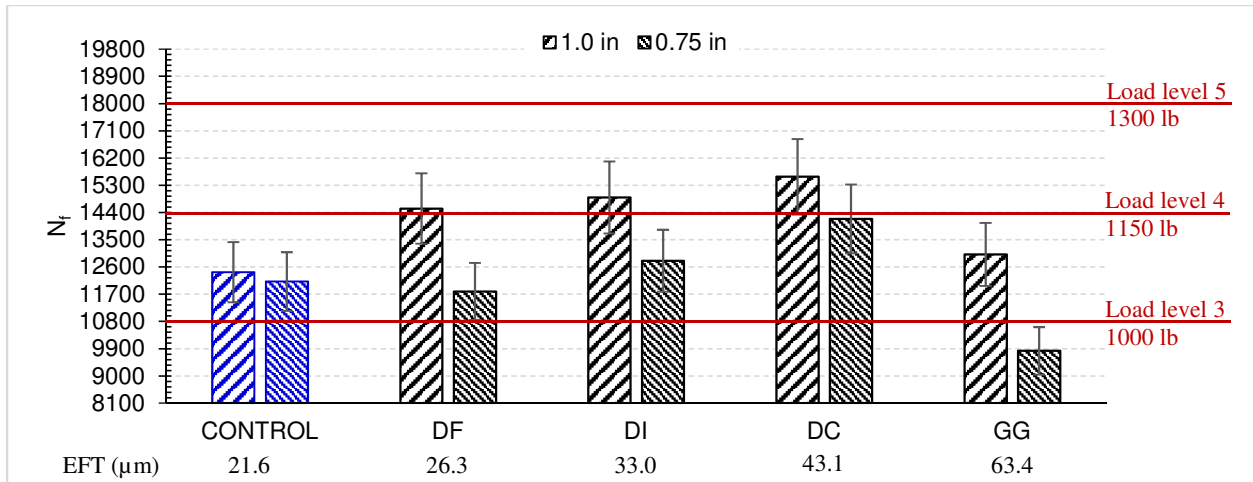


Figure 5-8. CSIC test results for 9.5-mm NMAS limestone interlayers.

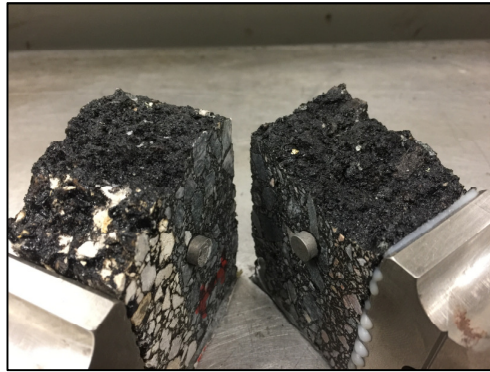


Figure 5-9. Comparison of failure surfaces between limestone and granite mixtures.

5.2.4 4.75-mm NMAS Limestone Interlayer Mixtures

Figure 5-10 shows that only the 4.75-mm dense-graded fine mixture, which had the highest DASR porosity (i.e. 74.9%), did not meet the APA requirement. Figure 5-11 shows that all 4.75-mm dense-graded limestone mixtures had improved reflective cracking performance relative to the control. It was also observed that CSIC results were sensitive to interlayer thickness and this sensitivity appeared to reduce as EFT increased. Only 4.75-mm dense-graded intermediate and coarse limestone mixtures appeared to be suitable as an FTSR interlayer, since the dense-graded fine mixture did not meet the APA requirement. For these interlayers, the 0.75 in thickness appeared to be necessary to provide adequate reflective cracking performance.

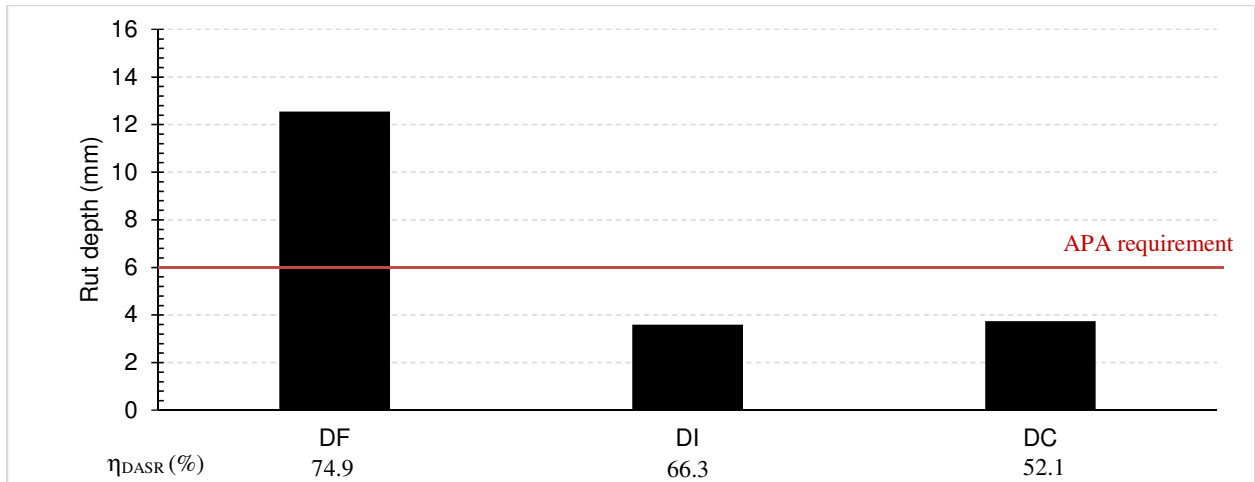


Figure 5-10. APA test result for 4.75-mm NMA limestone mixtures.

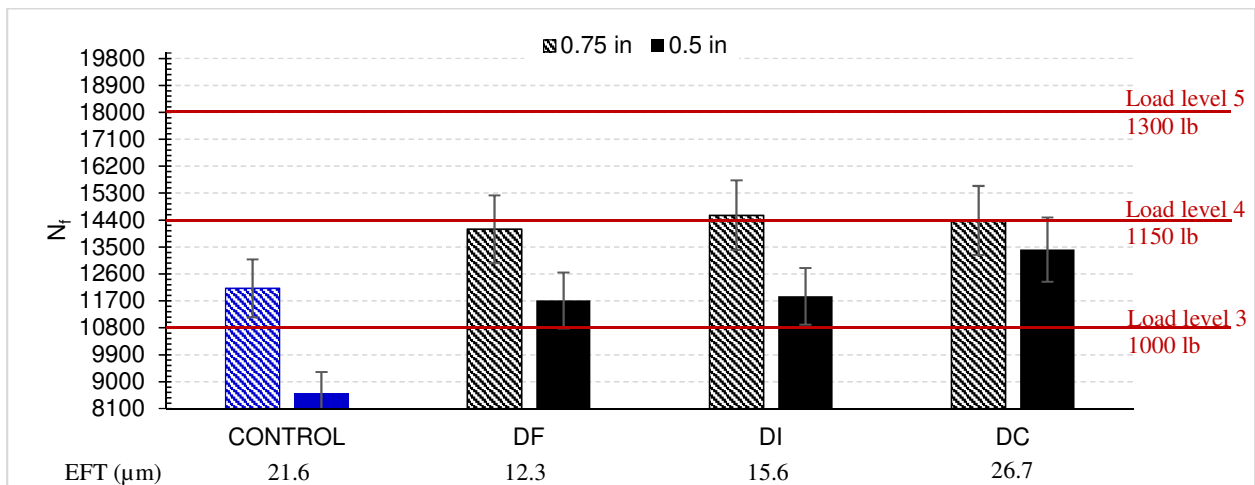


Figure 5-11. CSIC test results for 4.75-mm NMA limestone interlayers.

5.3 Identification of Preliminary Design Guidelines

It was generally observed that increase in gradation coarseness resulted in higher effective film thickness (EFT), which led to better reflective cracking performance and shear resistance for dense-graded interlayer mixtures tested in this study. Therefore, CSIC and APA test results were plotted against EFT to identify preliminary design guidelines for fracture-tolerant and shear-resistant (FTSR) interlayer mixtures.

5.3.1 Minimum EFT for 9.5-mm NMAS Interlayer Mixtures

Figure 5-12 shows that the CSIC results in terms of N_f did not change with EFT for 9.5-mm dense-graded granite mixtures used in both 0.75-in and 1.0-in interlayers and that reflective cracking resistance was insensitive to interlayer thickness. The 0.75-in thickness (the thinner option) appeared to be sufficient for all mixtures to provide good reflective cracking resistance, where N_f was greater than 14,400 cycles and reached Load Level 4 (1,150 lb). However, increase in EFT led to improved rutting performance (Figure 5-12) as well as considerable reduction in asphalt content of up to 1% (Figure 5-13).

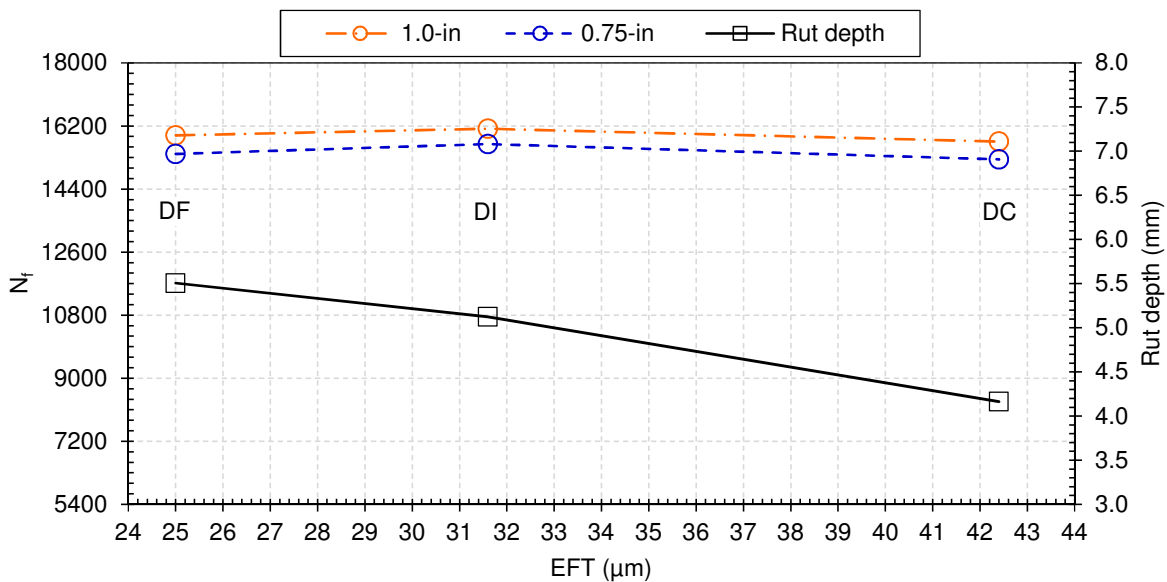


Figure 5-12. Effect of EFT on performance of 9.5-mm dense-graded granite mixtures.

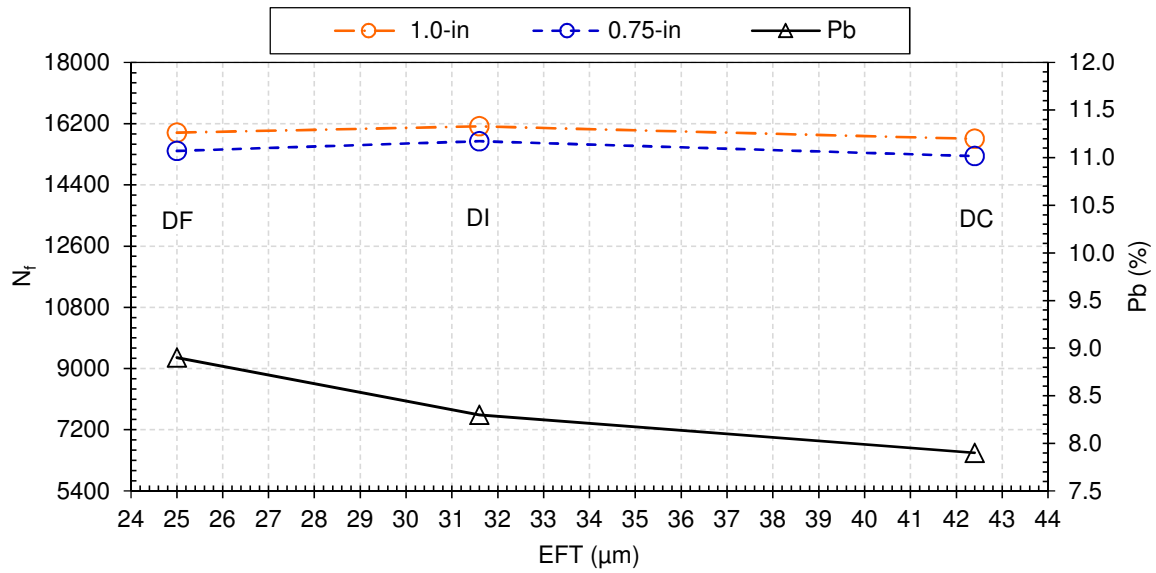


Figure 5-13. Effect of EFT on asphalt content of 9.5-mm dense-graded granite mixtures.

Unlike 9.5-mm dense-graded granite mixtures, limestone mixtures exhibited improved reflective cracking resistance as EFT increased for both 0.75-in and 1.0-in interlayer thicknesses (Figure 5-14). The reflective cracking resistance was sensitive to interlayer thickness and increase in EFT led to reduced sensitivity. Among all 0.75-in interlayers, only the dense-coarse limestone mixture reached an N_f close to 14,400 cycles. Figure 5-14 also shows that increase in EFT led to improved rutting performance.

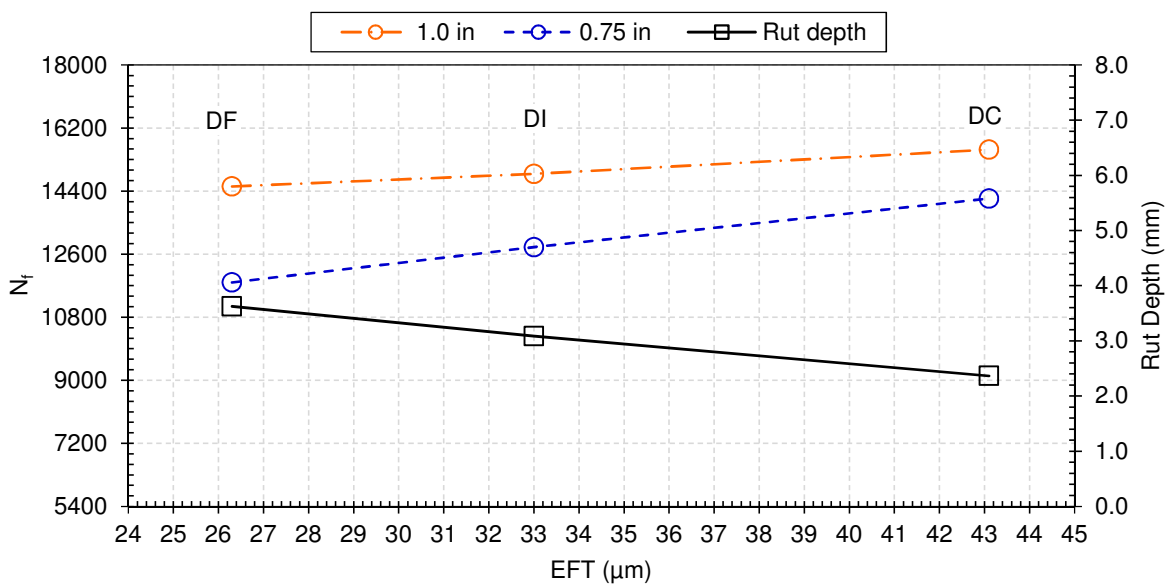


Figure 5-14. Effect of EFT on performance of 9.5-mm dense-graded limestone mixtures.

In an attempt to stay away from unstable reflective cracking performance that is sensitive to interlayer thickness, a minimum EFT requirement of 35 μm was proposed for design of 9.5-mm FTSR interlayer mixtures (Figure 5-15). The minimum EFT requirement also results in more economical design with lower asphalt content. As shown in Figure 5-15, asphalt content was higher for the dense-fine mixture with a relatively low EFT, but it reduced considerably for the dense-coarse limestone mixture with an EFT greater than 35 μm . It is recognized that the minimum EFT requirement was unnecessary for granite mixtures to reduce sensitivity to thickness and to improve reflective cracking resistance, but it resulted in lower asphalt content with equivalent performance. In other words, depending on availability of aggregates, a finer granite mixture with an EFT lower than the minimum requirement may be able to provide adequate performance, but it will result in higher cost.

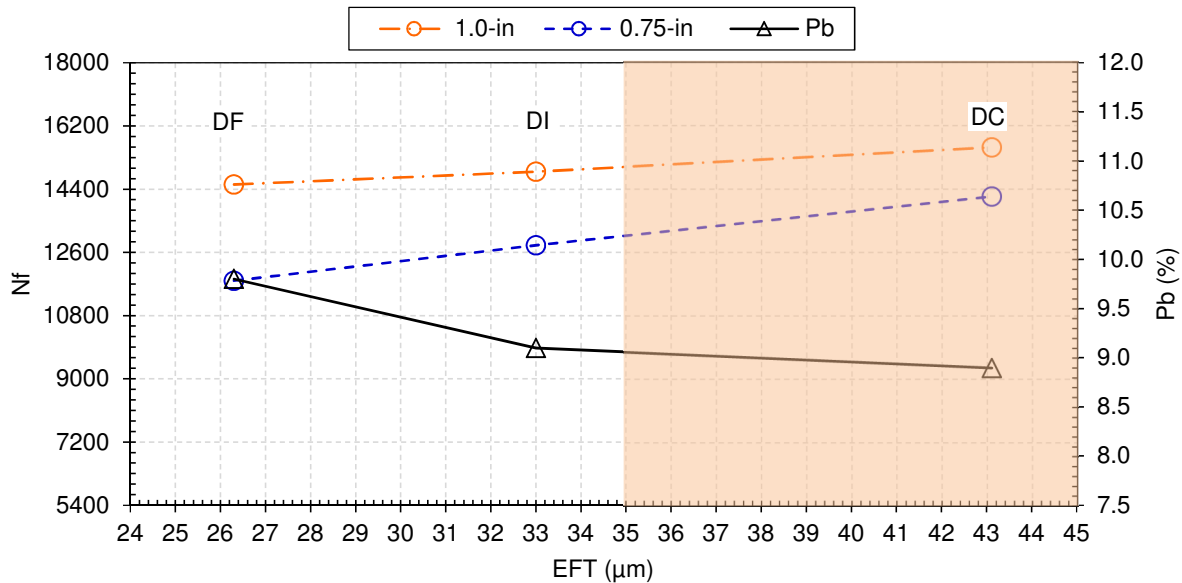


Figure 5-15. Effect of EFT on asphalt content of 9.5-mm dense-graded limestone mixtures and minimum EFT requirement.

It is important to note that a 9.5-mm gap-graded mixture will always meet the minimum EFT requirement. However, the characteristic stone-on-stone gap-graded design may result in breakage of weaker aggregates (such as Florida limestone) and poorer performance.

Furthermore, as compared to the dense-graded mixtures, the gap-graded mixtures required higher asphalt content and higher interlayer thickness to perform. Therefore, dense-graded mixtures with a minimum EFT of 35 μm are recommended for use as FTSR interlayer mixtures.

5.3.2 Minimum EFT for 4.75-mm NMAS Interlayer Mixtures

As indicated in Section 5.2, none of the 4.75-mm dense-graded granite mixtures were suitable as FTSR interlayer mixtures due to inadequate reflective cracking performance for fine-dense and intermediate-dense mixtures, and poor rutting performance for the coarse-dense mixture. Therefore, only results of the limestone mixtures were evaluated further for identification of minimum EFT.

Figure 5-16 shows that 4.75-mm dense-graded limestone mixtures generally exhibited improved reflective cracking resistance as EFT increased for 0.5-in interlayer thickness, and to a less extent for 0.75-in thickness. The reflective cracking resistance was sensitive to interlayer thickness and increase in EFT led to reduced sensitivity. Among all interlayers, only 0.75-in dense-intermediate and dense-coarse mixtures reached an N_f of 14,400 cycles (Load Level 4). Figure 5-16 also shows that asphalt content dropped considerably with increasing EFT from the dense-fine mixture to the dense-intermediate mixture produced with the same limestone source. However, further increase in EFT resulted in higher asphalt content in the dense-coarse mixture. This unexpected trend was likely caused by the introduction of a second limestone source which was necessary to produce the desired dense-coarse gradation.

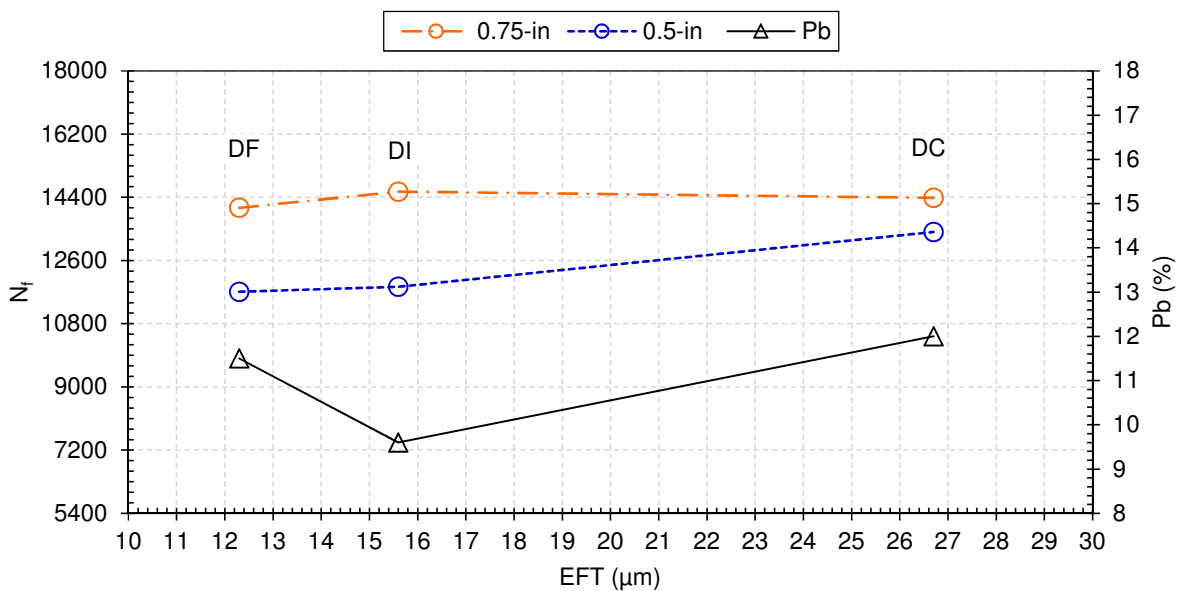


Figure 5-16. Effect of EFT on reflective cracking performance and asphalt content of 4.75-mm dense-graded limestone mixtures.

Figure 5-17 shows that increase in EFT led to considerably-improved rutting performance for two mixtures produced with the same limestone source: the dense-fine mixture with a low EFT of 12.3 μm had very high rut depth, while the dense-intermediate mixture with a higher EFT of 15.6 μm met the APA requirement. Further increase in EFT did not lead to additional reduction in rut depth for the dense-coarse mixture produced with the second limestone source, which had unexpectedly high asphalt content. In an attempt to stay away from rutting issues and to reduce sensitivity of reflective cracking performance to interlayer thickness, a minimum EFT requirement of 20 μm was proposed for design of 4.75-mm FTSR interlayer mixtures (Figure 5-17). The minimum EFT requirement may be used for other aggregate types, including granites. However, an independent check of rutting resistance is necessary.

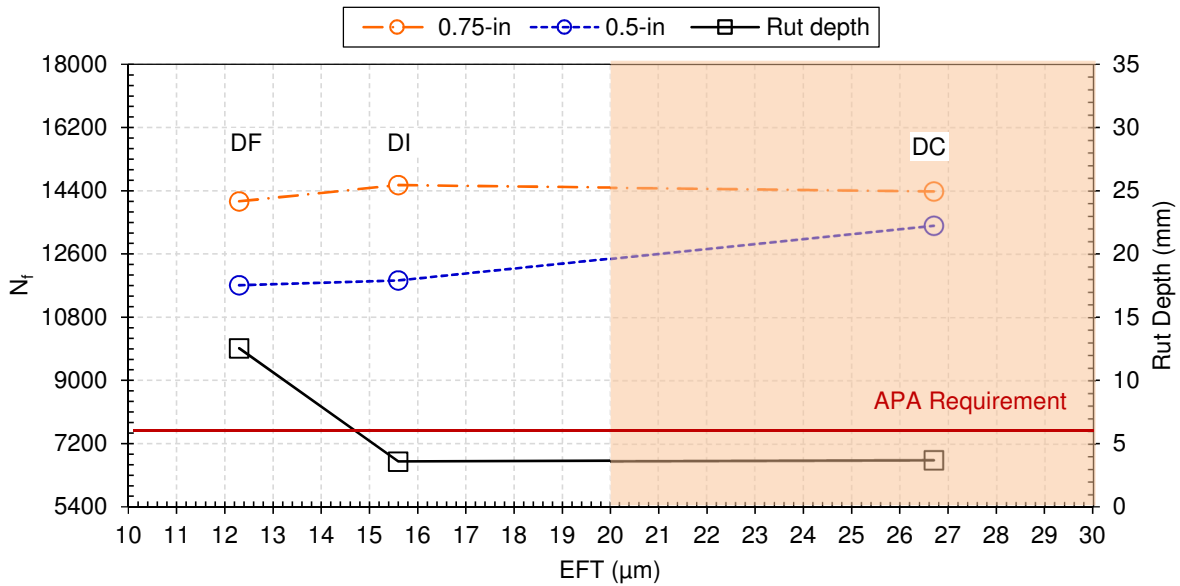


Figure 5-17. Effect of EFT on rutting performance of 4.75-mm dense-graded limestone mixtures and minimum EFT requirement.

5.3.3 Preliminary Design Guidelines

Table 5-1 summarizes preliminary design guidelines for FTSR interlayer mixtures. A portion of the guidelines are in line with the general idea employed by two existing interlayer mixtures (CAM and BRIC), i.e., using reduced N_{design} (50) and lower air void at N_{design} (2% for dense-graded and 4% for gap-graded) to allow for more asphalt content in interlayer mixtures as compared to structural mixtures. However, the general idea along with the gradation band established for CAM and BRIC do not necessarily guarantee production of mixtures that are fracture-tolerant and shear-resistant. The minimum EFT requirements developed as part of this study provide an important enhancement in terms of selecting appropriate gradations for adequate reflective cracking performance, sufficient shear resistance, and reduced cost. Figure 5-18 shows the gradation band for 9.5-mm dense-graded FTSR mixtures confined between an upper bound defined by the minimum EFT requirement of 35 μm and a lower bound defined by the maximum coarseness of SP-9.5 gradation. This gradation band has a narrow overlap with the gradation band for CAM. In fact, most of the 9.5-mm dense-graded FTSR mixtures are coarser than the CAM to achieve optimized performance. Similarly, the gradation band for 4.75-mm dense-graded FTSR mixtures, which is confined between an upper bound defined by the minimum EFT requirement of 20 μm and a lower bound defined by the maximum coarseness of SP-4.75 gradation, overlaps with the coarser portion of the gradation band for BRIC (Figure 5-19). Since 9.5-mm gap-graded mixtures naturally meet the minimum EFT requirement, the gradation band for gap-graded mixtures stays the same.

Table 5-1. Mix design requirements for FTSR interlayer mixtures.

| Parameter | Dense-Graded (DG) | | Gap-graded (GG) |
|----------------------------------|-------------------|-----------|-----------------|
| | 9.5 mm | 4.75 mm | 9.5 mm |
| EFT, μm min | 35 | 20 | 35 |
| η_{DASR} , % max | 50 | 60 | 50 |
| N_{design} | 50 | 50 | 50 |
| V_a at N_{design} , % | 2 | 2 | 4 |
| AC, % min | 7 | 7 | 6 |
| VMA, % min | 17 | 18 | 17 |
| Dust proportion | ≤ 1.4 | 0.6 – 1.2 | – |
| Draindown, % max | – | 0.1 | 0.3 |

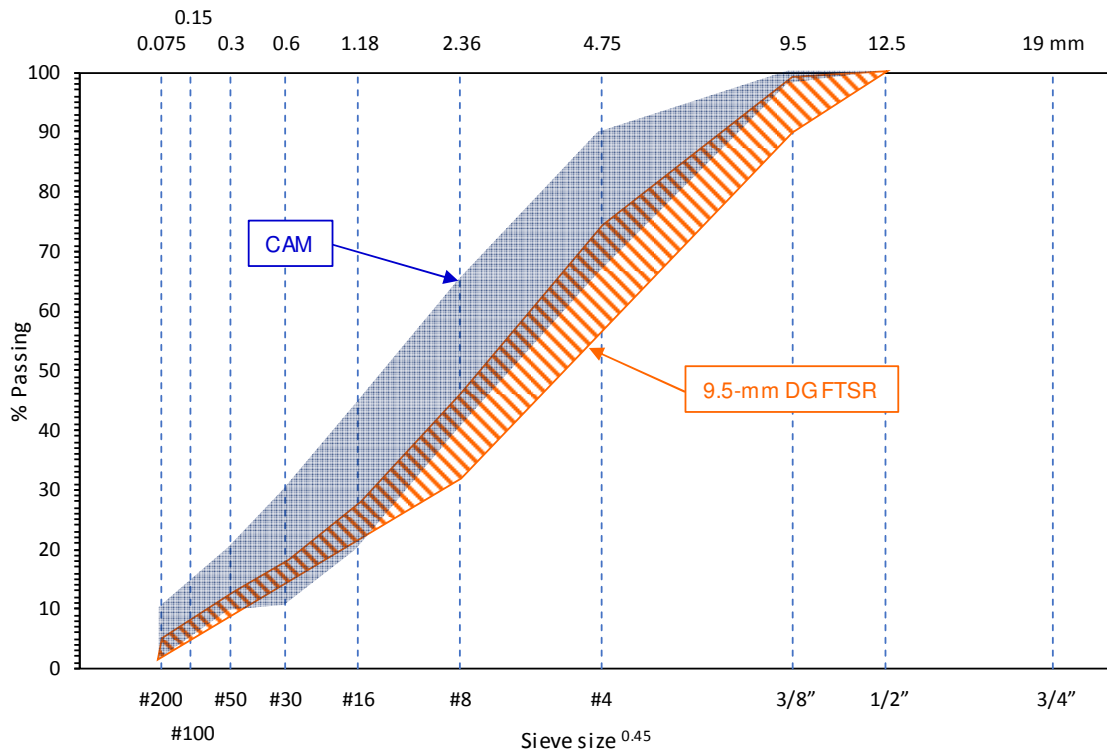


Figure 5-18. Comparison of gradation bands for 9.5-mm DG FTSR mixture and CAM.

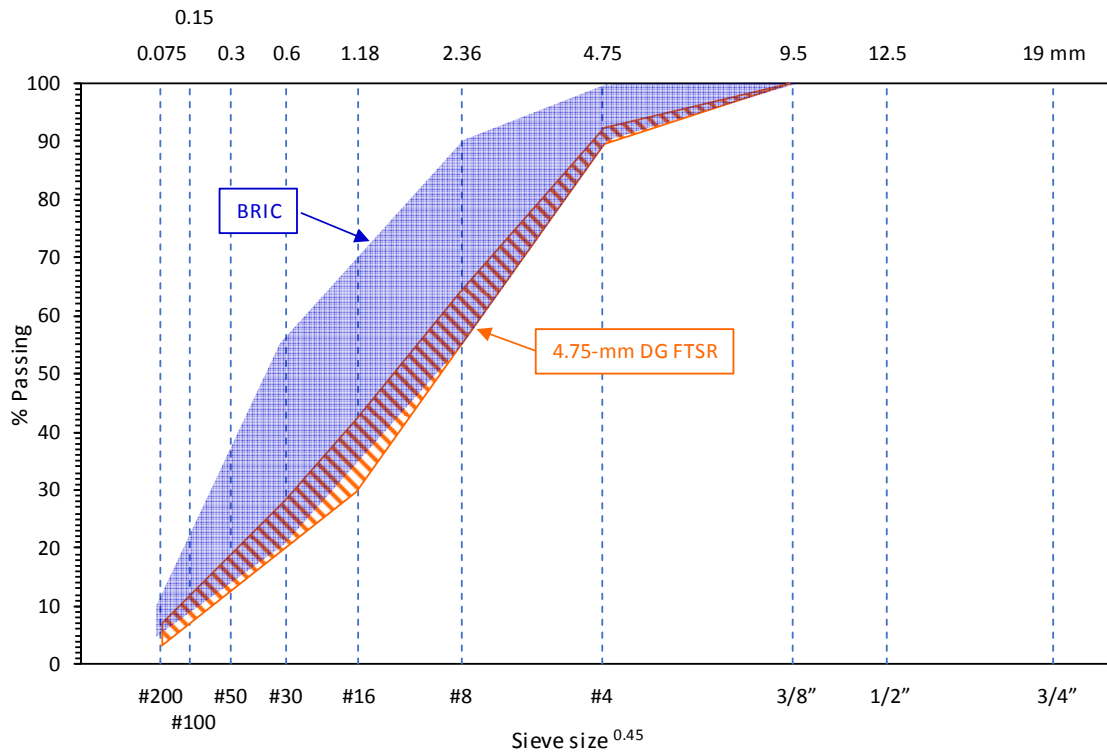


Figure 5-19. Comparison of gradation bands for 4.75-mm DG FTSR mixture and BRIC.

CHAPTER 6

CLOSURE

6.1 Summary of Findings

This study was conducted to develop guidelines for fracture-tolerant and shear-resistance (FTSR) interlayer mixtures to mitigate near-surface reflective cracking in overlays on asphalt pavement. Fourteen interlayer mixtures, covering a broad range of gradation, were designed based on the dominant aggregate size range – interstitial component (DASR-IC) model, which provides a framework for the design and modification of gradation to ensure sufficient aggregate interlock to resist permanent deformation as well as adequate cracking resistance. According to the DASR-IC model, coarser gradation results in lower DASR porosity and higher effective film thickness (EFT) which enhance shear resistance and fracture tolerance. A composite specimen interface cracking (CSIC) test developed in an earlier FDOT research project was enhanced with a new loading device, specimen preparation procedure, and loading procedure to more consistently evaluate reflective cracking performance of interlayer systems. In addition, asphalt pavement analyzer (APA) tests were performed to determine whether the interlayer mixtures had sufficient rutting resistance. A summary of findings based on results of tests and analyses is provided below:

- 9.5-mm dense-graded mixtures with a minimum EFT of 35 μm appear to be suitable as FTSR mixtures that provide good reflective cracking and rutting performance. Both granite and limestone can be used. However, limestone required greater interlayer thickness (1.0-in, as opposed to 0.75-in for granite) and more asphalt binder.
- As compared to CAM, 9.5-mm dense-graded FTSR mixtures exhibited equivalent performance with less asphalt binder when granite aggregate was used, or better performance and less sensitivity to interlayer thickness with less asphalt binder when limestone was used.
- 4.75-mm dense-graded limestone mixtures with a minimum EFT of 20 μm exhibited good reflective cracking performance at 0.75-in thickness and good rutting performance. However, due to higher asphalt content required, it is costlier than the 9.5-mm mixtures with the same thickness.

- The 4.75-mm dense-graded granite mixture with a minimum EFT of 20 μm also exhibited good reflective cracking performance at 0.75-in thickness, but were not suitable as an FTSR mixture due to high APA rut depth. Therefore, rutting resistance of 4.75-mm mixtures must be checked to ensure adequate shear resistance.
- As compared to BRIC mixture, 4.75-mm dense-graded limestone FTSR mixtures exhibited better performance and less sensitivity to interlayer thickness.
- The 9.5-mm gap-graded granite mixture provided superior performance at 1.0-in thickness. However, it is a costlier option relative to dense-graded mixtures due to greater thickness and more asphalt binder required. Weaker Florida limestone was not suitable for gap-graded design due to breakage of aggregates.
- 4.75-mm gap-graded mixtures cannot be designed with stockpiles available in Florida.
- The APA loading mechanism does not provide confinement in a manner similar to a real tire. Therefore, the APA test appears to be unsuitable for rutting performance evaluation of gap-graded mixture, which requires confinement to perform well. If gap-graded mixture is selected for use in the field, an alternative rut test (e.g., Hamburg wheel tracking test) is needed for independent verification.

6.2 Conclusions

The following conclusions were drawn based on the findings of this study:

- Use of lower compaction effort and reduced design air voids to allow for higher asphalt content does not necessarily ensure interlayer mixtures that are fracture-tolerant and shear-resistant.
- Interlayer mixtures designed by coarsening the gradation as reflected by a minimum EFT criterion results in better binder distribution for fracture tolerance and more suitable aggregate structure for shear resistance, even though design asphalt content is lower than for a finer-graded mixture.
- The DASR-IC model provides a systematic approach for design of FTSR interlayer mixture gradation with sufficient coarseness for improved reflective cracking and rutting performance, and reduced cost.

6.3 Recommendations and Future Work

Based on evaluations performed in this study, recommendations for further investigation are summarized below:

- A broader range of aggregate types, gradations, and interlayer thickness should be tested to refine the design guidelines.
- Development of a simpler test system (i.e. Superpave IDT along with HMA fracture mechanics) is recommended to complete the work needed for refinement of design guidelines.
- An HVS test or an experimental road test should be performed to verify further the guidelines for design of FTSR interlayer mixtures that were identified based on laboratory tests.

APPENDIX A
REVIEW OF REFLECTIVE CRACKING MITIGATION TREATMENT

A.1 Existing Asphalt Surface Modification

Modification of the existing asphalt surface is used to eliminate existing cracks in an asphalt pavement surface by removing the damaged surface prior placing the asphalt overlay. This treatment includes mainly three different approaches that can be used depending on the depth of the crack in the existing pavement: (1) mill and replace, (2) hot-in-place recycling (HIPR), and (3) full-depth-reclamation (FDR). The three approaches are described below.

A.1.1 Milling and Replacing

Mill and replace is similar to the full-depth-reclamation approach with the exception that only the wearing surface or upper asphalt layers are removed. It is typically used in pavement with good structural condition where cracks are confined to the surface layer. Figure A-1 a) shows the process of milling. The mitigation treatment seems to perform well if the discontinuity is completely removed. Otherwise, it is preferable to use the treatment in combination with other mitigation techniques (Von Quintus et al., 2009).

A.1.2 Hot-in-Place Recycling (HIPR)

Hot-in-place recycling (HIPR) is a treatment in which the existing pavement surface is removed (typically scarified) and mixed in-place with the application of heat. This technique may be considered in pavement with good structural condition where cracks extend below the wearing surface. Figure A-1 b) illustrates the equipment used for the HIPR process. Generally, this technique is not able to eliminate entirely the cracks in the existing pavement, which will eventually propagate through the new overlay. Moreover, further aging of the reclaimed asphalt pavement used to overlay the existing pavement can potentially result in thermal cracking (Von Quintus et al., 2009).

A.1.3 Full-Depth-Reclamation (FDR)

Full-depth-reclamation (FDR) is a cold-in-place recycling (CIPR) treatment in which the existing pavement is pulverized and mixed in-place without the use of heat. This strategy should be considered where cracks extend completely through the asphalt layer. Figure A-1 c) shows the equipment used for the CIPR process. This treatment seems to have high potential of success because the entire asphalt layer is remixed and compacted in-place, eliminating completely the discontinuities. However, due to the cost of the treatment, its use is recommended only when the pavement structure or the subgrade are severely damaged (Von Quintus et al., 2009).



(a) Milling and replacing
(www.wirtgen-group.com)



(b) HIPR (martec.ca)



(c) FDR (www.midlandasphalt.com)

Figure A-1. Existing asphalt surface modification.

A.2 Overlay Layer/Mixture Modification

Overlay layer/mixture modification includes two techniques: (1) thick asphalt overlays and (2) modified asphalt and specialty mixtures. The two approaches are described below.

A.2.1 Thick Asphalt Overlays

Thick asphalt overlays are used to reduce the stress level at the crack tip. A thicker overlay improves the load transfer across the crack, which results in a lower level of stress and strain developed at the crack tip. This treatment is shown in Figure A-2 a). This strategy is not meant to stop RC but to delay the appearance of cracks in the surface (Housel, 1962 and Van Breeman, 1963).

A.2.2 Modified Asphalt and Specialty Mixtures

Modified asphalt and specialty mixtures are typically used in combination with mill and replace. The purpose of this treatment is to improve the fracture tolerance of the overlay to resist high stress and strain developed at the crack tip in the existing pavement. Higher fracture resistance can be achieved by: (1) using a softer asphalt binder, (2) using additives to improve temperature susceptibility, (3) adding rubber to increase the flexibility to be extensible and highly elastic, and (4) employing mixtures with thick asphalt film thickness (i.e., using gap graded mix designs). Figure A-2 b) shows the application of a specialty mixture.

Chen et al. (2005) presented a case study of using specialty mixtures on a continuous reinforced concrete pavement (CRCP) in Beaumont district, Texas (US-96). After 40 years, the pavement was overlaid with a 3-in (76-mm) thick layer of gap graded mixture to solve the problem of spalling. The main concern in using this treatment was the potential for RC to develop due to the movement of the slabs. Five years after placement, it was reported to have good performance without visible cracks on the surface. This success was attributed to the cracking resistance of the gap graded mixture and to the good support and adequate load transfer of the pavement. As pointed out by Von Quintus et al. (2009), this treatment does not prevent RC from occurring, but it does help reduce the severity of reflective cracks.



(a) Thick overlay (www.graniterock.com)



(b) Modified asphalt and specialty mixture (www.terracon.com)

Figure A-2. Overlay layer/mixture modification.

A.3 Overlay Reinforcement

Reinforcement of asphalt overlay consists of a layer of reinforcing material installed between the existing pavement and the overlay to control or delay RC. The physical restraint provided by these products reduces the tensile and shear stress concentration in the overlay at the crack-tip. The most common materials used to manufacture these systems are geosynthetics and steel.

A.3.1 Geosynthetics

Geosynthetics refer to all planar synthetic products used in civil engineering application. In pavement rehabilitation the most common geosynthetic reinforcing systems are: (1) woven geotextiles, (2) geogrids, and (3) geocomposites. The three systems are described below.

A.3.1.1 Woven Geotextiles

Woven geotextiles, as shown in Figure A-3 a), are fabrics made of synthetic fibers using standard weaving machinery. The majority of these products are made of polypropylene or polyester. Due to their high tensile strength, they are typically used in pavement rehabilitation as an overlay reinforcement. These materials need to be in a state of tension to function properly. Therefore, in pavements where bending due to moving wheel load is the primary source of RC,

thick overlays are recommended. The Federal Aviation Administration (FAA) (2006) recommends not to use reinforcements if the overlay thickness is less than 3 in (75 mm). The minimum thickness requirement may have a negative impact on the cost-effectiveness of the treatment (Maurer and Malasheskie, 1989 and Buttlar et al., 2000).

A.3.1.2 Geogrids

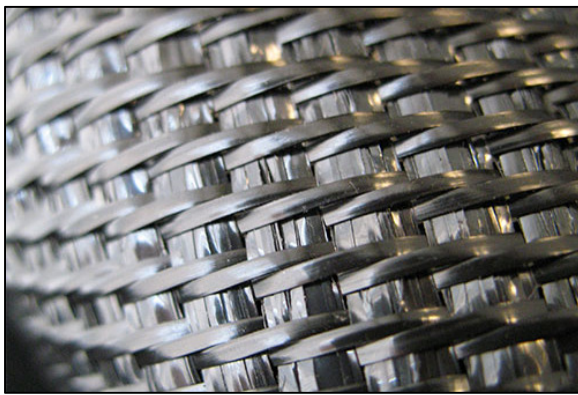
Geogrids are typically made from sheets of high-density polyethylene or polypropylene, as well as high-tenacity polymer yarns or fiberglass. These products come with open spaces (called apertures) of varying sizes. Based on the material and strength required, the size of the aperture ranges from 0.5 to 4.0 in (1.25 to 10 cm). Geogrids are installed with light asphalt binder (or an adhesive) to secure a good bond between the grid and the existing pavement. Figure A-3 b) depicts an example of geogrid application. These systems need to be engaged immediately as the moving load passes the discontinuity to avoid excessive overlay stretching. Therefore, good adhesion between the reinforcing layer and the overlay is required. However, achieving a proper level of adhesion is challenging due to the large openings, which generally occupy more than 80% of the surface area (Button and Lytton, 2007).

A.3.1.3 Geocomposites

Geocomposites consist of fabrics laminated into grids. These systems have been designed to combine the advantages of fabrics and grids. Fabrics provide a continuous surface to better bond with the existing pavement and the overlay, whereas grids provide additional strength to the new overlay (Von Quintus et al., 2009). Figure A-3 c) shows the application of geocomposites on top of an existing pavement. It is important to note that all these products, including woven geotextiles, geogrids, and geocomposites are difficult to install and very costly (Barazone, 1990 and Barazone, 2000).

A.3.2 Steel Mesh

Steel reinforcing was tested for the first time in the United States in 1950s. It was made with welded No.10 wire mesh. These products were gradually abandoned due to the poor performance and difficulty in installation (Davis, 1960). The introduction of a new configuration of steel mesh has helped in regaining interest in these systems (Al-Qadi and Elseifi, 2004). The steel mesh, as shown in Figure A-3 d), consists of a double-twist, hexagonal mesh with variable dimensions, which is transversally reinforced at regular intervals with steel wires inserted in the double-twist. No welding is required during the fabrication of these products. However, the use of steel mesh as reinforcement makes it impractical to mill the overlay. In addition, these products may corrode with time (Elseifi and Dhaka, 2015, Von Quintus et al., 2009).



(a) Woven geotextiles
(www.geosolutionsinc.com)



(b) Geogrids (<http://imaterialy.dumabyt.cz>)



(c) Geocomposites (www.ramalho1.com)



(d) Steel mesh interlayer
(www.externalworksindex.co.uk)

Figure A-3. Reinforcement of asphalt overlays.

A.4 Stress or Strain Relieving Layers

Stress or strain relieving interlayers consist of a layer of soft material installed between the existing pavement and the overlay to control or delay RC. These relatively low-stiffness systems are used over joints and cracks to increase the length over which strain development occurs. They are subdivided into two main categories based on their thickness: (1) cushion or crack relief layer (CRL), and (2) stress absorbing membrane interlayer (SAMI).

A.4.1 Crack Relief Layer (CRL)

Crack relief layers (CRL) are generally thick layers (more than 3 in), consisting of an open graded asphalt concrete (OGAC) mixture or unbound aggregate/crushed stone base material. Typically, the OGAC mixtures are composed of coarse aggregates (50-75 mm in NMAS), low fines, and high air voids (generally greater than 20 %) (Hensley, 1980, Von Quintus et al., 2009). The aggregates should be crushed stone from a hard and durable aggregate source. These systems are able to absorb and dissipate both horizontal and vertical movements before reaching the overlay. In addition, these thick layers provide interlock for load transfer, increasing the pavement structure capacity. Figure A-4 a) and b) show two examples of cushion or crack relief layer. Von Quintus et al. (2009) pointed out that there are two major issues associated with these strategies: (1) the total overlay thickness, which is generally much greater than that used in the other mitigation strategies, and (2) the risk for these layers to become a potential water conduit or reservoir between the overlay and existing pavement.



(a) Example 1 (www.epa.org)



(b) Example 2 (en.wikipedia.org)

Figure A-4. Cushion or crack relief layer.

A.4.2 Stress Absorbing Membrane Interlayers (SAMI)

Stress absorbing membrane interlayers (SAMI) are thin (less than 2 in) and flexible layers able to stretch horizontally without breaking. The intent of these systems is to dissipate the stress induced by horizontal movement at the discontinuity before reaching the overlay. These layers also provide protection to the pavement structure by reducing water infiltration. This category includes: (1) non-woven geotextile, (2) interlayer stress-absorbing composite (ISAC), (3) asphalt rubber membrane interlayer (ARMI), and (4) fracture-tolerant interlayer system. The four approaches are explained below.

A.4.2.1 Non-Woven Geotextiles

Non-woven geotextiles have high elongation and low modulus, which ensure high strain tolerance. These treatments provide an interior plane able to absorb the tack coat. When saturated, the fabrics behave as a waterproof membrane with the role of protecting the pavement structure and subgrade. These products are typically made of thermoplastic materials such as polypropylene or polyester. Polypropylene is cheaper but easier to damage during installation than polyester. Figure A-5 a) shows the geotextile installation on top of the existing pavement. Generally, these treatments are impractical and non-cost-effective due to the difficulty encountered during installation and the high cost. Particular care needs to be taken to avoid formation of wrinkles and overlaps in the fabric as a potential source of cracks in the overlay. Prevention of these defects is difficult, especially with complex pavement geometries. Tack coat application is another issue. Insufficient tack coat may induce debonding, whereas excessive tack coat may cause slippage. The correct amount may vary based on weight and thickness of the fabric and conditions of the old pavement. Unfortunately, the large amount of products and specifications make the selection of the installation procedure very complicated (Barazone, 1990 and Barazone 2000).

A.4.2.2 Interlayer Stress Absorbing Composite (ISAC)

Interlayer stress absorbing composite (ISAC) systems combine the advantages of having a low stiffness geotextile as a bottom layer to fully bond with the existing pavement, a viscoelastic membrane as a core to absorb the stress induced by the movement of the underlying pavement,

and a high stiffness geosynthetic as a top layer to provide reinforcement to the new overlay. Figure A-5 b) shows the installation of the ISAC.

Vespa (2005) evaluated the performance of ISAC on jointed reinforced concrete pavement (JRCP) as a RC mitigation treatment. The use of ISAC appeared to help delay RC. However, the high cost of the treatment makes it non-cost-effective. In addition, Von Quintus et al. (2009) mentioned that these systems are difficult to install.

A.4.2.3 Asphalt Rubber Membrane Interlayer (ARMI)

Asphalt rubber membrane interlayer (ARMI) was designed to make the overlay behave independently from the underlying structure. It is important to note that ARMI is an FDOT term, while Asphalt Rubber SAMI is a more widely used term around the country. As shown in Figure A-5 c), ARMI installation is a two-step procedure consisting of spraying a 0.25 in (6 mm) to 0.40 in (10 mm) thick layer of soft material (asphalt rubber binder) on top of the existing pavement surface, followed by the application of relatively coarse aggregates. The aggregates are then seated into the layer using a pneumatic rubber tire roller.

This treatment has been found to increase susceptibility of overlay to rutting, which has been observed in both field and laboratory studies. Work carried out by Greene et al. (2012) as part of the FDOT's accelerated pavement testing (APT) program showed rut depths at least twice as high in sections containing an ARMI than in the control section (without an ARMI). A possible explanation was that introduction of an interlayer like ARMI may have promoted the development of a global shear plane along which slip occurred. Regarding cracking, Chen et al. (2013) conducted a study using the composite specimen interface cracking (CSIC) test developed at the University of Florida. Overall, results showed that specimens without ARMI exhibited a lower damage accumulation rate and a greater number of cycles to failure, and thus better performance than specimens with ARMI. Theoretical analysis suggested that the bridging effect between the single aggregates was the primary cause of stress concentration, which dramatically accelerated RC (Sun, 2011).

A.4.2.4 Fracture-Tolerant Interlayer

Fracture-tolerant interlayer systems, as shown in Figure A-5 d), consist of a relatively thin layer (typically less than 1 in [25 mm]) of high fracture-resistant mixtures, which are typically fine aggregate mixtures with a high asphalt binder content. In most cases, polymer-modified binders, such as styrene-butadiene-styrene (SBS), ethylene-vinyl acetate (EVA) co-polymer, and styrene-butadiene (SB) are used for this application. Sand mix, sand anti-fracture (SAF), NovaChip and STRATA belong to this category.

Fracture-tolerant interlayer systems have been used in the U.S. since the early 1950s. Several states have implemented these treatments and promising results have been reported as described below. Although most of the work reported in the literature involved use of these systems for asphalt overlay on PCC, they offered interesting insight that may be helpful in mitigating RC in asphalt overlay on flexible pavements.

In Alabama, a large number of techniques have been evaluated to provide guidance and recommendations to the Federal Aviation Administration (FAA) for mitigation of RC in rigid and flexible pavements. Based on the results of the evaluation, it appeared that fracture-tolerant interlayer system were effective treatments for existing pavement with good support and subjected to horizontal movements (Von Quintus, 2009). In 2014, the Louisiana Department of Transportation and Development conducted an in-depth literature review of research projects on RC. The objective of the study was to evaluate and compare different RC strategies considering performance, economic worthiness, constructability, and long-term benefits. Based on the results of the study, the research team identified fracture-tolerant interlayer systems as most promising techniques to mitigate RC in asphalt overlay of flexible pavements (Elseifi and Dhakal, 2015).

The Florida Department of Transportation carried out a study on State Road 10 (SR-10) with the scope of exploring the effectiveness of alternative methods to mitigate RC. SR-10 was a two-lane highway consisting of a 7-in Portland cement concrete (PCC) pavement. After the expansion of the road to four lanes, RC was noticed on the two inside lanes. Five field sections

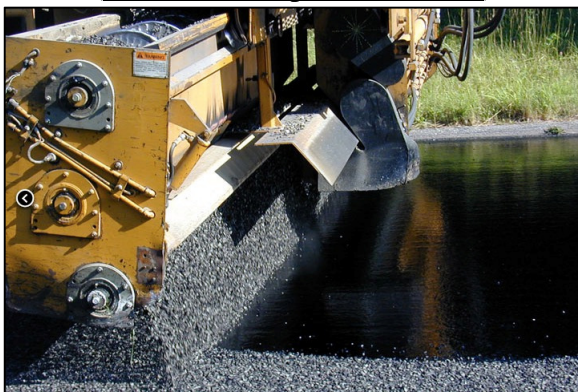
located within the eastbound and the westbound traffic lanes were included in the study. The rehabilitation, which was performed in 2010, consisted of milling 3-inches of the existing asphalt and putting back 1.5-in of Superpave (SP) 12.5-mm structural course in Sections 1, 2, 4 and 5, and 2.5-in of the same material in Section 3 (control section). In addition, Section 1 received a 0.5-inch asphalt overbuild, Section 4 received a 1.0-inch open-graded crack relief layer (OGCR), and Section 5 received a 0.5-inch ARMI. The performance of these treatments was evaluated based on deflection, cracking, rutting and ride quality. The latest data have shown that the sections with a OGCR have not performed as well as the control and the sections with an SP-9.5 overbuild (Chun et al., 2016).



(a) Nonwoven geotextiles
(www.missouripetroleum.com)



(b) ISAC (www.tensar.co.uk)



(c) ARMI (www.asmg.com)



(d) Fracture-tolerant interlayer system
(www.midlandasphalt.com)

Figure A-5. Stress and strain relief interlayer.

APPENDIX B
AGGREGATE STOCKPILE INFORMATION

Table B-1. Aggregate stockpiles used for granite mixtures.

| Type of Material | FDOT Code | Producer | Pit | Terminal |
|------------------|-----------|------------------------|-----------------|----------|
| # 89 Stone | C53 | Junction City Mining | GA-553 | TM-561 |
| W-10 Screenings | F22 | Junction City Mining | GA-553 | TM-561 |
| M-10 Screenings | F23 | Martin Marietta | GA-753 | TM-337 |
| M-10 Screenings | F23 | Martin Marietta | NS-315 | TM-579 |
| Local Sand | - | V.E. Whitehurst & Sons | Starvation Hill | |

Table B-2. Aggregate stockpiles used for limestone mixtures.

| Type of Material | FDOT Code | Producer | Pit | Terminal |
|------------------|-----------|----------|--------|----------|
| S-1-B Stone | C55 | CEMEX | 87-090 | TM-445 |
| Screenings | F21 | CEMEX | 87-090 | TM-447 |
| Screenings | F23 | CEMEX | 87-090 | TM-445 |
| Screenings | F24 | CEMEX | 08-012 | - |

APPENDIX C

GRADATIONS DESIGNED FOR INTERLAYER MIXTURES

Table C-1. Granite interlayer mixture gradations

| Sieve Size | (mm) | 9.5-mm NMAS | | | | 4.75-mm NMAS | | |
|------------|-------|-------------|-------|-------|-------|--------------|-------|-------|
| | | (%) | (%) | (%) | (%) | (%) | (%) | (%) |
| | | DF | DI | DC | GG | DF | DI | DC |
| 3/4 | 19.0 | 100.0 | 100.0 | 100.0 | 100.0 | 100.0 | 100.0 | 100.0 |
| 1/2 | 12.5 | 100.0 | 100.0 | 100.0 | 100.0 | 100.0 | 100.0 | 100.0 |
| 3/8 | 9.5 | 99.7 | 99.4 | 99.1 | 98.4 | 100.0 | 100.0 | 100.0 |
| #4 | 4.75 | 88.4 | 77.2 | 67.7 | 46.9 | 99.8 | 97.4 | 90.3 |
| #8 | 2.36 | 64.2 | 52.6 | 42.6 | 22.5 | 86.4 | 76.4 | 61.0 |
| #16 | 1.18 | 39.9 | 33.0 | 27.0 | 17.3 | 68.5 | 51.9 | 40.6 |
| #30 | 0.60 | 25.1 | 20.9 | 17.3 | 13.8 | 53.7 | 36.5 | 23.1 |
| #50 | 0.30 | 15.6 | 13.3 | 11.3 | 12.0 | 37.3 | 22.8 | 13.3 |
| #100 | 0.150 | 9.6 | 8.5 | 7.5 | 10.9 | 22.4 | 12.4 | 7.5 |
| #200 | 0.075 | 4.0 | 4.0 | 4.0 | 9.9 | 6.0 | 6.0 | 6.0 |

Table C-2. Limestone interlayer mixture gradations

| Sieve Size | (mm) | 9.5-mm NMAS | | | | 4.75-mm NMAS | | |
|------------|-------|-------------|-------|-------|-------|--------------|-------|-------|
| | | (%) | (%) | (%) | (%) | (%) | (%) | (%) |
| | | DF | DI | DC | GG | DF | DI | DC |
| 3/4 | 19.0 | 100.0 | 100.0 | 100.0 | 100.0 | 100.0 | 100.0 | 100.0 |
| 1/2 | 12.5 | 100.0 | 100.0 | 100.0 | 100.0 | 100.0 | 100.0 | 100.0 |
| 3/8 | 9.5 | 98.9 | 97.1 | 95.8 | 92.6 | 100.0 | 100.0 | 100.0 |
| #4 | 4.75 | 84.3 | 74.4 | 67.2 | 50.7 | 100.0 | 93.5 | 94.2 |
| #8 | 2.36 | 63.8 | 51.0 | 41.9 | 21.7 | 89.3 | 74.9 | 61.5 |
| #16 | 1.18 | 44.9 | 35.7 | 29.0 | 16.2 | 67.8 | 54.0 | 38.3 |
| #30 | 0.60 | 26.4 | 21.3 | 17.6 | 13.1 | 50.2 | 36.8 | 21.9 |
| #50 | 0.30 | 17.6 | 14.6 | 12.3 | 12.0 | 36.5 | 24.9 | 11.3 |
| #100 | 0.150 | 7.1 | 6.6 | 6.1 | 10.7 | 16.0 | 10.5 | 7.1 |
| #200 | 0.075 | 4.0 | 4.0 | 4.0 | 9.9 | 6.0 | 6.0 | 6.0 |

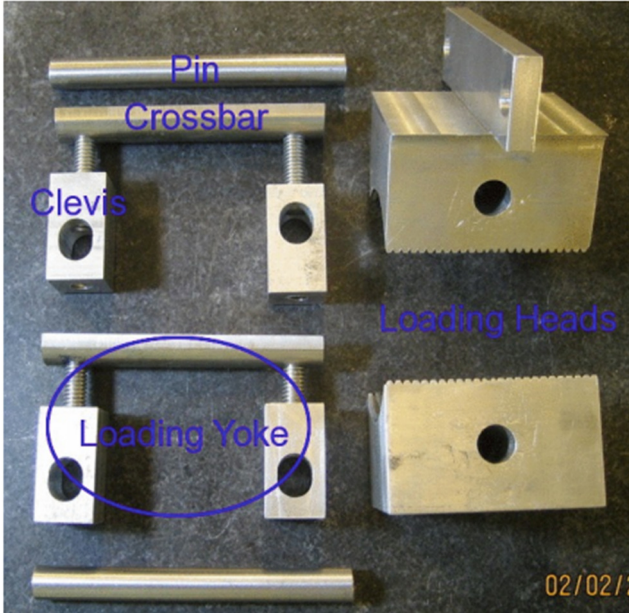
APPENDIX D
ENHANCEMENT OF THE CSIC TEST

The composite specimen interface cracking (CSIC) test developed in an earlier FDOT research project was enhanced with a new loading device, specimen configuration (and associated preparation procedure), and loading procedure to improve test repeatability and simplify the test setup (specimen installation) as described below.

D.1 New Loading Device

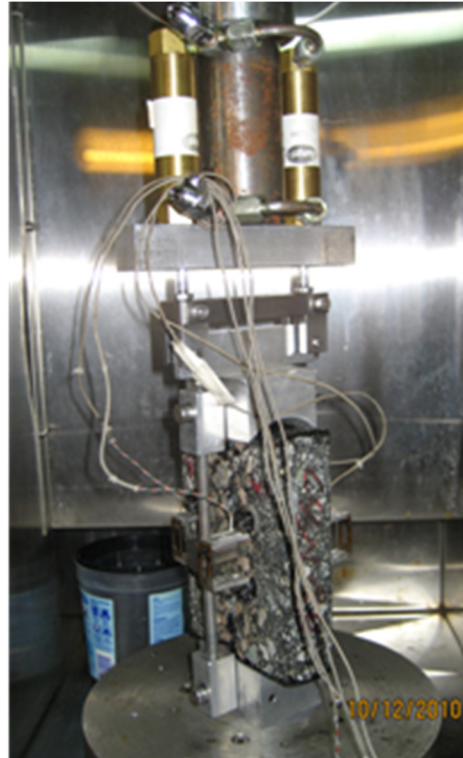
The original loading assembly (Figure D-1(a)) consisted of two loading heads (top and bottom), two pins, two crossbars (split cylinders through which the load was applied to the specimen) and four clevises that formed two sets of loading yokes. Mounting the specimen on the MTS frame included multiple steps: i) The two crossbars were inserted into the central hole of the specimen and connected to the clevises through treaded bars. The length of the threaded bars was adjusted such that the specimen will be evenly pulled during the test; ii) The clevises were connected to the loading heads through two pins; and iii) The loading heads were connected to the MTS frame. It is noted that an additional dual cylinder loading assembly was required along with the original loading device to equalize the load applied on the two sides of the composite specimen (Figure D-1(b)).

The new loading device is more rugged and easier to assemble. The new loading assembly consists of two loading heads (Figure D-2(a)), two crossbars (Figure D-2(b)), and four socket cap screws (Figure D-2(c)). The top loading head was designed with four slots (two on each side) to allow for the insertion of two steel bars (one on each side) from the bottom loading head. This design minimizes the potential of misalignment during load application, which is a problem associated with the original loading device. The two crossbars were inserted into the central hole of the specimen and connected directly to the loading device through the four socket cap screws (Figure D-3(a)). The test setup with the new loading assembly is shown in Figure D-3(b).

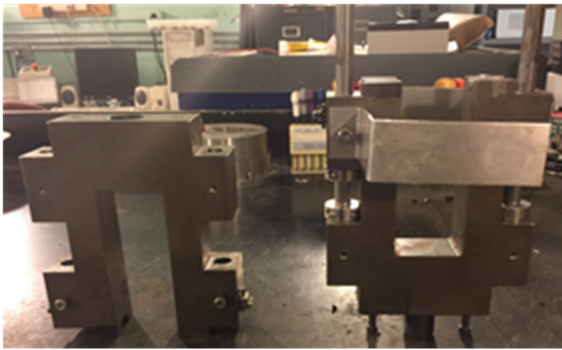


(a) Loading assembly

Figure D-1. Original loading device.



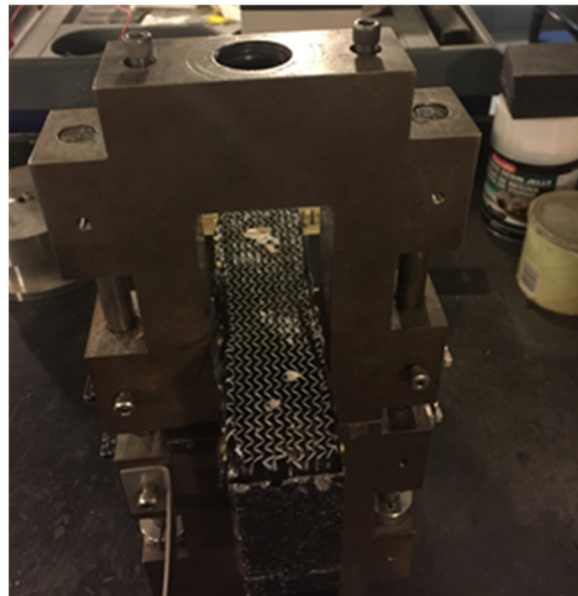
(b) Test setup



(a) Loading heads

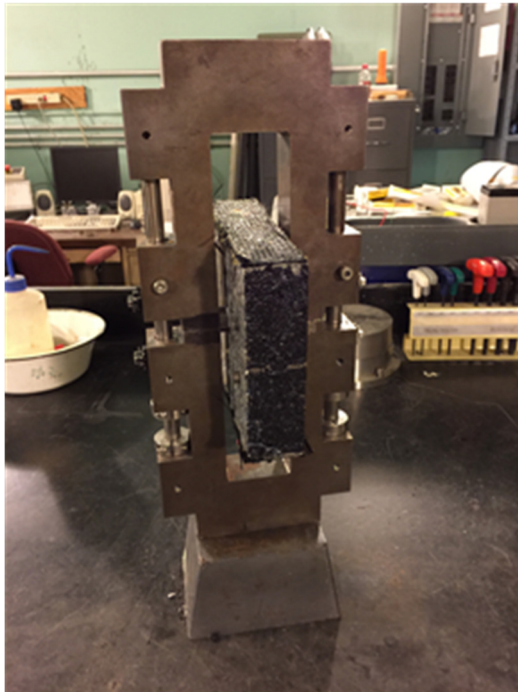


(b) Cross bars

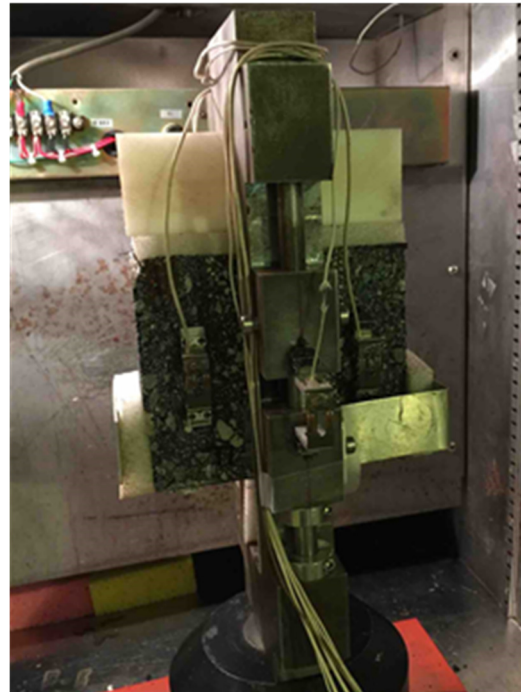


(c) Socket cap screws

Figure D-2. New loading assembly.



(a) Specimen placement



(b) Test setup

Figure D-3. Test setup with new loading device.

D.2 New Specimen Configuration

The original specimen configuration (Figure D-4(a)) consists of two composite layers with identical geometry glued (using epoxy) along the plane of symmetry. Each composite layer includes three layers: a 1.5-in overlay, an interlayer of desired thickness, and a 0.75-in underlying layer with a through gap in the center. A 0.75-in diameter hole was drilled in the center of the specimen for application of repeated load. The underlying layers were obtained from pre-compacted dense-graded samples sliced into 0.75-in thin layers. These layers were cut in half along the diametrical axis (Figure D-4(b)). A Teflon spacer was placed between the two half layers (Figure D-4(c)) to simulate old pavement with an existing crack.



(a) Original configuration



(b) Underlying layer cut in half



(c) Underlying layer with Teflon spacer

Figure D-4. Original specimen configuration.

The new specimen configuration has less asphalt layers (less variables) and is easier to produce. As shown in Figure D-5(a), two metal spacers were created to replace the pre-compacted underlying layer used in the original configuration. The metal spacers, when assembled, formed a 0.75-in diameter central hole in connection with two thin gaps (Figure D-5(b)). As a result, neither installation of Teflon spacer nor drilling is required to fabricate the new specimen.

The position metal panels (Figure D-5(c)) were created to enhance the process of specimen assembly in terms of more accurate alignment of two composite layers and placement of gauge points. As shown in Figure D-5(b), the positioning metal panels held tight the assembled specimen through four pins (two on each side) that are connected to the metal spacers. Gauge points were then placed to the surface of the specimen at pre-determined locations. Figure D-5(d) presents the complete composite specimen with the new configuration.



(a) Metal spacer



(c) Positioning metal panel



(b) Assembled CSIC specimen

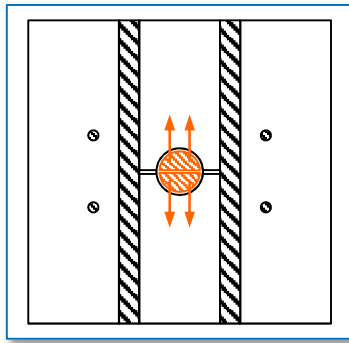


(d) New configuration

Figure D-5. New specimen assembly.

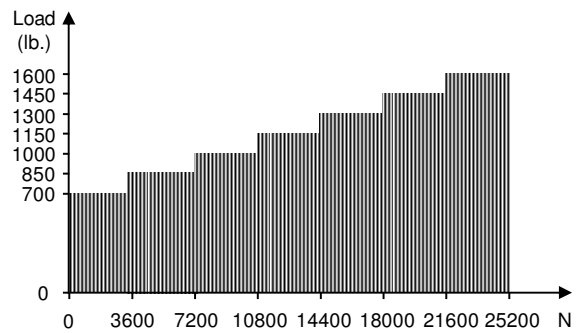
D.3 New Loading Procedure

Similar to the original design, a repeated haversine tensile load consisting of 0.1s loading and 0.9s rest period was applied through two crossbars placed inside the central hole of the specimen (Figure D-6(a)). In lieu of the constant amplitude loading procedure employed in the prior studies, a new loading procedure (called amplitude sweep loading) was established to ensure completion of CSIC testing in one working day without compromising accuracy in ranking of mixture performance.



(a) Loading applied through crossbars

Figure D-6. New loading procedure.



(b) Amplitude sweep loading

As shown in Figure D-6(b), the amplitude sweep loading procedure had an initial load of 700 lb and a constant increment of 150 lb for every one hour of loading until reaching 1,600 lb. Based on trial tests conducted on composite specimens with a range of interlayer mixtures, it was observed that almost no damage was induced to the specimen below the 700-lb load level. The constant load increment of 150 lb resulted in gradual accumulation of damage over a series of load levels. All specimens evaluated failed before reaching 1600 lb and the test duration was typically no greater than 6 hours.

APPENDIX E
MIXTURE TEST RESULTS

Table E-1. CSIC test results for 9.5-mm mixtures and the control at 1.0-in thickness.

| (Rock) | (R#) | Number of cycles to failure | | | | |
|-----------|-----------|-----------------------------|-------------------|-------------------|-------------------|-------------------|
| | | (N _f) | (N _f) | (N _f) | (N _f) | (N _f) |
| Granite | Replicate | Control | DF | DI | DC | GG |
| | R1 | 12449 | 16234 | 16121 | 16740 | - |
| | R2 | 12404 | 16254 | - | 15715 | 18000 |
| | R3 | - | 15318 | - | 14805 | 18000 |
| | Average | 12427 | 15935 | 16121 | 15754 | 18000 |
| Limestone | Replicate | | DF | DI | DC | GG |
| | R1 | | 13158 | 14755 | 16142 | 14752 |
| | R2 | | 14744 | 15048 | - | 12024 |
| | R3 | | 15692 | 14883 | 14961 | 12264 |
| | R4 | | - | - | 15644 | - |
| | Average | | 14532 | 14896 | 15583 | 13014 |

Table E-2. CSIC test results for 9.5-mm mixtures and the control at 0.75-in thickness.

| (Rock) | (R#) | Number of cycles to failure | | | | |
|-----------|-----------|-----------------------------|-------------------|-------------------|-------------------|-------------------|
| | | (N _f) | (N _f) | (N _f) | (N _f) | (N _f) |
| Granite | Replicate | Control | DF | DI | DC | GG |
| | R1 | 12961 | 15342 | 15648 | 15131 | 14400 |
| | R2 | 11826 | 15454 | 15469 | 16207 | 15360 |
| | R3 | 11569 | - | 15937 | 14400 | 15701 |
| | Average | 12119 | 15398 | 15684 | 15246 | 15153 |
| Limestone | Replicate | | DF | DI | DC | GG |
| | R1 | | 12025 | 13108 | 13371 | 9709 |
| | R2 | | - | 13164 | 14730 | 7360 |
| | R3 | | 11558 | 12138 | 12579 | 12411 |
| | R4 | | - | - | 16071 | - |
| | Average | | 11792 | 12803 | 14188 | 9827 |

Table E-3. CSIC test results for 4.75-mm mixtures and the control at 0.75-in thickness.

| (Rock) | (R#) | Number of cycles to failure | | | | |
|-----------|-----------|-----------------------------|-------------------|-------------------|-------------------|-------------------|
| | | (N _f) | (N _f) | (N _f) | (N _f) | (N _f) |
| Granite | Replicate | Control | DF | DI | DC | DCM |
| | R1 | 12961 | 13217 | 12870 | 13358 | 11775 |
| | R2 | 11826 | 12132 | 13149 | 15196 | 12980 |
| | R3 | 11569 | 13067 | 12834 | 16516 | 12779 |
| | Average | 12119 | 12805 | 12951 | 15023 | 12511 |
| Limestone | Replicate | | DF | DI | DC | |
| | R1 | | 13059 | 13610 | 13188 | |
| | R2 | | - | 16666 | 15126 | |
| | R3 | | 15148 | 13406 | 14849 | |
| | Average | | 14099 | 14561 | 14388 | |

Table E-4. CSIC test results for 4.75-mm mixtures and the control at 0.50-in thickness.

| (Rock) | (R#) | Number of cycles to failure | | | | |
|-----------|-----------|-----------------------------|-------------------|-------------------|-------------------|-------------------|
| | | (N _f) | (N _f) | (N _f) | (N _f) | (N _f) |
| Granite | Replicate | Control | DF | DI | DC | DCM |
| | R1 | 8974 | 11685 | 9241 | 16178 | 8154 |
| | R2 | - | 9610 | 9532 | 12418 | - |
| | R3 | 8283 | 9117 | 12063 | 14943 | 8222 |
| | Average | 8629 | 10137 | 10279 | 14512 | 8188 |
| Limestone | Replicate | Control | DF | DI | DC | |
| | R1 | - | 12058 | 11558 | 12400 | |
| | R2 | - | 11929 | 12098 | 12858 | |
| | R3 | - | 11143 | 11898 | 14981 | |
| | Average | - | 11710 | 11851 | 13413 | |

Table E-5. APA test results for interlayer mixtures.

| (Rock) | | 9.5-mm NMAS | | | 4.75-mm NMAS | | | | |
|-----------|-------|-------------|-------|-------|--------------|--------|-------|--------|-------|
| | | (mm) | (mm) | (mm) | Rut Depth | | (mm) | (mm) | (mm) |
| | Set | DF | DI | DC | GG | DF | DI | DC | DCM |
| Granite | Left | 5.484 | 4.956 | 3.812 | 14.000 | 14.000 | 6.079 | 11.214 | 2.632 |
| | Right | 5.528 | 5.761 | 4.514 | 10.919 | 14.000 | 7.034 | 14.000 | 2.734 |
| | Ave. | 5.506 | 5.125 | 4.163 | 12.460 | 14.000 | 6.557 | 12.607 | 2.683 |
| | | | | | | | | | |
| Limestone | Left | 3.808 | 2.842 | 2.276 | 4.484 | 14.000 | 3.366 | 4.067 | |
| | Right | 3.444 | 3.330 | 2.454 | 4.944 | 11.073 | 3.813 | 3.416 | |
| | Ave. | 3.626 | 3.086 | 2.365 | 4.714 | 12.537 | 3.589 | 3.742 | |
| | | | | | | | | | |

LIST OF REFERENCES

- AASHTO. (2010). Standard method of test for determining rutting susceptibility of hot mix asphalt (HMA) using the asphalt pavement analyzer (APA), AASHTO T 340, Washington, D.C.
- Al-Qadi, I. L. & Elseifi, M. A. (2004). Field installation and design considerations of steel reinforcing netting to reduce reflection of cracks. In *Proceedings of the 5th International RILEM Conference: Cracking in Pavements–Mitigation, Risk Assessment, and Prevention* (pp. 97-104). Limoges, France.
- Baek, J. & Al-Qadi, I. (2011). Sand Mix Interlayer to Control Reflective Cracking in Hot-Mix Asphalt Overlay. *Transportation Research Record: Journal of the Transportation Research Board*, 2227, 53–60.
- Barazone, M. (1990). Paving fabric interlayer membranes and installation procedures over the past 20 years. *Geotechnical Fabrics Report*, 10(4).
- Barazone, M. (2000). Installing paving synthetics--overview of correct installation procedure (part two of three). *Geotechnical Fabrics Report*, 18(3).
- Bennert, T., Fee, F., Sheehy, E., Blight, R., & Sauber, R. (2011). Implementation of Performance-Based HMA Specialty Mixtures in New Jersey. *Journal of the Association of Asphalt Paving Technologists*, 80.
- Blankenship, P., Iker, N. & Drbohlav, J. (2004). Interlayer and design considerations to retard reflective cracking. *Transportation Research Record*, (1896), 177–186.
- Buttlar, W. G., Bozkurt, D. & Dempsey, B. J. (2000). Cost-effectiveness of paving fabrics used to control reflective cracking. *Transportation Research Record*, (1730), 139–149.
- Button, J., & Lytton, R. (2007). Guidelines for Using Geosynthetics with Hot-Mix Asphalt Overlays to Reduce Reflective Cracking. *Transportation Research Record: Journal of the Transportation Research Board*, (2004), 111–119.
- Chen, D. H., Scullion, T., Bilyeu, J., & Won, M. (2005). Detailed forensic investigation and rehabilitation recommendation on interstate highway-30. *Journal of Performance of Constructed Facilities*, 19(2), 155-164.
- Chen, Y., Lopp, G., & Roque, R. (2013). Effects of an asphalt rubber membrane interlayer on pavement reflective cracking performance. *Journal of Materials in Civil*

- Engineering*, 25(12), 1936-1940.
- Chen, Y., Tebaldi, G., Roque, R., Lopp, G., & Exline, M. (2013). A mechanistic test to evaluate effects of interface condition characteristics on hot-mix asphalt overlay reflective cracking performance. *Road Materials and Pavement Design*, 14(sup1), 262-273.
- Choubane, B., Page, G., & Musselman, J. (2000). Suitability of asphalt pavement analyzer for predicting pavement rutting. *Transportation Research Record: Journal of the Transportation Research Board*, (1723), 107-115.
- Cooley, L.A. & Brown, E.R. (2003). Potential of using stone matrix asphalt for thin overlays. NCAT Report 03-01, National Center for Asphalt Technology.
- Chun, S., Nazef, A., Offei, E., Greene, J., & Choubane, B. (2016). *Effectiveness of Crack Relief Techniques to Mitigate Reflective Cracking in Asphalt Overlaid Concrete Pavement*, TRB (No. 16-1609).
- Davis, N. M. (1960). A field study of methods of preventing reflection cracks in bituminous resurfacing of concrete pavements. Report No. 12, University of Toronto, Toronto, Ontario.
- Drakos, C. A., Roque, R., Birgisson, B., & Novak, M. (2005). Identification of a physical model to evaluate rutting performance of asphalt mixtures. *Journal of ASTM International*, 2(3), 1-21.
- Elseifi, M. & Dhaka, N. (2015). Mitigation Strategies of Reflection Cracking in Pavements, In *Report No. FWHA/LA.14/541*. Luisiana Department of Transportation and Development.
- FAA. (2006). Airport pavement design and evaluation. AC-150/5320-6, Federal Aviation Administration, U.S. Department of Transportation.
- Ghauch, Z. G., & Abou-Jaoude, G. G. (2013). Strain response of hot-mix asphalt overlays in jointed plain concrete pavements due to reflective cracking. *Computers & Structures*, 124, 38-46.
- Greene, J., Choubane, B., Chun, S., & Kim, S. (2012). Effect of asphalt rubber membrane interlayer (ARMI) on instability rutting and reflection cracking of asphalt mixture. In *Report No. FL/DOT/SMO/12-552*. Florida Department of Transportation.
- Guarin, A., Roque, R., Kim, S., & Sirin, O. (2013). Disruption factor of asphalt mixtures. *International Journal of Pavement Engineering*, 14(5), 472-485.
- Hensley, M. J. (1980). Open-graded asphalt concrete base for the control of reflective cracking.

- Journal of the Association of Asphalt Paving Technologists, 49, 368-381.
- Housel, W. S. (1962). Design, Maintenance and Performance of Resurfaced Pavements at Willow Run Airfield. *Highway Research Board Bulletin*, (322).
- Isola, M., Chun, S., Roque, R., Zou, J., Koh, C., & Lopp, G. (2014). Development and evaluation of laboratory conditioning procedures to simulate mixture property changes effectively in the field. *Transportation Research Record: Journal of the Transportation Research Board*, (2447), 74-82.
- Kim, S., Roque, R., Guarin, A., & Birgisson, B. (2006). Identification and assessment of the dominant aggregate size range (DASR) of asphalt mixture. *Journal of Asphalt Paving Technologists*, 75, 789-814.
- Lea, J. & Harvey, J. T. (2004). Data mining of the caltrans pavement management system (PMS) database. Technical report, University of California, Berkeley, Pavement Research Center, Richmond, California, 94804.
- Lu, Q. & Harvey, J. T. (2012). Laboratory Performance Comparison of Promising Asphalt Surface Mixes. In *CICTP 2012: Multimodal Transportation Systems—Convenient, Safe, Cost-Effective, Efficient*, 3451-3462.
- Luther, M. S., Majidzadeh, K., & Chang, W. (1976). Mechanistic investigation of reflective cracking of asphalt overlays. In *Transportation Research Record 572*, TRB, National Research Council, Washington, D. C., pp. 111-122.
- Lytton, R. L. (1989). Use of geotextiles for reinforcement and strain relief in asphalt concrete. *Geotextiles and Geomembranes*, 8(3), 217-237.
- Maurer, D. A. & Malasheskie, G. J. (1989). Field performance of fabrics and fibers to retard reflective cracking. *Geotextiles and Geomembranes*, 8(3), 239-267.
- Mukhtar, M. T. & Dempsey, B. J. (1996). *Interlayer stress absorbing composite (ISAC) for mitigating reflection cracking in asphalt concrete overlays* (No. UILU-ENG-96-2006). Department of Civil Engineering, University of Illinois at Urbana-Champaign.
- Nam, B. H., Golestani, B., Noori, M., Tatari, O., and An, J. (2014). Investigation of reflective cracking mitigation techniques. Final Report, Contract No. BDK78 977-17, Florida Department of Transportation.
- Penman, J. and Hook, K.D. (2008). The Use of Geogrids to Retard Reflective Cracking on Airport runways, taxiways and aprons. In Al-Qadi, I.L., Scarpas, T., and Loizos, A.

- (Editors). Pavement Cracking. Mechanisms, Modeling, Detection, Testing and Case Histories, pp. 713-720. CRC/Taylor & Francis Group, London, UK.
- NCHRP Report 673. A manual for design of hot mix asphalt with commentary. Transportation Research Board, 2011.
- Roque, R., Chun, S., Zou, J., Lopp, G., & Villiers, C. (2011). Continuation of Superpave projects monitoring. *Final Report of Florida Department of Transportation*.
- Roque, R., Koh, C., Chen, Y., Sun, X., & Lopp, G. (2009). Introduction of Fracture Resistance to the Design and Evaluation of Open Graded Friction Courses in Florida. *Florida Department of Transportation, Contract BD 545-53*.
- Scullion, T. (2010). *Technical Bulletin on Design and Construction of Crack Attenuating Mixes (CAM)* (No. Report 0-5598-P1). Texas Transportation Institute, Texas A & M University System.
- Sherman, G. b. (1974). Reflective Cracking. *Pavement Rehabilitation: Proceedings of a Workshop. Federal Highway Administration, U.S. Department of Transportation, Washington, D.C, FHWA-RD-74*, 151–157.
- Smit, A.F., Prasad, S., Prozzi, J., and Tahmoressi, M. (2011). Cam Mix Design with Local Aggregates (No. Report FHWA/TX-12/0-6435-1). University of Texas at Austin.
- Sun, X. (2011). *Modeling Analysis Of Pavement Layer Interface Bonding Condition Effects On Cracking Performance*. PhD Dissertation, University of Florida.
- Van Breemen, W. (1963). Discussion of Possible Designs of Composite Pavements. *Highway Research Record*, (37).
- Vespa, J. W. (2005). *An evaluation of interlayer stress absorbing composite (ISAC) reflective crack relief system* (No. FHWA/IL/PRR 150). Illinois. Dept. of Transportation. Bureau of Materials and Physical Research.
- Von Quintus, H. L., Mallela, J., Weiss, W., & Shen, S. (2009). Techniques for Mitigation of Reflective Cracks, Technical Guide APTP Project 05-04. *Airfield Asphalt Pavement Technology Program, Auburn University, Alabama, USA*.
- Wu, R. (2005). Finite element analysis of reflective cracking in asphalt concrete overlays. PhD Dissertation, University of California, Berkeley.